Generating curvature perturbations in a contracting universe

Aaron M. Levy

A Dissertation
Presented to the Faculty
of Princeton University
in Candidacy for the Degree
of Doctor of Philosophy

Recommended for Acceptance
by the Department of
Physics
Adviser: Paul J. Steinhardt

April 2017

Abstract

This thesis studies bouncing cosmologies in which the present-day expansion of the universe was preceded not by a "big bang"− before which time and space ceased to have meaning− but by a contracting phase that then bounced. We discuss two competing paradigms for generating the observed, scale-invariant spectrum of primordial density perturbations during the contracting phase: "the matter bounce scenario" and "ekpyrosis." First, we discuss the matter bounce scenario, and in particular, its fine-tuning instability to the growth of anisotropic stress. Then, we examine ekpyrosis. In the best-understood ekpyrotic models, one scalar field drives the background evolution of the universe while another (entropic) scalar field generates the density perturbations. We study the stability of these models, showing that in contrast to previous theorems, the simplest (as measured by parameters and degrees of freedom), observationally viable realizations are dynamical attractors. Finally, we present a new mechanism called "warm ekpyrosis," which eliminates altogether the need for the second (entropic) scalar field. Rather, a single field falls down its ekpyrotic potential, smoothing and flattening the universe, while simultaneously, through couplings to lighter degrees of freedom, decaying into hot, ultrarelativistic matter. This decay allows both for the production of a scale-invariant density perturbation and for a possible mechanism of reheating.

Acknowledgements

I would like to thank my advisor, Paul Steinhardt. I would also like to express my sincerest gratitude to my senior colleague, Lasha Berezhiani, for helpful discussions and insights; David Spergel for his consistently sound advice; Frans Pretorius and Chris Tully for serving on my prethesis committee; Herman Verlinde for his valuable counsel as Director of Graduate Studies; Lyman Page for his indispensable role as Department Chair; Peter Meyers for being my experimental advisor; Joaquin Turiaci for our fun collaboration; and my friends and family for their unwavering love and encouragement.

Contents

Chapter 1

Introduction

1.1 Olbers' paradox and the beginning of the Universe

The darkness of the night sky immediately presents a paradox [1], named after the German astronomer Heinrich Wilhelm Olbers, that sheds... well... light on the nature of the cosmos. For if the Universe were eternal and static and filled more or less uniformly with stars like the sun, then the intensity of light observed at the Earth would be infinite; that is, the night sky would be bright, not dark. To see this, note that in a spherical shell around the Earth of width dr at radius r containing a number density n of stars, there would exist $4\pi r^2 n dr$ stars. If each one emitted at luminosity L, then an Earth-bound observer would measure an intensity, dI, from this shell that is independent of radius, *i.e.,*

$$dI = (4\pi r^2 n)\frac{L}{4\pi r^2}dr = nLdr. \tag{1.1}$$

Therefore, the total intensity would diverge, *i.e.,* $I = \int dI = nL\int_0^\infty dr = \infty$, indicating an infinitely bright sky.

The resolution, encoded in Einstein's equations of general relativity [2], is that the Universe is not static. Space is not merely a fixed background through which particles move, but rather stretches and bends in response to them. In our Universe, as a result of this stretching, distant regions grow ever more distant over time. As a corollary, in the past, the Universe was smaller and denser. Extrapolating Einstein's equations back through this high density regime reveals a singularity approximately 13.8 billion years ago, an event Fred Hoyle famously derided in 1949 as a "big bang." Ever since then, light, which travels at finite speed, can have traversed only a finite distance. In turn, this means that Earth-bound observers today can see only a finite distance away and therefore finitely many stars [3]. Therefore, the total intensity is finite; the night sky is dark.

1.2 The cosmic microwave background

When we observe an object that is one light year away, it appears to us as it was one year ago, since this is when the light was emitted, only having reached us after a year of transit. By extension, the farther out we look in distance, the further back we are looking in time. By observing very distant light sources, we are in effect studying the Universe in its nascency. Unfortunately, there is a limit to how far we can see. The farthest light we can detect originates from the time when the Universe, having burst into existence hot and dense after the big bang, had stretched and cooled enough that free electrons, from which photons had previously Thomson scattered, bound to protons to form neutral hydrogen. Over the last 13.8 billion years, these old photons have been free streaming through space, carrying a snapshot of the Universe as it was 380,000 years after the big bang. First detected in 1964 by Penzias and Wilson [4] and measured today by precision ground-based [5, 6, 7, 8], balloon-borne [9, 10] and satellite telescopes [11, 12, 13], this "cosmic microwave background" (CMB)

radiation has a nearly ideal blackbody spectrum at a temperature of 2.73 K and is isotropic except for minuscule anisotropic fluctuations of order but 10^{-5} (ignoring the dipole anisotropy induced by the peculiar motion of the Earth with respect to the cosmological rest frame of the CMB). According to the theory of general relativity, these fluctuations grew via gravitational instability to form the foam-like cosmic web of large-scale structure we observe today.

1.3 Big bang problems and the inflationary proposal

Given the great success of explaining the growth of large-scale structure from these initial fluctuations, it is natural to ask what caused them. In searching for an explanation, in 1969, Charles Misner realized something troubling, a conundrum he referred to as the "horizon paradox" [14]. Due to the finite time since the big bang and the finite speed of light, there is a greatest possible distance– a particle horizon– over which physical information can travel. Cosmic microwave background photons that subtend an angle of more than $\approx 2^\circ$ on the sky were beyond each other's particle horizon, meaning they were out of causal contact, at the time they decoupled from matter. Nevertheless, the CMB radiates as a nearly perfect isotropic blackbody. It is as though distant regions achieved thermal equilibrium, despite insufficient time for any physical mechanism to induce it. Therefore, the Universe began with a density profile that is inexplicably smooth. In that same year, Robert Dicke noticed a similar problem: the Universe began with a spatial geometry that is inexplicably flat [15].

Reflecting on these problems, Misner remarked, "Things that you don't understand can be a constant to ten or twenty percent, but to one percent, it requires an explanation." Since 1981, the conventional explanation for the initial smoothness and flatness of the Universe has been the inflation scenario [16, 17, 18]. In its ideal formulation, typical conditions arising from the big bang allow small, causally

connected regions of the Universe to undergo a period of rapid, accelerated expansion, *i.e.,* inflation, before nucleosynthesis. The accelerated expansion smoothes and flattens the local geometry, while simultaneously stretching quantum fluctuations to cosmological scales. These quantum fluctuations [19, 20, 21, 22, 23] imprint the observed anisotropies onto the CMB and form the density perturbations that seed the formation of large-scale structure.

However, this idealization has been criticized for several weaknesses. First, although it was introduced to explain the required smoothness and flatness, inflation requires special initial conditions of its own, conditions certain entropic arguments suggest are extremely, exponentially unlikely [24]. For example, applying the canonical Liouville measure to homogeneous, isotropic universe, the authors of Ref. [25] demonstrate that such universes are exponentially less likely to result from long periods of inflation than from no inflation at all. Concordantly, the quantum argument given in Ref. [26] concludes that constituent quanta at sub-Planckian energy densities are exponentially unlikely to initiate inflation, even when weighted by volume.

Second, the inflationary paradigm is versatile to the point of being unfalsifiable. By adding parameters and adjusting their values, inflationary models can accommodate nearly any cosmological observables [27]. Unfortunately, for the models most favored by observation– those involving a single field with a flat, plateau-like potential– initiating inflation requires smoothness over scales much greater than the Hubble radius [28], the very condition inflation was supposed to provide. Without it, gradients and inhomogeneities rapidly dominate the evolution of the Universe, preventing inflation from ever starting. Thus, "inflation does not predict smoothness and flatness– it assumes it" [29].

Third, given a particular model, inflation leads almost unavoidably to the multiverse, according to which *any* outcome is possible [30, 31, 32, 33, 34, 35]. In most regions, quantum fluctuations of the inflaton field exert small effects– the ones respon-

sible for the temperature anisotropy observed in the CMB. In these places, inflation terminates when the classically evolving inflaton field falls far enough down its potential function. But in rare regions, the quantum fluctuations deliver large kicks back up the potential, impeding the classical descent of the inflaton, thereby prolonging the exponential expansion. In short order, these rare eternally inflating regions dominate the volume of space, and the process repeats anew. Far from the uniformity inflation was intended to provide, the universe obtains a fractal-like structure as small pocket universes terminate inflation at different times and with different cosmological properties. Some are flat and smooth with a scale-invariant spectrum of density fluctuations like ours, but an infinite number are not. According to Guth, "Anything that can happen will happen; in fact, it will happen infinitely many times" [36]. With no selection rule– no probability measure– to favor pocket universes like our own, the multiverse renders inflation unpredictive.

Finally, inflating universes have been shown to be geodesically past-incomplete [37]. This implies that inflation is fundamentally unable to explain the nature of the big bang singularity. Rather, some unknown physics is required. These issues have motivated the search for better answers.

1.4 Bouncing cosmologies

One approach is to replace the initial big bang singularity with a big bounce. In contrast to inflation, one-time bouncing cosmologies (and their cyclic cousins) can be past-eternal [38], meaning the universe has no creation event because it always exists. As a happy consequence, the pre-bounce contracting phase offers plenty of time for resolving Misner's horizon paradox: in a past-eternal universe, particle horizons are infinite, so distant regions enjoy perennial causal contact. Moreover, bouncing

cosmologies resolve the flatness problem since contraction, like inflation, is a natural flattener.

The earliest cyclic solution to Einstein's equations predates inflation by nearly 60 years, way back to Friedmann's "periodic world" of 1922 [39]. In it, Friedmann argued that a homogeneous universe with a cosmological constant and a supercritical matter density executes eternal, regular periods of expansion and contraction with bouncing transitions in between. These ideas generated significant interest amongst the founders of the big bang theory (*e.g.,* Einstein [40, 41] and Lemaître [42]) until Tolman emphasized a serious thermodynamic flaw [43, 44]. He argued that as a direct consequence of the second law of thermodynamics, the regular periods of expansion and contraction should increase in duration over time. Backtracking, then, the periods universe achieves zero size a finite time in the past, thereby reintroducing the creation event the model was designed to avoid.

Another problem for contracting universes, first shown by Belinksii, Khalatnikov, and Lifshitz (BKL) in the 1960s, is their instability to the growth of anisotropic stresses [45]. In expanding universes, anisotropies are usually ignored, since they dilute much faster than other stress-energy components and therefore quickly become negligible. In contracting universes, however, BKL showed that the opposite is true: as space contracts, anisotropies grow more important. In short order, they drive the universe towards a Kasner-like evolution in which one spatial direction expands while the other two contract. If spatial curvature is present, then every so often, sudden jumps between Kasner-like solutions switch the directions and rates of contraction in a manner reminiscent of a kitchen mixer [14]. Over time, inhomogeneities in the curvature induce asynchronies between jumps at different locations, leading ultimately to a highly inhomogeneous crunch that is incompatible with the large-scale homogeneity observed today.

As a result of Tolman's entropy problem and the BKL instability, cyclic cosmologies fell into disfavor until Steinhardt and Turok proposed an innovation that resolves both. Initially formulated in the language of M-theory, their new cyclic model [46] posited that the observable Universe occupies one of two parallel 3-branes whose regular collisions punctuate long periods of intra-brane stretching and manifest as big crunch/big bang transitions. The stretching of the branes dilutes the entropy density, thereby circumventing Tolman's problem. Meanwhile, the inter-brane potential responsible for the periodic collisions generates an ultra-slow contracting phase, called ekpyrosis [47], that evades the BKL instability before the bounce [48]. Over time, this new cyclic model was understood to admit an effective 3+1-dimensional description using the same ingredients, *i.e.*, scalar fields, as inflation. In this framework, the ekpyrotic phase derives from an effective scalar whose pressure exceeds its energy density, so that the field dominates all other stress-energy components, even anisotropies, and the Universe contracts homogeneously.

In light of these successes, bouncing cosmologies have resurged in recent years. Many mechanisms have been proposed for achieving a bounce, both singular (see, *e.g.,* [49, 50, 51, 52, 53, 54])– in which quantum gravity effects introduce bounce-inducing deviations from conventional general relativity– and nonsingular (*e.g.,* [55, 56, 57, 58, 59, 60, 61, 62])– in which the density remains sub-Planckian and the transition from contraction to expansion evolves classically via a violation of the null energy condition. Both approaches face difficult challenges, although recent progress on cubic Galileon theories [63, 64] has provided classically stable nonsingular bounces that avoid many pathologies plaguing other models, *e.g.*, ghosts, gradient instabilities, super-luminal sound speeds, etc.

Whether singular or nonsingular, any bouncing model must ultimately explain the nearly scale-invariant spectrum of primordial fluctuations observed in the CMB. Since fluctuations on length scales of cosmological interest originate in the contracting

phase preceding the bounce, predictions for primordial spectra depend critically on the gravitational dynamics, *i.e.,* the equation of state of the dominant energy component, during the contracting phase. In this thesis, we consider two popular contracting scenarios, examining the stability and spectra of each: the matter bounce scenario (chapter 2) and ekpyrosis (chapters 3 and 4). We will assess to what extent these scenarios address the standard fine-tuning problems without introducing additional tunings of their own.

This thesis is organized as follows: In chapter 2, we show that the BKL instability poses a serious fine-tuning challenge for any bouncing cosmology involving a matter-like phase of contraction to generate the observed spectrum of perturbations. In chapter 3, we argue that, in contrast to previous theorems, precisely the opposite is true of the simplest, observationally viable, two-field models of ekpyrosis. In particular, we prove that these models are strong attractors for a wide range of initial conditions. Finally, in chapter 4, we propose an ekpyrotic mechanism for generating the observed spectrum that is also an attractor. Termed "warm ekpyrosis," the model involves a single ekpyrotic field coupled to a thermal bath of radiation into which it continuously decays. The decay allows a scale-invariant spectrum to be generated without the need for a second field. It also provides a possible mechanism for reheating the post-bounce universe without recourse to stringy, high energy physics.

Chapters 2, 3, and 4 are based on work published in Refs. [65, 66, 67], respectively.

Chapter 2

Fine-tuning challenges for the matter bounce scenario

This chapter was published in Ref. [65] as an Editor's Suggestion.

2.1 Introduction

Matter bounce models were introduced to provide a simple mechanism for generating a scale-invariant spectrum of adiabatic perturbations in accord with observations [68, 69, 70, 71]. The basic idea is that quantum fluctuations naturally generate a scale-invariant spectrum of adiabatic curvature perturbations during a contracting phase if the dominant density is a pressureless (*i.e.,* matter-like) fluid, such as a scalar field rolling along an exponential potential [72, 73, 74]. If the matter-like phase is followed by a nonsingular bounce, say, the scale-invariant spectrum can be preserved after the bounce and provide an explanation of the observed fluctuations in the microwave background and of the large-scale structure of the universe. This scenario is referred to as "matter bounce" [75]. It resolves the horizon problem (and in some incarnations, the flatness problem) of standard Big Bang cosmology [76], generates the observed

perturbations, and avoids the multiverse problem [77, 31, 32, 33, 34, 35] of inflation [78, 17, 18].

One well-known problem with the matter bounce scenario is its overproduction of tensor fluctuations during the matter-like contracting phase. This issue has been studied extensively [62, 79, 80] with various proposed resolutions [81, 82, 83, 84, 85]. But perhaps the biggest problem for the matter bounce scenario is the instability of the contracting matter-like phase to anisotropy. If unchecked, anisotropy rapidly dominates the energy budget of the universe– spoiling the equation of state responsible for the scale-invariant spectrum– and ultimately leading to chaotic Belinskii-Khalatnikov-Lifshitz (BKL) behavior [45].

Most works attempting to resolve the anisotropy problem focus on avoiding BKL instability after the matter-like contracting phase and thus after the generation of scale-invariant superhorizon perturbations [62, 86, 79]. They argue that if anisotropy is subdominant by the end of the matter-like contraction, then an ensuing phase of ekpyrosis will render it negligible thereafter. Suppressing the anisotropy after the matter-like phase is far too late, though, as we emphasize in this chapter. Unless the anisotropy is exponentially suppressed before the matter-like phase begins, it rapidly overtakes the energy density of matter before a sufficient number of scale-invariant modes have been generated.

In this chapter, we examine the anisotropy problem and demonstrate that it requires extreme, exponential tuning of the initial conditions– in some cases, exponentially more tuning than required to resolve the flatness problem, for example. In Sec. 2.2, we summarize the anisotropy problem along lines similar to those in Ref. [87]. In Sec. 2.3, we argue that suppressing the anisotropy requires a protracted isotropizing phase *prior* to the matter-like phase, and moreover that the degrees of freedom responsible for the matter-like phase must be coupled to those driving the isotropizing phase. In Sec. 4.4, we construct an example of this sort involving a canonical

scalar field with a specially constructed potential. In Sec. 2.5, we show how resolving the anisotropy problem requires extreme fine-tuning of this potential. In Sec. 2.6, we conclude, arguing that this extreme fine-tuning is a generic property of the matter bounce scenario.

In what follows, we employ reduced Planck units ($8\pi G = 1$) and metric signature $(-+++)$.

2.2 Quantifying the anisotropy problem

In this section, we review the anisotropy problem for matter-dominated, contracting universes, demonstrating that the growth of anisotropy is exponentially sensitive to the number of modes that leave the horizon during the matter-like phase. This result is summarized in Eq. (2.5).

In a flat Friedmann-Robertson-Walker universe driven by a stress-energy component, X, with a constant equation of state $\epsilon = -\dot{H}/H^2$, the scale factor, a, is related to the Hubble parameter, $H \equiv \dot{a}/a$, in the following way

$$\frac{a_f}{a_i} = \left(\frac{H_i}{H_f}\right)^{1/\epsilon}, \tag{2.1}$$

where subscripts i and f denote initial and final values. In the above, overdots denote derivatives with respect to coordinate time, t. The ratio of the energy density in anisotropy ($\propto a^{-6}$) to that in X ($\propto a^{-2\epsilon}$), $f \equiv \rho_\sigma/\rho_X$, scales as

$$\frac{f_f}{f_i} = \left(\frac{a_f}{a_i}\right)^{2(\epsilon-3)} = \left(\frac{H_i}{H_f}\right)^{2\left(1-\frac{3}{\epsilon}\right)}, \tag{2.2}$$

where the second equality follows from Eq. (2.1). A perturbation with comoving wavenumber k will exit the horizon when, $k = a|H|$. As the universe evolves, $a|H|$ grows (for $\epsilon > 1$), taking shorter and shorter wavelengths outside the horizon. That

is, between times t_f and t_i

$$N \equiv \ln\left(\frac{a_f H_f}{a_i H_i}\right) = \left(1 - \frac{1}{\epsilon}\right) \ln\left(\frac{H_f}{H_i}\right) \tag{2.3}$$

e-foldings of scales will have exited the horizon. Combining Eqs. (2.3) and (2.2) yields

$$\frac{f_f}{f_i} = \exp\left(-2N\left(\frac{\epsilon - 3}{\epsilon - 1}\right)\right). \tag{2.4}$$

During ekpyrosis, $\epsilon > 3$, so the right side of Eq. (2.4) decreases exponentially with N, reflecting the isotropizing power of ekpyrosis. By contrast, during matter-dominated contraction, $\epsilon = 3/2$, so the right side of Eq. (2.4) *grows* exponentially with N,

$$f_f/f_i = e^{6N}. \tag{2.5}$$

This quantifies the anisotropy problem of matter-dominated contraction. Unless f_i is fantastically small, Eq. (2.5) shows that anisotropy will overtake matter after only a few e-foldings of scales have left the horizon.

Past works have simply *assumed* f_i to be small, arguing that if f_f does not exceed unity by the end of the matter-like contraction, then an ensuing phase of ekpyrotic contraction will ensure that it never does. The problem with the above logic is in assuming $f_i \sim \mathcal{O}(e^{-360})$ (if 60 e-foldings of scales are generated). For comparison, consider the flatness problem of standard Big Bang cosmology. In its most extreme version, wherein radiation-dominated expansion is assumed to begin at or near Planckian energy density, the fractional contribution of spatial curvature, $\Omega_K \propto 1/(aH)^2$, increases by a factor of $(\Omega_K)_f/(\Omega_K)_i = (\dot{a}_i/\dot{a}_f)^2 = t_f/t_i = (T_i/T_f)^2 \sim e^{146}$, where T is temperature, and for simplicity, we have assumed radiation domination all the way to present day at $T_f = 2.7K$. Thus, (for $N = 60$)[1] the anisotropy problem of the

[1]Of course, reducing N (to as low as ≈ 7.6 to satisfy the minimum required by observations [88, 69]) reduces the fine-tuning in Eq. (2.5). But doing so introduces a different kind of tuning,

matter bounce scenario is many, *many* orders of magnitude worse than the flatness problem of standard Big Bang cosmology: it involves a factor of e^{-214} more tuning.

2.3 The necessity of coupling

Without a powerful isotropizing phase before matter domination, it is clear from the last section that anisotropy quickly spoils the generation of scale-invariant modes. But suppressing anisotropy before matter domination is impossible unless the degrees of freedom responsible for the isotropizing phase are coupled to those responsible for the matter-like phase, as we now show.

Consider a universe with three components: anisotropy, pressureless matter, and a third stress-energy component, X, which will be used to suppress anisotropy. Since anisotropy grows faster than matter, suppressing anisotropy with X requires that X grows faster than both anisotropy and matter. For example, X might be an ekpyrotic field. Thereafter, this component, which begins greater than matter and grows faster than matter must somehow give way to matter. If X is decoupled from the matter, such a transition is impossible. Either X must decay directly into matter, or else it must drive the matter-like phase itself. In either case, suppressing the anisotropy imposes extreme fine-tuning requirements on the Hubble parameter, as we will show below.

The decay scenario suffers additionally from the tight constraint that the decay products must gravitate like nonrelativistic matter and nothing stiffer that might spoil a matter-like background. For example, from the reasoning of the previous section, any relativistic species, produced even in modest amounts, will grow faster than matter by a factor of $\exp(2N)$, quickly spoiling the matter-like phase. Therefore,

namely in ensuring these modes are today cosmological. That is, it is not enough to generate 7.6 e-foldings of scale-invariant modes; these modes must also be pushed far outside the horizon before the bounce– but after the matter-like phase– by some mechanism that does not amplify anisotropy, *i.e.,* ekpyrosis, but that pushes them to just the right distance so that they re-enter the horizon today. This tuning can exceed that captured by Eq. (2.5).

we will focus on the scenario without decay, presenting one realization in which X is a scalar field whose potential is specially constructed to produce both phases, first (stiff) ekpyrotic- and then (soft) matter-like contraction. We show that suppressing the anisotropy is possible only if the potential is extremely fine-tuned. Thus, the tuning of the anisotropy is traded for a tuned potential, and hence a tuned Hubble parameter.

2.4 Stiff-to-soft model

In this section, we present a toy model in which the universe undergoes a phase of ekpyrotic contraction before transitioning into matter-like contraction. The stiff-to-soft transition is possible because both phases are driven by the same scalar field, ϕ, whose potential energy density, $V(\phi)$, pictured schematically in Fig. 2.1, is specially constructed to obtain this behavior. As ϕ moves from the far right of Fig. 2.1 to the left, the universe contracts with an ekpyrotic equation of state $\epsilon_{ek} > 3$ until it crosses the kink in the middle of the figure. Thereafter, the field runs *up* the potential, driven by Hubble *anti*friction, and the universe contracts with the same equation of state as pressureless matter, $\epsilon_{md} \equiv 3/2$. As discussed, the purpose of the ekpyrotic phase is to suppress the anisotropy so that the succeeding phase remains matter-like and thereby generates a scale-invariant spectrum of adiabatic perturbations.

2.4.1 The equations of motion and the solution

The Lagrangian density is

$$\mathcal{L} = \frac{1}{2}R - \frac{1}{2}(\partial\phi)^2 - V(\phi), \tag{2.6}$$

where R is the Ricci scalar,

$$
\begin{aligned}
V(\phi) &= V_{md}(\phi) + \Theta\left(\frac{\phi-\phi_e}{\Delta\phi}\right) \times \left(V_{ek}(\phi) - V_{md}(\phi)\right), && (2.7)\\
V_{ek}(\phi) &\equiv -V_{ek}^f \exp\left(-\sqrt{2\epsilon_{ek}}(\phi-\phi_e)\right), && (2.8)\\
V_{md}(\phi) &\equiv V_{md}^i \exp\left(-\sqrt{2\epsilon_{md}}(\phi-\phi_e)\right), && (2.9)\\
\Theta(\phi) &\equiv (1+\tanh\phi)/2, && (2.10)
\end{aligned}
$$

$V_{ek}^f > 0$ is the magnitude of the potential energy density at the end of ekpyrosis, $V_{md}^i > 0$ is the magnitude of the potential energy density at the onset of matter domination, ϕ_e is the field value at which ekpyrosis transitions into matter domination, and $\Delta\phi$ sets the width of the transition. We will consider the limit of a rapid transition, namely $\Delta\phi \to 0$, so that the changeover from ekpyrosis to matter domination can be approximated by a Heaviside θ function, *i.e.,* $\Theta(\frac{\phi-\phi_e}{\Delta\phi}) \to \theta(\phi-\phi_e)$. In this limit,

$$
V(\phi) \approx \begin{cases} V_{ek}(\phi) & \text{for } \phi > \phi_e \\ V_{md}(\phi) & \text{for } \phi < \phi_e, \end{cases} \qquad (2.11)
$$

so the scalar field generates ekpyrotic contraction to the right of the kink and matter-like contraction to the left of the kink. The solution to the equations of motion,

$$
\begin{aligned}
H^2 &= \frac{1}{2}\left(\frac{1}{2}\dot{\phi}^2 + V(\phi)\right), && (2.12)\\
0 &= \ddot{\phi} + 3H\dot{\phi} + V_{,\phi}, && (2.13)
\end{aligned}
$$

is given by

$$
\begin{aligned}
a_{ek}(t) &= a_e\left(1 + (t_e - t)\sqrt{\frac{V_{ek}^f}{\epsilon_{ek}-3}}\epsilon_{ek}\right)^{1/\epsilon_{ek}} && (2.14)\\
\phi_{ek}(t) &= \phi_e + \sqrt{2\epsilon_{ek}}\ln\left(\frac{a_{ek}(t)}{a_e}\right) && (2.15)
\end{aligned}
$$

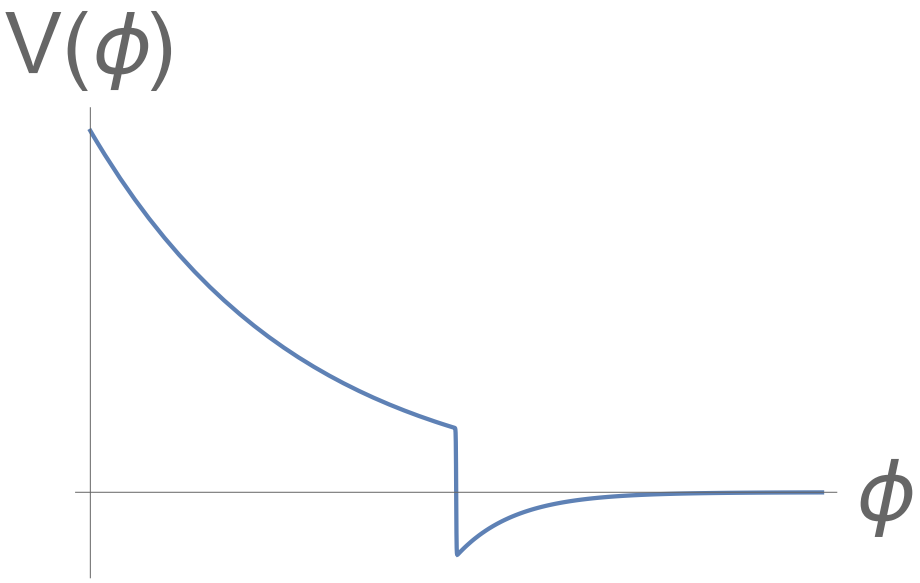

Figure 2.1: This shows the potential in Eq. (2.7). The field moves from right to left across the figure, transitioning from ekpyrotic to matter-like contraction after the kink.

for $t < t_e$ and by

$$a_{md}(t) = a_e \left(1 + (t_e - t)\sqrt{\frac{V^i_{md}}{3 - \epsilon_{md}}}\epsilon_{md}\right)^{1/\epsilon_{md}} \tag{2.16}$$

$$\phi_{md}(t) = \phi_e + \sqrt{2\epsilon_{md}} \ln\left(\frac{a_{md}(t)}{a_e}\right), \tag{2.17}$$

for $t > t_e$, where t_e is the time at which $\phi = \phi_e$, $a_e \equiv a(t_e)$, and $V^i_{md} = 3V^f_{ek}/(2(\epsilon_{ek}-3))$. Figure 2.2 shows excellent agreement between this analytic solution and a numerical solution to the equations of motion. Since the rest of this section is devoted to a derivation of this solution, the casual reader may skip to Sec. 2.5 with no loss of continuity.

2.4.2 Analytical derivation

We can gain insight into these dynamics by analyzing the equations of motion in the dimensionless "Ω-variables" (or more properly their square roots)

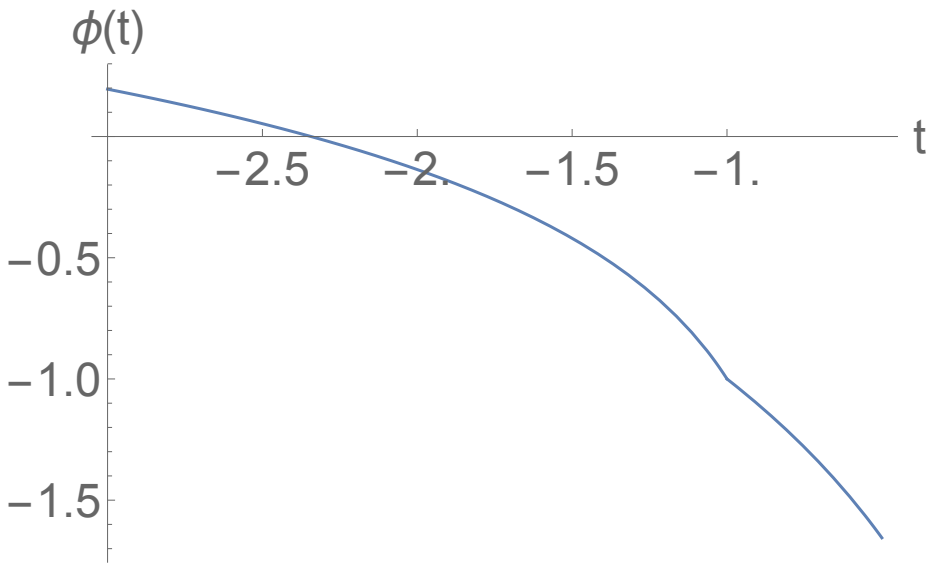

Figure 2.2: This shows a numerical solution to Eq. (2.13) superimposed over the analytic result in Eqs. (2.15) and (2.17) (where $\phi_e = t_e = -V^i_{md} = -1$, $\epsilon_{ek} = 6$, and $\Delta\phi = 10^{-4}$). The two curves are indistinguishable. For $t < t_e$, the solution is ekpyrotic, and for $t > t_e$ it is matter-like.

$(x, y) \equiv (\frac{\dot\phi}{\sqrt{6}H}, -\frac{\sqrt{|V|}}{\sqrt{3}H})$, characterizing respectively the fractional kinetic and potential energy density in the ϕ field. In these variables, the Friedmann equation, Eq. (4.10), takes the simple form $y = \sqrt{\pm(x^2 - 1)}$, where the upper sign corresponds to the case $V < 0$ as in the ekpyrotic phase and the lower sign corresponds to $V > 0$ as in the matter-like phase. Thus, during ekpyrosis, $x > 1$, and during matter domination, $x < 1$. In either case, the scalar field equation, Eq. (2.13), can be rewritten as

$$\frac{dx}{d\ln a} = 3(x^2 - 1)\left(x - \sqrt{\frac{\epsilon}{3}}\right). \tag{2.18}$$

The function on the right side of Eq. (2.18) is plotted in Fig. 2.3. There is a fixed-point, scaling solution at $x = \sqrt{\epsilon/3}$. At first, when $\epsilon = \epsilon_{ek} > 3$, this solution corresponds to the red dot in Fig. 2.3(a). If the transition is rapid (which we can ensure by taking $\Delta\phi$ small), then the function plotted in Fig. Fig. 2.3(a), which applies during the ekpyrotic phase, changes rapidly into that shown in Fig. 2.3(b), which applies during the matter-dominated phase. Since in the matter-dominated

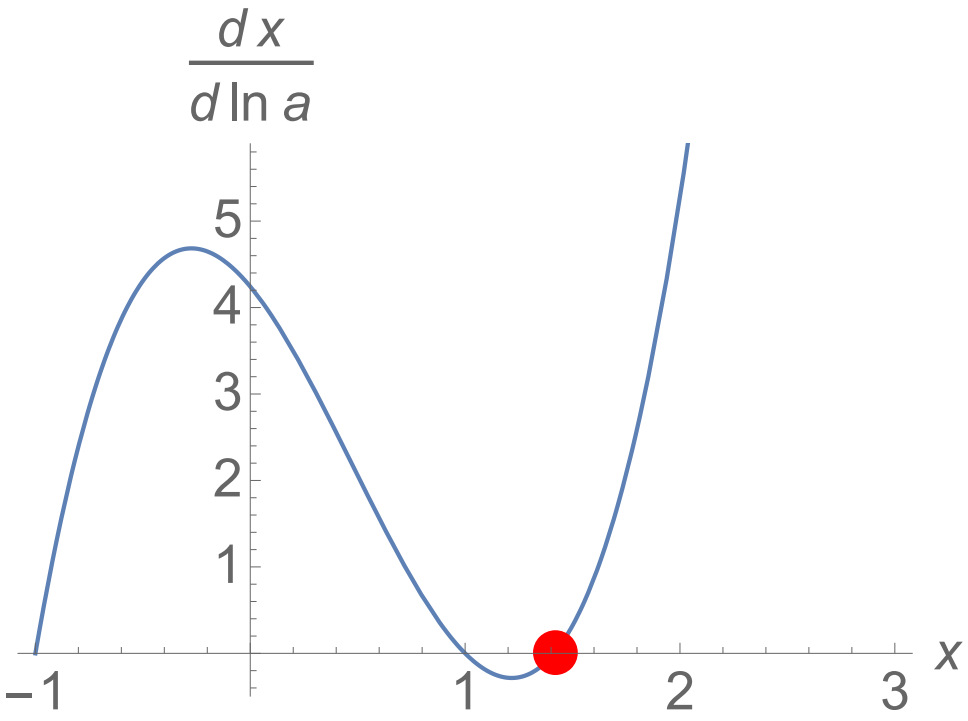

(a)

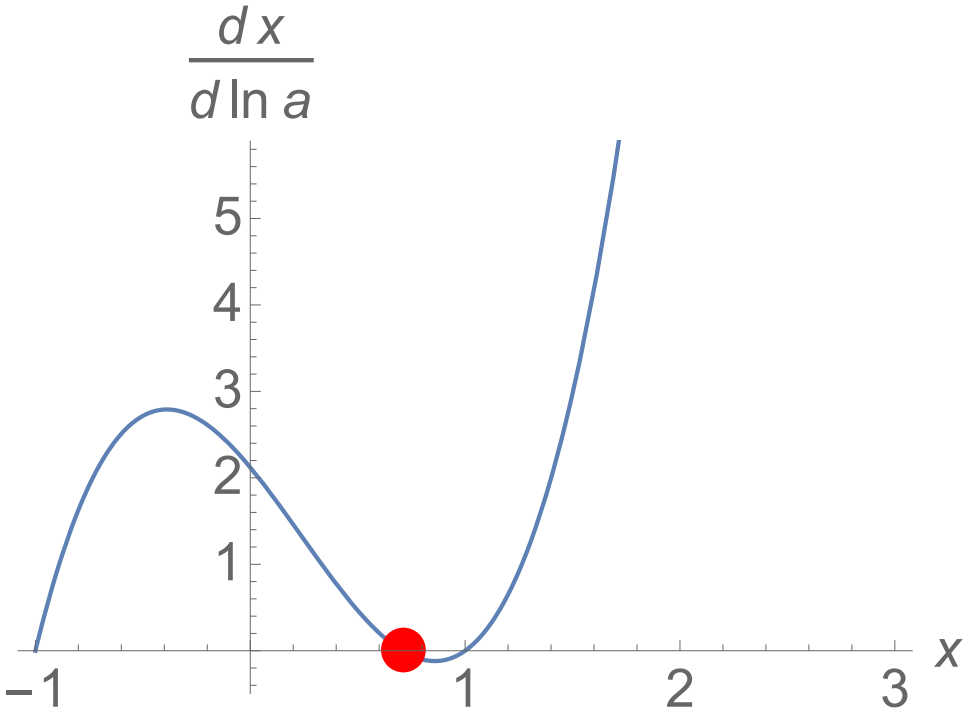

(b)

Figure 2.3: This shows the right side of Eq. (2.18) during (a) ekpyrosis (for the choice $\epsilon = 6$) and (b) matter domination ($\epsilon = 3/2$). In both cases, the fixed-point solution $x = \sqrt{\epsilon/3}$ is indicated by a red dot. In (a), the blue curve slopes upward at the fixed point, indicating stability. In (b), the blue curve slopes downward at the fixed point, indicating instability.

phase, $\epsilon = \epsilon_{md} = 3/2$, the fixed-point solution corresponding to the red dot is now at $x = 1/\sqrt{2}$. As explained in Fig. 2.3, the fixed-point solution is an attractor during ekpyrosis and a repeller during matter domination. Thus, to ensure that matter domination lasts long enough to generate 60 e-foldings of scale-invariant modes, the transition must leave the system very close to $x = 1/\sqrt{2}$. We now show how to achieve this.

Recall that t_e is the time at which ϕ crosses the kink in the potential separating ekpyrosis from matter domination. To find the matching conditions at t_e for the solutions in the two regimes, we first multiply Eq. (2.13) by $\dot{\phi}$ to obtain

$$\frac{d}{dt}\left(\frac{1}{2}\dot{\phi}^2 + V\right) = -3H\dot{\phi}^2, \tag{2.19}$$

where the last term on the left side follows from the identity $\dot{V} = V_{,\phi}\dot{\phi}$. Now we integrate over time from $t_e - \delta$ to $t_e + \delta$ and take the limit $\delta \to 0$. Assuming the right side is finite (though possibly discontinuous) in some neighborhood of the kink, this yields "conservation of energy" across the kink, *i.e.,*

$$\Delta(\dot{\phi}^2) = -2\Delta(V), \tag{2.20}$$

where $\Delta(F) \equiv F(t_e^+) - F(t_e^-)$ for any function $F(t)$. Note that this implies continuity of ϕ and H across the kink. There is, however, a discontinuity in $\dot{\phi}$: the kinetic energy of the field is reduced by the height of the kink.

Therefore, to ensure that the transition carries the ekpyrotic solution at $x_{before} = \sqrt{\epsilon_{ek}/3}$ to the matter-like solution at $x_{after} = \sqrt{\epsilon_{md}/3}$, the height, ΔV, of the kink must be chosen to satisfy

$$\frac{1}{\sqrt{2}} \stackrel{!}{=} x_{after} = \frac{\dot{\phi}_{after}}{\sqrt{6}H^f_{ek}} = \sqrt{x^2_{before} - \frac{\Delta V}{3(H^f_{ek})^2}}. \tag{2.21}$$

Since $(H^f_{ek})^2 = V^f_{ek}/(3(x^2_{before} - 1))$ and $x_{before} = \sqrt{\epsilon_{ek}/3}$, this gives $\Delta V = (1 + \frac{3}{2(\epsilon_{ek}-3)})V^f_{ek}$ or

$$V^i_{md} = \frac{3}{2(\epsilon_{ek} - 3)} V^f_{ek}, \tag{2.22}$$

as claimed below Eq. (2.17).

2.5 Analysis of fine-tuning

We have constructed a cosmological model in which soft (pressureless) matter overtakes stiff (ekpyrotic) matter. This is necessary for the matter bounce scenario to explain the initial smallness of the anisotropy at the onset of the matter-like phase. Unfortunately, as we will now show, small anisotropy requires an extremely fine-tuned potential.

First, note that generating N_{md} e-foldings of scales during the matter-like phase immediately requires

$$V^f_{md}/V^i_{md} = \exp\left(6N_{md}\right). \tag{2.23}$$

or equivalently, that $|H|$ must grow during the matter-like phase by a factor $\exp\left(3N_{md}\right)$. Although we have modeled the pressureless matter as a scalar field, it is clear from Eq. (2.3) that this growth in Hubble is independent of the nature of the pressureless matter (so long as it can support density fluctuations, *e.g.*, a scalar field with the same equation of state as matter). During this period, recall from Eq. (2.5) that the fractional energy density in anisotropy will have grown by a factor of $\exp\left(6N_{md}\right)$. Therefore, the preceding ekpyrotic phase must suppress anisotropy by at least this much. This requires

$$V^f_{ek}/V^i_{ek} > \exp\left(\frac{6N_{md}}{1 - \frac{3}{\epsilon_{ek}}}\right), \tag{2.24}$$

or equivalently that $|H|$ must grow by a factor of at least $\exp(3N_{md})$ during the ekpyrotic phase. Therefore, combining Eqs. (2.23) and (2.24) with Eq. (2.22), we find that from the beginning of the ekpyrotic phase to the end of the matter-like phase, the potential must grow by many orders of magnitude such that

$$V_{md}^f/V_{ek}^i > \frac{3}{2(\epsilon_{ek}-3)} \exp\left(\left(12+\frac{18}{\epsilon_{ek}-3}\right)N_{md}\right), \tag{2.25}$$

or equivalently, that $|H|$ must grow by a factor $\exp(6N_{md})$. This is independent of the nature of the degrees of freedom driving ekpyrosis. Thus, we have shown that resolving the anisotropy problem requires an extremely fine-tuned potential.

2.6 Discussion

In this chapter, we have emphasized some of the difficulties imposed by the anisotropy problem on the matter bounce scenario. Collecting the model-independent observations of the previous section, these are:

1. Generating N_{md} e-foldings scale-invariant modes with matter-like contraction requires that H change by $\approx 2.6N_{md}$ orders of magnitude. During such a phase, the fractional energy density in anisotropy grows by twice as many orders of magnitude, $\approx 5.2N_{md}$.

2. Therefore, without a powerful suppression mechanism *before* the matter-like contraction, anisotropy rapidly overtakes the matter, thereby spoiling the background required for the scale-invariant spectrum. Previous arguments invoking an isotropizing phase *after* the anisotropy has already grown by this exponentially large factor are analogous to invoking present-day dark energy as a resolution to the flatness problem of standard Big Bang cosmology.

3. If ekpyrosis is that suppression mechanism, any implementation will require another phase during which H changes by another $2.6N_{md}$ orders of magnitude. It will also require that soft, pressureless matter somehow overtake stiff, ekpyrotic matter. This is impossible unless the degrees of freedom responsible for ekpyrotic contraction are coupled somehow to the pressureless matter. (In the toy model presented here, in which both the stiff and the soft phases result from the same scalar field, this requires fine-tuning a potential over $5.2N_{md}$ orders of magnitude with a kink of just the right height in between. The only other possibility is to arrange for direct decay of an ekpyrotic field into pressureless matter, which introduces the additional problems discussed in Sec. 2.3.)

Other attempted resolutions to the problem of small initial anisotropy, involving high-energy, nonlinear modifications to the gravitational action [89] or to the equation of state of matter after the matter-like phase [87], suffer from the same fine-tuning constraint discussed in Sec. 2.2: it is too late. Anisotropy must be exponentially suppressed by the onset of the matter-dominated phase. This was appreciated in Ref. [87].

Having discussed the anisotropy problem, it is worthwhile to consider the other big challenge for the matter bounce scenario, which was discussed in Sec. 2.1, namely the overproduction of tensor fluctuations during the matter-like phase. For a wide class of single-field models, it has been argued [79, 80] that satisfying current limits on the tensor-to-scalar ratio requires violating current limits on primordial non-Gaussianities. This conclusion applies quite generally to any non-singular bouncing model in which 1) the matter-like contraction is due to a single (not necessarily canonical) scalar field, 2) the same scalar field allows for the violation of the null energy condition required to produce the nonsingular bounce, 3) the fluctuations are sourced from Bunch-Davies vacuum, and 4) general relativity holds at all scales. This seriously constrains the viability of matter bounce cosmology. The only remaining

models must violate one or more of these quite general assumptions, for example through the inclusion of multiple fields (as in the matter bounce curvaton mechanism [81]) or through modifications to Einstein gravity (as in *e.g.,* [90, 91, 82, 92]). Both approaches spoil the aesthetic advantage of requiring only a single, simple extra degree of freedom. Given these phenomenological challenges and in light of the anisotropy problem– which plagues even these modified versions– the matter bounce scenario is not very promising.

Chapter 3

Scale-invariant perturbations in ekpyrotic cosmologies without fine-tuning of initial conditions

Parts of this chapter were published in Ref. [66] in collaboration with Dr. Anna Ijjas and Professor Paul Steinhardt.

3.1 Introduction

To recapitulate, in chapter 1 we explained that a prime motivation for studying contracting universes is that they naturally resolve the fine-tuning problems of standard big bang cosmology. In chapter 2, we examined a subset of contracting universes with the additional feature that they naturally generate the observed (nearly) scale-invariant spectrum of primordial fluctuations. We showed that these "matter bounce scenarios" come at a price because they introduce a new fine-tuning problem that is many orders of magnitude worse than the standard fine-tuning problems: in these scenarios, anisotropy rapidly grows to dominate the energy budget of the universe, spoiling the equation of state responsible for the fluctuations and leading ultimately

to chaotic mixmaster behavior. We argued that the only salvation for such scenarios is to invoke an ekpyrotic phase beforehand, since ekpyrosis suppresses anisotropy. This same instability to anisotropy applies quite generally, not just to matter-dominated contraction, but to any contracting phase driven by stress-energy components with softer equations of state than that of anisotropy. In light of this, the remainder of this thesis will explore ekpyrotic cosmologies in greater detail.

Ekpyrotic bouncing cosmologies are designed to smooth and flatten the universe via a matter component whose energy density grows to dominate all other forms of stress-energy, including inhomogeneities, spatial curvature, and most importantly anisotropy (see Eq. (2.4) with $\epsilon > 3$) [47]. The universe undergoes an ultra-slow contraction such that quantum fluctuations in the ekpyrotic energy component, ρ_ϕ, that drives the contraction exit the Hubble radius (see Eq. (2.3) with $\epsilon > 3$). A key question is whether these superhorizon quantum fluctuations can explain the observed, scale-invariant spectrum without introducing additional fine-tuning problems.

The earliest models of ekpyrosis involving a single scalar field cannot; they produce an adiabatic spectrum with a strong blue tilt [93, 94, 95, 96, 97] that is inconsistent with observations. The best known ekpyrotic models that produce the observed fluctuations involve two scalar fields. In these examples, the potentials are chosen such that the universe contracts with an ekpyrotic equation of state while simultaneously, vacuum-sourced entropy fluctuations exit the Hubble radius with a scale-invariant spectrum. After the ekpyrotic smoothing phase, these perturbations convert via a curvaton-like "entropic mechanism" into a scale-invariant spectrum of adiabatic perturbations [58, 98, 99, 100, 101]. In the first examples of this kind, the background cosmological solution describing the evolution of the two fields along the potential energy surface is unstable, which means finely tuned initial conditions are required to begin the ekpyrotic phase [102, 103, 104, 105]. Tolley and Wesley studied a wide range of ekpyrotic models and suggested that this problem may be generic [106], namely

that generating a scale-invariant spectrum of adiabatic or entropic fluctuations is only possible if the ekpyrotic phase begins with finely tuned initial conditions. Their argument hinged on a phase plane analysis which revealed that the background solutions are not attracted to a fixed point. From this, they concluded that the scenario suffers from a sensitivity to initial conditions. If true, this argument represents a serious blow to bouncing cosmologies because it implies that ekpyrosis cannot resolve the standard puzzles without introducing another fine-tuning problem of its own.

In this chapter, we present simple ekpyrotic models that generate a scale-invariant, nearly Gaussian spectrum of density perturbations but do *not* require fine-tuning of initial conditions. Although these models belong in the class considered by Tolley and Wesley, we show that the background solutions are attracted to a fixed curve along which scale-invariant fluctuations are generated. The existence of such a fixed curve is sufficient to ensure that the observational predictions are insensitive to the choice of initial conditions. In other words, being attracted to a fixed point is not necessary to avoid fine-tuning.

In Section 3.2, we summarize the general argument that suggests the need for finely tuned initial conditions. In Section 3.3, we review a simple ekpyrotic model for which we find a fixed-curve but no fixed-point attractor. In Section 3.4, we describe how to construct more general examples that also avoid the need for fine-tuning of initial conditions. Finally, we discuss the implications for cosmology.

3.2 Scaling solutions, scale-invariance and instability

Scaling solutions are solutions to the equations of motion for which there exists a set of field variables such that all contributions (treating the kinetic and potential energy densities as distinct) to the total energy density scale identically with time, keeping their fractional contributions constant. Scaling background solutions are particularly

important because they are exactly solvable and can yield a scale-invariant spectrum of perturbations.

In Ref. [106], Tolley and Wesley presented an instability argument that applies to contracting, ekpyrotic, scaling solutions derived from two-derivative, two-field actions

$$S = \int d^4x\sqrt{-g}\left(\frac{1}{2}R - \sum_{a,b=1}^{2}\frac{1}{2}G^{ab}(\Phi)g^{\mu\nu}\partial_\mu\Phi_a\partial_\nu\Phi_b - V(\Phi)\right) \tag{3.1}$$

that possess a continuous symmetry generated by a parameter κ such that

$$\frac{d\Phi_a}{d\kappa} = \xi_a(\Phi), \quad g_{\mu\nu} \to e^{\kappa}g_{\mu\nu}, \quad S \to e^{\kappa}S. \tag{3.2}$$

Here $g_{\mu\nu}$ is the spacetime metric with $(-+++)$ signature convention, R is the Ricci scalar, $\xi_a(\Phi)$ is a function of two scalar fields $\Phi = \{\Phi_a\}$ where $a = 1, 2$, G^{ab} is the metric on field space, and $V(\Phi)$ is the potential energy density; reduced Planck units ($8\pi G_N = 1$ where G_N is Newton's gravitational constant) are used throughout. This symmetry guarantees the existence of a set of field variables $(\Phi_1, \Phi_2) \mapsto (\phi, \sigma)$ such that the Lagrangian density can be rewritten as

$$\mathcal{L} = \frac{1}{2}R - \frac{1}{2}(\partial\sigma)^2 - \frac{1}{2}f(\sigma)(\partial\phi)^2 - V_0e^{-c\phi}h(\sigma), \tag{3.3}$$

where c is a real constant, and $V_0 < 0$ (that is, the ekpyrotic potential $V(\phi, \sigma)$ is negative). Along the background solution, $f(0) = h(0) = 1$ and $\sigma = 0$.

It proves useful to introduce the dynamical variables

$$(w, x, y, z) \equiv \left(\frac{\sqrt{f(\sigma)}\phi'}{\sqrt{6}\mathcal{H}}, \frac{\sigma'}{\sqrt{6}\mathcal{H}}, -\frac{a\sqrt{-V_0h(\sigma)}e^{-\frac{c}{2}\phi}}{\sqrt{3}\mathcal{H}}, \sigma\right) \tag{3.4}$$

where τ is conformal time running from large negative to small negative values, a prime denoting a derivative with respect to conformal time, a is the scale factor, and

$\mathcal{H} \equiv a'/a$ is the conformal Hubble parameter. The four variables are dimensionless using reduced Planck units. With these variables, the Friedmann-Robertson-Walker (FRW) equations of motion become

$$w_{,N} = 3(w^2+x^2-1)\left(w - \frac{c}{\sqrt{6f(z)}}\right) - \sqrt{\frac{3}{2}}\frac{f_{,z}}{f(z)}xw, \tag{3.5}$$

$$x_{,N} = 3(w^2+x^2-1)\left(x + \frac{1}{\sqrt{6}}\frac{h_{,z}}{h(z)}\right) + \sqrt{\frac{3}{2}}\frac{f_{,z}}{f(z)}w^2, \tag{3.6}$$

$$z_{,N} = \sqrt{6}x. \tag{3.7}$$

Here we introduced the dimensionless time variable $N \equiv \ln a$ that denotes the number of e-folds of ekpyrotic contraction and runs from large positive to small positive values. We eliminated y using the Friedmann constraint

$$w^2 + x^2 - y^2 = 1. \tag{3.8}$$

The equation of state takes the simple form

$$\epsilon \equiv 1 - \frac{\mathcal{H}'}{\mathcal{H}^2} = 3(w^2+x^2). \tag{3.9}$$

From the Friedmann constraint, we also see that the square of each variable w, x, and y is a fractional contribution to the total energy density: w^2 is the ϕ-kinetic energy; x^2 is the σ-kinetic energy; and y^2 is the potential energy. The equation-of-state parameter ϵ is the sum of kinetic energies.

As can be verified by direct substitution, the background Eqs. (3.5)-(3.7) admit a fixed-point solution,

$$(w,x,y,z) = \left(\frac{c}{\sqrt{6}}, 0, \sqrt{\frac{c^2}{6}-1}, 0\right), \tag{3.10}$$

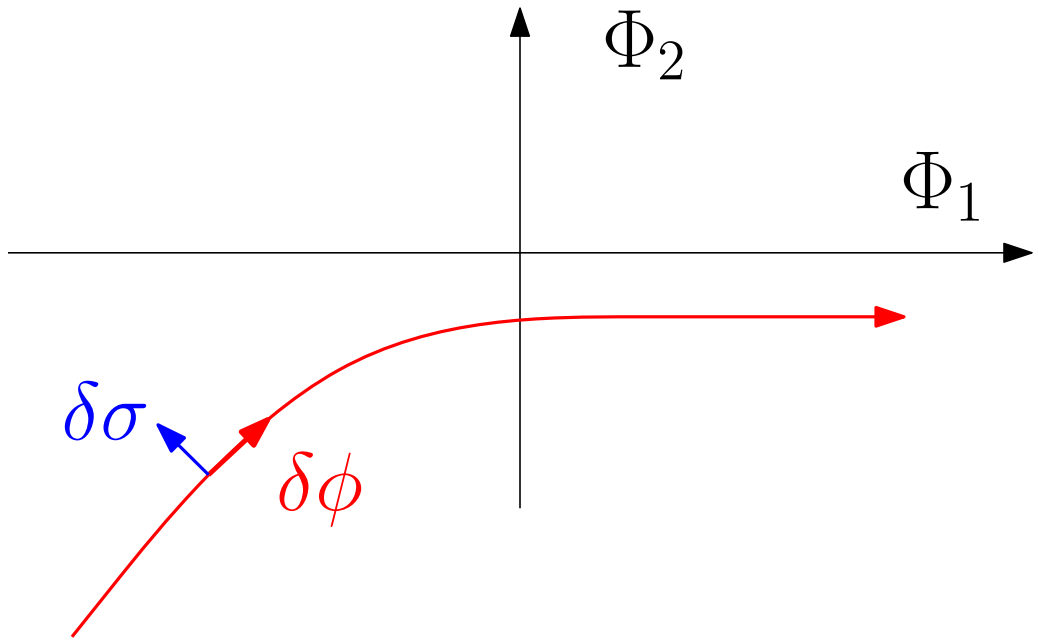

Figure 3.1: **A schematic trajectory of a solution through field-space:** The field variables (ϕ, σ) were constructed so that, along the field-space trajectory in Eq. (3.10), only ϕ varies and $\sigma = 0$. Perturbations $\delta\phi$ are tangent to the trajectory and are adiabatic; perturbations $\delta\sigma$ are orthogonal to the trajectory and are entropic.

in which $\sigma = 0$ and only ϕ is changing, provided the constraint $h_{,\sigma}(0) = -c^2 f_{,\sigma}(0)/(c^2 - 6)$. Obviously, this is a scaling solution since any fractional contribution to the total energy density, w^2, x^2, and y^2, is constant.

The cosmological background solutions correspond to a field-space trajectory like the one shown in Fig. 3.1. Perturbations of this trajectory can be decomposed into those along the red curve (*adiabatic* perturbations) and perpendicular to it (*entropic* perturbations).

The instability argument connects the stability of the solution in Eq. (3.10) with the spectral indices of its perturbations. The basic idea makes use of the fact that, since $z \equiv \sigma = 0$ in the background solution, the second order action and, hence, the perturbation spectra derived from it are determined by a few parameters

$$\{c; f_{,\sigma}(0); f_{,\sigma\sigma}(0); h_{,\sigma\sigma}(0)\}. \tag{3.11}$$

Linearized around the fixed point in Eq. (3.10), the background Eqs. (3.5)-(3.7) reduce to a matrix equation, where the parameters in Eq. (3.11) determine the eigenvalues of the matrix. Tolley and Wesley's analysis showed that any combination of the parameters in Eq. (3.11) that results in a scale-invariant spectrum of perturbations (entropic or adiabatic) renders the background solution dynamically unstable to perturbations in the sense that the matrix associated with the linearized system has at least one negative eigenvalue. In a contracting universe, a negative eigenvalue means a dynamically unstable direction in $(w - x - z)$ space.

An example is given by the Lagrangian density

$$\mathcal{L} = \frac{1}{2}R - \frac{1}{2}(\partial\Phi_1)^2 + \frac{1}{2}(\partial\Phi_2)^2 - \tilde{V}_0 e^{-c_1\cdot\Phi_1} - \tilde{V}_0 e^{-c_2\cdot\Phi_2}, \tag{3.12}$$

where c_1, c_2 are positive-definite constants and $\tilde{V}_0 < 0$. The corresponding FRW equations of motion admit a scaling solution with $\Phi_i = A_i \ln|\tau| + B_i$ and $c_1 A_1 = c_2 A_2$ that has been shown [98, 99] to generate a scale-invariant spectrum of entropic perturbations. According to the instability argument, it should have an unstable background which in this simple case ($G_{ab} = \delta_{ab}$) can be depicted as in Fig. 3.2.

For the purpose of illustration, we briefly outline how the instability emerges from a negative eigenvalue of the linearized system. The change of variables,

$$\phi = \frac{c_2\Phi_1 + c_1\Phi_2}{\sqrt{c_1^2 + c_2^2}}, \tag{3.13}$$

$$\sigma = \frac{c_1\Phi_1 - c_2\Phi_2}{\sqrt{c_1^2 + c_2^2}} + \sigma_0 \tag{3.14}$$

with $\sigma_0 = 2\ln(c_2/c_1)/(c_1^2 + c_2^2)$, brings the Lagrangian density in Eq. (3.12) to the form of Eq. (3.3). The coupling function to the kinetic energy of ϕ, $f(\sigma)$, and the

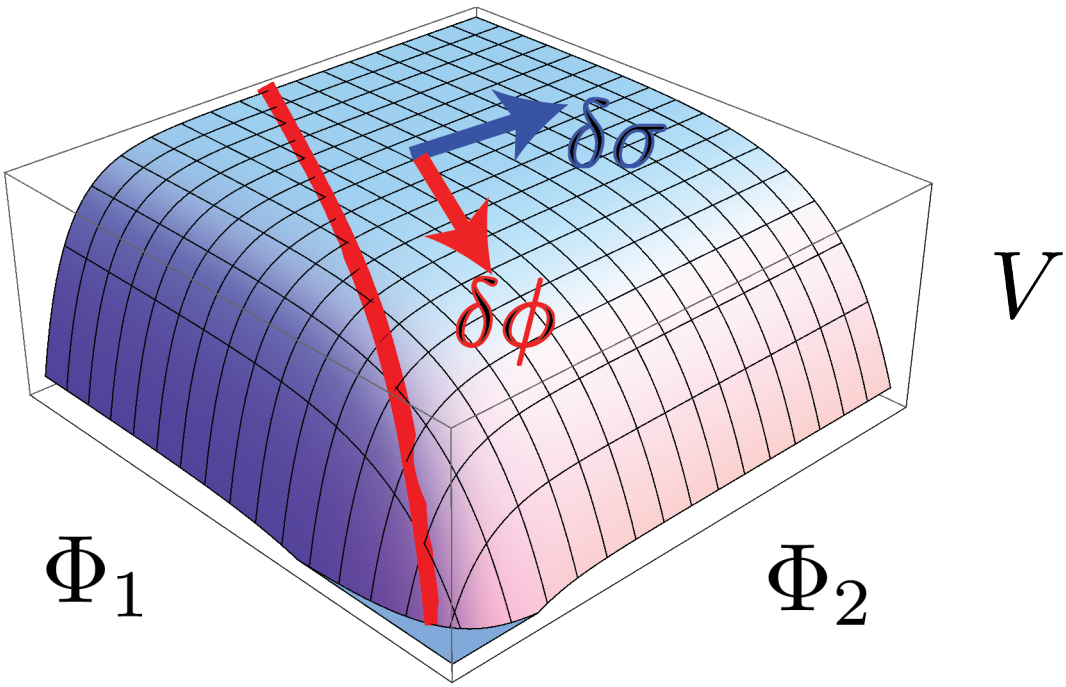

Figure 3.2: **The instability of the scaling solution corresponding to the action in Eq.** (3.12): The background cosmological solution corresponds to a trajectory along the ridge of the potential as indicated by the red arrow and red curve. Quantum fluctuations along the trajectory produce a blue spectrum of adiabatic perturbations and fluctuations normal to the trajectory produce a scale-invariant spectrum of entropic perturbations. After the ekpyrotic phase, the entropic perturbations convert into adiabatic perturbations due to the bending of the trajectory curve (not shown here). The fact that the background trajectory is a ridge means that it is unstable if the initial conditions are sufficiently far from the ridge.

coupling function to the potential energy of ϕ, $h(\sigma)$, are given by

$$f(\sigma) = 1, \tag{3.15}$$

$$h(\sigma) = 1 + \frac{c^2}{2}\sigma^2 + \mathcal{O}(\sigma^3), \tag{3.16}$$

and the parameters, c and V_0 are defined such that

$$\frac{1}{c^2} = \frac{1}{c_1^2} + \frac{1}{c_2^2}, \tag{3.17}$$

$$V_0 = \left(\left(\frac{c_2}{c_1}\right)^{\frac{2c_1^2}{c_1^2+c_2^2}} + \left(\frac{c_1}{c_2}\right)^{\frac{2c_2^2}{c_1^2+c_2^2}} \right) \tilde{V}_0. \tag{3.18}$$

Linearizing the background Eqs. (3.5)-(3.7) about the fixed point in Eq. (3.10), the perturbations $(\delta w, \delta x, \delta z) \equiv (w - \frac{c}{\sqrt{6}}, x, z)$ satisfy

$$\begin{pmatrix} \delta w_{,N} \\ \delta x_{,N} \\ \delta z_{,N} \end{pmatrix} = M \cdot \begin{pmatrix} \delta w \\ \delta x \\ \delta z \end{pmatrix} \tag{3.19}$$

with M defined as

$$M \equiv \begin{pmatrix} \frac{1}{2}(c^2-6) & 0 & 0 \\ 0 & \frac{1}{2}(c^2-6) & \frac{c^2(c^2-6)}{2\sqrt{6}} \\ 0 & \sqrt{6} & 0 \end{pmatrix}. \tag{3.20}$$

The eigenvalues of M are $(c^2-6)/2$ and $(c^2-6) \pm \sqrt{9c^4 - 60c^2 + 36}/4$. Note that the smallest eigenvalue is negative for ekpyrosis, as is clear from substituting Eq. (3.10) into the equation of state, Eq. (3.9): $\epsilon > 3$ requires $c > \sqrt{6}$. Therefore, as the universe contracts, N decreases, and perturbations along the eigenvector corresponding to the negative eigenvalue grow so that the system is carried away from the fixed-point solution in Eq. (3.10). In this case, the negative eigenvalue means that the initial conditions for the fields must be fine-tuned to lie close to the trajectory or else the fields will evolve far-off course as illustrated in Fig. 3.2.

3.3 Ekpyrosis and scale-invariance without fine tuning

In this section, we describe the case where the negative eigenvalue exists but is physically irrelevant. As we will show, the occurrence of the negative eigenvalue only means that the attractor is a fixed curve rather than a fixed point.

We consider the Lagrangian density first discussed by Li in Ref. [107],

$$\mathcal{L} = \frac{1}{2}R - \frac{1}{2}(\partial\psi)^2 - \frac{1}{2}e^{-\lambda\psi}(\partial\chi)^2 - \tilde{V}_0 e^{-\lambda\psi}, \tag{3.21}$$

where λ is positive and $\tilde{V}_0 < 0$. The model involves an ekpyrotic field, ψ, with a negative potential, similar to ordinary, single-field ekpyrosis. The novel feature is the non-canonical, exponential coupling to the massless spectator field, χ. We begin with the simple case where $V(\psi) = 0$. This corresponds to the borderline ekpyrotic equation of state $\epsilon = 3$. Then, we generalize to $V(\psi) \neq 0$ ($\epsilon > 3$) and provide a full, analytic treatment.

3.3.1 $V(\psi) = 0$

The basic idea is captured in Fig. 3.3(a), which illustrates background trajectories corresponding to different initial conditions in the space $(\tilde{w}, \tilde{x}, \tilde{y}^{\,0}, \tilde{z}) \equiv$

$$\left(\frac{\psi'}{\sqrt{6}\mathcal{H}}, \frac{e^{-\frac{\lambda}{2}\psi}\chi'}{\sqrt{6}\mathcal{H}}, \cancelto{0}{-\frac{a\sqrt{-\tilde{V}_0}e^{-\frac{\lambda}{2}\psi}}{\sqrt{3}\mathcal{H}}}, e^{-\frac{\lambda}{2}\psi}(\chi - \chi_0) \right). \tag{3.22}$$

We use the superscript $\sim$ to distinguish quantities expressed in (ψ, χ) variables from those expressed in the special (ϕ, σ) variables that were used to derive the original instability argument.

Any set of initial conditions for a, ψ, ψ', χ, and χ' corresponds to a particular point on the cylinder. The background solution follows the blue arrow originating at this point. There are two special initial conditions at the points $(\tilde{w}, \tilde{x}, \tilde{z}) = (\pm 1, 0, 0)$; the one with the $+$ sign corresponds to the red arrow in Fig. 3.3(a). These two points are special because the blue arrows vanish here; *i.e.,* if the background solution starts here, it stays here. Hence, these are fixed-point solutions.

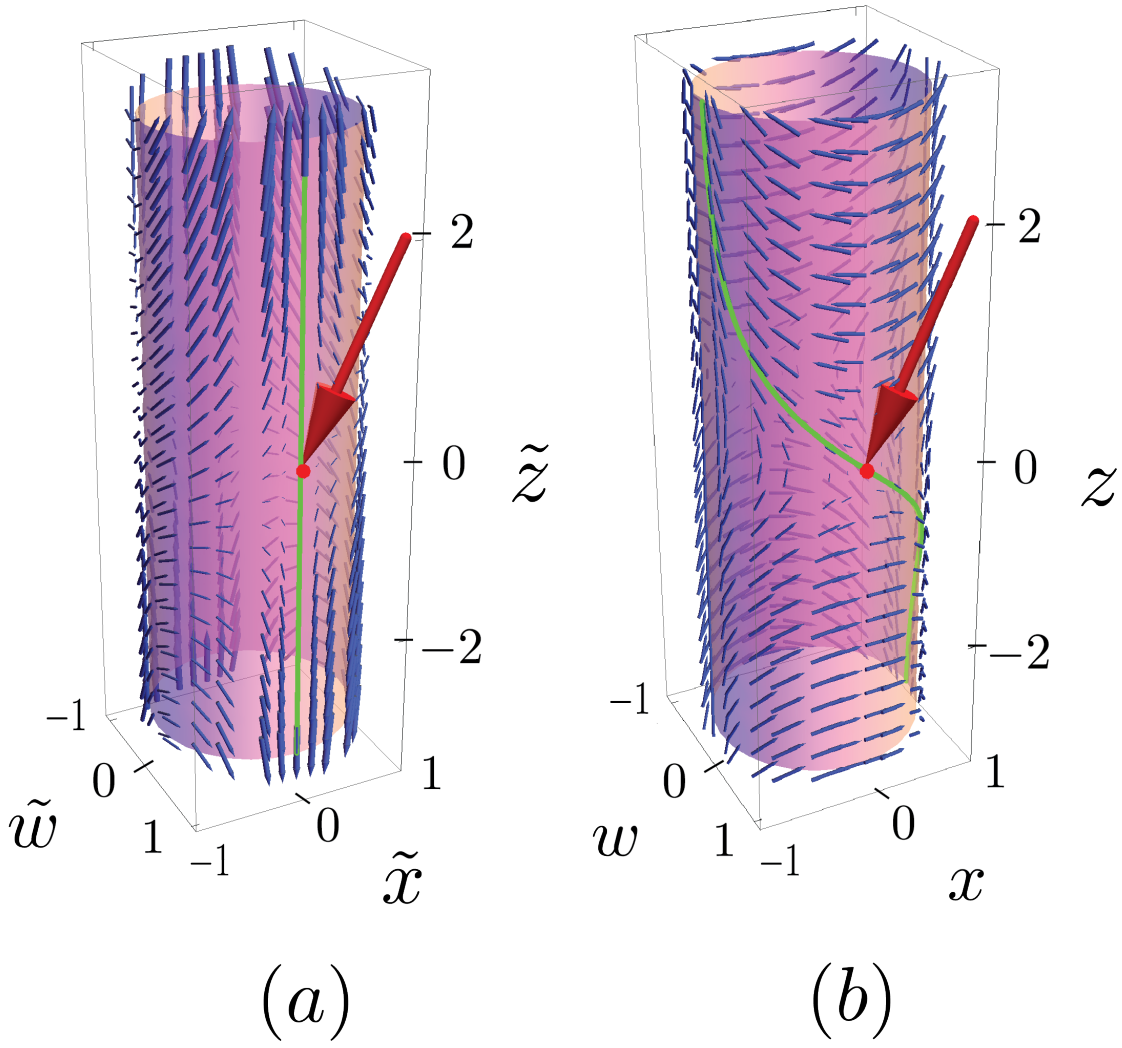

Figure 3.3: The Lagrangian density in Eq. (3.21) with $V = 0$ and $\lambda = \sqrt{6}$: Green curves and red arrows map onto each other according to the transformations in Eqs. (3.38)-(3.41). Solutions follow the blue arrows. (a) **The trajectories in (ψ, χ) variables:** For $\tilde{y} = 0$, $(\tilde{w}, \tilde{x}, \tilde{z}) \equiv \left(\psi'/(\sqrt{6}\mathcal{H}), e^{-\frac{\lambda}{2}\psi}\chi'/)\sqrt{6}\mathcal{H}), e^{-\frac{\lambda}{2}\psi}(\chi - \chi_0)\right)$. The green curve is the fixed-curve attractor $(\tilde{w}, \tilde{x}, \tilde{z}) = (1, 0, \tilde{z})$. The red arrow points to the fixed point $(\tilde{w}, \tilde{x}, \tilde{z}) = (1, 0, 0)$. (b) **The trajectories in (ϕ, σ) variables:** For $y = 0$, $(w, x, z) \equiv \left(\sqrt{f(\sigma)}\phi'/(\sqrt{6}\mathcal{H}), \sigma'/(\sqrt{6}\mathcal{H}), \sigma\right)$. The green curve, $(w, x, z) = \left(\mathrm{sech}(\frac{\lambda}{2}z), -\tanh(\frac{\lambda}{2}z), z\right)$, is the fixed-curve attractor. The red arrow points to the fixed point $(w, x, z) = (1, 0, 0)$.

For any other initial conditions, (*i.e.,* any other point on the cylinder), the blue arrows carry the background solution toward the green curve. The green curve is therefore a strong attractor for generic initial conditions. Henceforth, we call such an attractor curve a "fixed-curve attractor." Solutions evolving along this curve are scaling solutions since $\tilde{w}, \tilde{x}$, and $\tilde{y}$ are constant. They describe a universe dominated by the kinetic energy of the adiabatic field, ψ; the entropic field, χ, is constant. For the case ($\lambda = \sqrt{6}$) depicted in Fig. 3.3, these solutions can be shown to generate a scale-invariant spectrum of perturbations in the entropic field, χ.

As for the negative eigenvalue associated with the linearized equations of motion, in the cases discussed in this chapter, it only indicates the existence of a fixed-curve attractor instead of a fixed-point attractor. The existence of a fixed-curve attractor means there is no need for fine-tuning of initial conditions.

One can describe the same dynamics in the special (ϕ, σ) variables (see Fig. 3.3(b)). Since the Lagrangian density in Eq. (3.21) has the shift symmetry of Eq. (3.2) assumed by the instability argument, it can be put into the form of Eq. (3.3) through a variable transformation $(\psi, \chi) \mapsto (\phi, \sigma)$,

$$\psi = \phi + \frac{2}{\lambda} \ln \left[\operatorname{sech} \left(\frac{\lambda \sigma}{2} \right) \right] + \psi_0, \tag{3.23}$$

$$\chi = \frac{2}{\lambda} e^{\frac{\lambda}{2}(\phi + \psi_0)} \tanh \left(\frac{\lambda \sigma}{2} \right) + \chi_0, \tag{3.24}$$

where ψ_0 is a real constant (see Appendix A). Substituting this transformation into Eq. (3.21) yields the Lagrangian density in Eq. (3.3) with $f(\sigma) = h(\sigma) = \cosh^2(\frac{\lambda\sigma}{2})$ and $c = \lambda$. The two Lagrangian densities describe the same theory in different field variables: the cylinder on the right is a twisted version of the one on the left. It is clear from the blue arrows that the green curve in Fig. 3.3(b) is an attractor, just like the green curve in Fig. 3.3(a). Solutions along the green-curve attractor generate a scale-invariant spectrum of entropic perturbations.

3.3.2 $V(\psi) \neq 0$

We extend our analysis to the more general form of the Lagrangian density in Eq. (3.21) that applies both to $V(\psi) = 0$ and to $V(\psi) \neq 0$.

Extremizing the action with respect to variations of the fields (ψ, χ) yields the field equations

$$\psi'' + 2\mathcal{H}\psi' - \lambda \tilde{V}_0 e^{-\lambda\psi} a^2 + \frac{\lambda}{2} e^{-\lambda\psi} \chi'^2 = 0, \tag{3.25}$$

$$\chi'' + 2\mathcal{H}\chi' - \lambda\psi'\chi' = 0. \tag{3.26}$$

The Friedmann constraint is

$$\mathcal{H}^2 = \frac{1}{6}\left(\psi'^2 + e^{-\lambda\psi}\chi'^2 + 2a^2\tilde{V}_0 e^{-\lambda\psi}\right). \tag{3.27}$$

Using the variables defined in Eq. (3.22), these equations can be recast as the autonomous, dynamical system

$$\tilde{w}_{,N} = 3(\tilde{w}^2 + \tilde{x}^2 - 1)\left(\tilde{w} - \frac{\lambda}{\sqrt{6}}\right) - \sqrt{\frac{3}{2}}\lambda\tilde{x}^2, \tag{3.28}$$

$$\tilde{x}_{,N} = 3\tilde{x}(\tilde{w}^2 + \tilde{x}^2 - 1) + \sqrt{\frac{3}{2}}\lambda\tilde{w}\tilde{x}, \tag{3.29}$$

$$\tilde{z}_{,N} = -\sqrt{\frac{3}{2}}\lambda\tilde{w}\tilde{z} + \sqrt{6}\tilde{x}. \tag{3.30}$$

If $V \neq 0$, this system admits three fixed-point solutions at $(\tilde{w}, \tilde{x}, \tilde{y}, \tilde{z}) =$

$$(-1, 0, 0, 0)\,, \tag{3.31}$$

$$(+1, 0, 0, 0)\,, \tag{3.32}$$

$$\left(\frac{\lambda}{\sqrt{6}}, 0, \sqrt{\frac{\lambda^2}{6} - 1}, 0\right), \tag{3.33}$$

all of which are unstable (*i.e.,* associated with a negative eigenvalue). The third fixed-point solution given by Eq. (3.33) bisects two fixed-*curve* solutions

$$(\tilde{w}, \tilde{x}, \tilde{y}, \tilde{z}) = \left(\frac{\lambda}{\sqrt{6}}, 0, \sqrt{\frac{\lambda^2}{6} - 1}, \pm \tilde{Z} \right) \tag{3.34}$$

with $\tilde{Z} \propto e^{-\frac{\lambda^2}{2} N}$, that generate a scale-invariant spectrum of entropic perturbations, as shown in Ref. [107].

If $V = \tilde{y} = 0$, λ^2 must be 6 in order for the fixed point in Eq. (3.33) to be a solution. For $\lambda = \sqrt{6}$, this coincides with the fixed point in Eq. (3.32) and corresponds to the red arrow shown in Fig. 3.3(a); Eq. (3.34) parameterizes the vertical, green, fixed-curve attractor.

Changing variables $(\psi, \chi) \mapsto (\phi, \sigma)$ as defined in Eqs. (3.23) and (3.24), the Lagrangian density in Eq. (3.21) takes the form of Eq. (3.3) with $f(\sigma) = h(\sigma) = \cosh^2\left(\frac{\lambda}{2}\sigma\right), c = \lambda$, and $V_0 = \tilde{V}_0 e^{-\lambda\psi_0}$. Repeating the same analysis in the new variables defined in Eq. (3.4), the equations of motion become

$$w_{,N} = 3(w^2 + x^2 - 1)\left(w - \frac{\lambda}{\sqrt{6}} \text{sech}\,(\lambda z) \right) - \sqrt{6} c \tanh(\lambda z) x w, \tag{3.35}$$

$$x_{,N} = 3(w^2 + x^2 - 1)\left(x + \sqrt{\frac{2}{3}} \lambda \tanh(\lambda z) \right) + \sqrt{6} c \tanh(\lambda z) w^2, \tag{3.36}$$

$$z_{,N} = \sqrt{6} x. \tag{3.37}$$

The variable transformations as defined in Eqs. (3.23) and (3.24) imply the following relationship between the variables $(w, x, y, z) \mapsto (\tilde{w}, \tilde{x}, \tilde{y}, \tilde{z})$:

$$\tilde{w} = \operatorname{sech}\left(\frac{\lambda}{2}z\right) w - \tanh\left(\frac{\lambda}{2}z\right) x, \tag{3.38}$$

$$\tilde{x} = \tanh\left(\frac{\lambda}{2}z\right) w + \operatorname{sech}\left(\frac{\lambda}{2}z\right) x, \tag{3.39}$$

$$\tilde{y} = y, \tag{3.40}$$

$$\tilde{z} = \frac{2}{\lambda}\sinh\left(\frac{\lambda}{2}z\right). \tag{3.41}$$

If $V = 0$, these transformations quantify how to "twist" Fig. 3.3(b) to generate Fig. 3.3(a).

The fixed-point solutions in Eqs. (3.31)-(3.33) are given in the new variables (w, x, y, z) as

$$(-1, 0, 0, 0)\,, \tag{3.42}$$

$$(+1, 0, 0, 0)\,, \tag{3.43}$$

$$\left(\frac{\lambda}{\sqrt{6}}, 0, \sqrt{\frac{\lambda^2}{6} - 1}, 0\right), \tag{3.44}$$

and the fixed-curve solutions in Eq. (3.34) are

$$\left(\frac{\lambda}{\sqrt{6}}\operatorname{sech}\left(\frac{\lambda}{2}z\right), -\frac{\lambda}{\sqrt{6}}\tanh\left(\frac{\lambda}{2}z\right), \sqrt{\frac{\lambda^2}{6} - 1}, \pm Z\right) \tag{3.45}$$

with $Z = (2/\lambda)\sinh^{-1}\left(\lambda\tilde{Z}/2\right)$. These fixed curves lie on the surface of the cylinder $w^2 + x^2 = \frac{\lambda^2}{6}$. For $V = 0$ and $\lambda = \sqrt{6}$, Eq. (3.45) corresponds to the twisted green curve that is confined to the surface of the unit cylinder in Fig. 3.3(b).

Direct substitution verifies that the curves in Eq. (3.34) and Eq. (3.45) are solutions to the background equations given in Eqs. (3.28)-(3.30) and Eqs. (3.35)-(3.37) for both $V = 0$ with $\lambda = \sqrt{6}$ and for $V \neq 0$.

To show the existence of a negative eigenvalue, we linearize the equations of motion about the fixed points, in Eq. (3.33) and (3.44), respectively, for the two sets of variables. Linearizing Eqs. (3.28)-(3.30) about Eq. (3.33) yields a matrix equation like that given in Eq. (3.19) with $(\delta\tilde{w}, \delta\tilde{x}, \delta\tilde{z}) \equiv \left(\tilde{w} - \lambda/\sqrt{6}, \tilde{x}, \tilde{z}\right)$ and

$$\tilde{M} \equiv \begin{pmatrix} \frac{\lambda^2}{2} - 3 & 0 & 0 \\ 0 & \lambda^2 - 3 & 0 \\ 0 & \sqrt{6} & -\frac{\lambda^2}{2} \end{pmatrix}. \tag{3.46}$$

Similarly, linearizing Eqs. (3.36)-(3.37) about Eq. (3.44) yields Eq. (3.19) with $(\delta w, \delta x, \delta z) \equiv \left(w - \lambda/\sqrt{6}, x, z\right)$ and

$$M \equiv \begin{pmatrix} \frac{\lambda^2}{2} - 3 & 0 & 0 \\ 0 & \frac{\lambda^2}{2} - 3 & \frac{\lambda^2\left(\lambda^2-3\right)}{2\sqrt{6}} \\ 0 & \sqrt{6} & 0 \end{pmatrix}. \tag{3.47}$$

Both $\tilde{M}$ and M have eigenvalues $\{-\lambda^2/2, \lambda^2/2 - 3, \lambda^2 - 3\}$, the first of which is negative. In the first set of variables, the eigenvector corresponding to the eigenvalue $-\lambda^2/2$ is parallel to the unit vector in the $\tilde{z}$-direction, which is tangent to the fixed-curve solution in Eq. (3.34). In the second set of variables, the eigenvector associated with eigenvalue $-\lambda^2/2$ is parallel to a linear combination of unit vectors $\hat{x}, \hat{z}$, namely $\hat{z} - \lambda^2/(2\sqrt{6})\hat{x}$, which is tangent to the fixed-curve solution in Eq. (3.45).

For the case, $V = 0$ and $\lambda = \sqrt{6}$, these eigenvectors are tangent to the green fixed curves in Fig. 3.3 at the red arrows. The existence of a negative eigenvalue in this model is harmless, since it only means that the system is attracted to a fixed-curve solution (instead of a fixed-point solution) that generates a scale-invariant spectrum of entropic perturbations.

3.3.3 Further generalizations

Although the remainder of this chapter will consider actions with the shift symmetry in Eq. (3.2), our results can be generalized to cases without shift symmetry. For example, the field contribution to the shift-symmetric Lagrangian density in Eq. (3.21) is a special case of the more general Lagrangian density

$$\mathcal{L} = \frac{1}{2}R - \frac{1}{2}(\partial\psi)^2 - \frac{1}{2}e^{-\lambda\psi}(\partial\chi)^2 - V_0 e^{-\mu\psi}\left[1 + r(\chi)\right] + q(\chi) \tag{3.48}$$

with $\mu = \lambda$ and $r(\chi) = q(\chi) = 0$. The addition of $q(\chi)$ and $r(\chi)$ breaks the shift symmetry since

$$\begin{aligned} V &= \left(1 + r(\chi)\right) V_0 e^{-\mu\psi} + q(\chi) \\ &\to \left(1 + r(\chi_0 + e^{\frac{\lambda}{2\mu}\kappa}(\chi - \chi_0))\right) V_0 e^{-\mu\psi - \kappa} + q(\chi_0 + e^{\frac{\lambda}{2\mu}\kappa}(\chi - \chi_0)) \\ &\neq e^{-\kappa} V. \end{aligned} \tag{3.49}$$

If $\mu = \lambda$, the ekpyrotic Lagrangian density in Eq. (3.48) admits a scaling solution that is a fixed-curve attractor with $\chi' = 0$ and that generates a scale-invariant spectrum of entropic perturbations. This is due to the fact that as $\chi' \to 0$, $r(\chi)$ and $q(\chi)$ approach constants $r(\chi_0)$ and $q(\chi_0)$. The first, $r(\chi_0)$, can be reabsorbed into V_0, and the second, $q(\chi_0)$, is negligible along the fixed-curved attractor.

3.4 Constructing new models

In this section, we derive the most general ekpyrotic, two-field Lagrangian density with shift symmetry that admits scaling solutions which are either fixed-point or fixed-curve attractors and generate a scale-invariant spectrum of entropy perturbations.

First, we consider the Lagrangian density in Eq. (3.3) with arbitrary parameters and couplings,

$$\{V_0 < 0, c \in \mathbb{R}, h(\sigma) > 0, f(\sigma) > 0\}. \tag{3.50}$$

In Appendix B, we show that the combined conditions of shift symmetry, scaling solution, fixed-curve attractor and scale-invariant spectrum of perturbations imply the following properties:

P1: $\lim_{|\sigma|\to\infty} f(\sigma) = \infty$ monotonically;

P2: $\lim_{|\sigma|\to\infty} h(\sigma) \propto e^{-\mu\sigma}$;

P3: $\lim_{|\sigma|\to\infty} (w, x, y, z) = \left(0, \frac{\mu}{\sqrt{6}}, \sqrt{\frac{\mu^2}{6} - 1}, -\text{sgn}(\mu)\infty\right)$;

P4: $|\mu| > \sqrt{6}$.

Property P1 says that the coupling $f(\sigma)$ must grow without bound. Property P2 constrains the form of the potential energy density to be exponential at late times. Property P3 defines the scaling solution. It implies $w = 0$ so that the ϕ field is fixed; furthermore, since the background equations in Eqs. (3.5)-(3.7) depend explicitly on σ, which will vary, it also implies that the scaling solution is a fixed curve (rather than a fixed point) in $(w-x-z)$ space. Property P4 is necessary for ekpyrosis ($\epsilon > 3$) as follows from substituting this solution into the equation of state, Eq. (3.9).

The example from the last section has these four properties. At late times, the fixed-curve attractor in Eq. (3.45) goes to $z \equiv \sigma \to \pm\infty$. In this limit, $f(\sigma) = h(\sigma) = \cosh^2(\lambda\sigma/2)$ is dominated by the single exponential $e^{|\lambda\sigma|}/4$. For example, if $\lambda > 0$ and $\sigma \to -\infty$, choosing $\mu = \lambda$ in the solution in property P3 reproduces Eq. (3.45) at late times. Similar arguments apply for the different combinations of $\text{sgn}(\lambda)$ and $\text{sgn}(\sigma)$.

Assuming properties P1 through P4, the only remaining degrees of freedom are the parameters, c, V_0, and the late-time behavior of $f(\sigma)$, modulo property P1. We

show now that, given these four properties, it is possible to obtain a scale-invariant spectrum for the entropic modes but not for the adiabatic modes.

We perturb Einstein's equations about the fixed-curve solution specified by Property P3, working in the longitudinal gauge [108, 23] where the metric takes the form

$$\mathrm{d}s^2 = a^2\left(-(1+2\Phi)\mathrm{d}\tau^2 + (1-2\Phi)\mathrm{d}\vec{x}^2\right). \tag{3.51}$$

Since $\phi' = 0$ along the background solution in property P3, the quantity $Q_s \equiv \sqrt{f(\sigma)}\delta\phi$ is automatically gauge invariant and represents the entropy perturbation; the Mukhanov-Sasaki variable $Q_\sigma \equiv \delta\sigma + (\sigma'/\mathcal{H})\Phi$ is also gauge invariant and represents the adiabatic perturbation [109, 110]. Property P3 implies that the equation of state $\epsilon = \mu^2/2$ and, therefore, the conformal Hubble parameter is $\mathcal{H}^{-1} = (1-\epsilon)(-\tau) < 0$. Then, the mode functions $u_\sigma \equiv aQ_\sigma$ and $u_s \equiv aQ_s$ satisfy

$$u_\sigma'' + \left(k^2 - \frac{\theta^\sigma}{(-\tau)^2}\right)u_\sigma = \frac{\alpha}{(-\tau)^2}u_s + \frac{\beta}{(-\tau)}u_s', \tag{3.52}$$

$$u_s'' + \left(k^2 - \frac{\theta^s}{(-\tau)^2}\right)u_s = \frac{\gamma}{(-\tau)^2}u_\sigma + \frac{\delta}{(-\tau)}u_\sigma', \tag{3.53}$$

where the background-dependent quantities can be derived, for example, from the expressions in Ref. [111]:

$$\theta^{\sigma} = -\frac{2\left(\mu^2-4\right)}{\left(\mu^2-2\right)^2} - \frac{\left(\mu^2-6\right)^2}{\mu^2(\mu^2-2)^2}\frac{c^2}{f}, \tag{3.54}$$

$$\theta^{s} = -\frac{2(\mu^2-4)}{(\mu^2-2)^2} + 3\frac{\mu^2-6}{\mu^2(\mu^2-2)}\frac{c^2}{f} - \frac{\mu(\mu^2-6)}{(\mu^2-2)^2}\frac{f_{,\sigma}}{f} - \frac{\mu^2}{(\mu^2-2)^2}\left(\frac{f_{,\sigma}}{f}\right)^2 + \frac{2\mu^2}{(\mu^2-2)^2}\frac{f_{,\sigma\sigma}}{f}, \tag{3.55}$$

$$\alpha = 4\frac{\mu^2-6}{\mu(\mu^2-2)^2}\frac{c}{\sqrt{f}} + 2\frac{\mu^2-6}{(\mu^2-2)^2}\frac{c}{\sqrt{f}}\frac{f_{,\sigma}}{f}, \tag{3.56}$$

$$\beta = 2\frac{\mu^2-6}{\mu(\mu^2-2)^2}\frac{c}{\sqrt{f}}, \tag{3.57}$$

$$\gamma = -4\frac{\mu^2-6}{\mu\left(\mu^2-2\right)^2}\frac{c}{\sqrt{f}}, \tag{3.58}$$

$$\delta = -\beta. \tag{3.59}$$

These variables are generally time dependent because $f = f(\sigma)$ is a function of τ. Substituting the expression for $\mathcal{H}^{-1}$ into the definition of x given in Eq. (3.4), we find

$$f_{,\sigma} = \frac{f'}{\sigma'} = -f'\frac{\mu^2-2}{2\mu}(-\tau). \tag{3.60}$$

Using this expression, Eqs. (3.55), (3.56) can be rewritten as

$$\theta^{s} = -2\frac{\mu^2-4}{(\mu^2-2)^2}\frac{c^2}{f} - \frac{2}{\mu^2-2}\frac{f'}{f}(-\tau) - \frac{1}{4}\left(\frac{f'}{f}(-\tau)\right)^2 + \frac{1}{2}\frac{f''}{f}(-\tau)^2, \tag{3.61}$$

$$\alpha = 4\frac{\mu^2-6}{\mu(\mu^2-2)}\frac{c}{\sqrt{f}} + \frac{\mu^2-6}{\mu(\mu^2-2)}\frac{c}{\sqrt{f}}\frac{f'}{f}(-\tau). \tag{3.62}$$

Eqs. (3.52) and (3.53) are a coupled, linear system of differential equations which must be solved as $\tau \to 0^-$ to find the spectra. Depending on the growth rate of the coupling function $f(\sigma)$, different terms in Eqs. (3.54), (3.61), (3.62), (3.57), (3.58), and (3.59) come to dominate in this regime. For example, the first term in θ^{σ} always

dominates over the second since $f \to \infty$ as $\tau \to 0^-$. By contrast, the relative sizes of the different terms in θ^s depend on the magnitude of f'/f.

For clarity, we define the symbol "$\gtrsim$" to mean

$$|A(\tau)| \gtrsim |B(\tau)| \quad \text{if} \quad \frac{d\ln|A(\tau)|}{d\ln|\tau|} < \frac{d\ln|B(\tau)|}{d\ln|\tau|} \quad \text{as} \quad \tau \to 0^-. \tag{3.63}$$

Similarly, we define "$\sim$" to mean

$$A(\tau) \sim B(\tau) \quad \text{if} \quad \frac{d\ln|A(\tau)|}{d\ln|\tau|} = \frac{d\ln|B(\tau)|}{d\ln|\tau|} \quad \text{as} \quad \tau \to 0. \tag{3.64}$$

For example, $1/(-\tau)^2 \gtrsim 1/(-\tau)$ and $3/(-\tau) \sim 2/(-\tau)$.

There are three qualitatively different cases to consider: fast growth, $|f_{,\sigma}/f| \gtrsim 1$; slow growth, $|f_{,\sigma}/f| \lesssim 1$; and "just-so" growth, $|f_{,\sigma}/f| \sim 1$.

3.4.1 Fast growth: $|f_{,\sigma}/f| \gtrsim 1$

If $|f_{,\sigma}/f| \gtrsim 1$, then $|f'/f| \gtrsim |1/\tau|$. Let us assume that

$$\frac{\gamma}{(-\tau)^2}u_\sigma, \frac{\delta}{(-\tau)}u'_\sigma \ll \frac{\theta^s}{(-\tau^2)}u_s \tag{3.65}$$

so that to leading order, the entropic mode evolves independently:

$$u_s'' - \frac{1}{2}\left(\frac{f''}{f} - \frac{1}{2}\left(\frac{f'}{f}\right)^2\right)u_s = 0. \tag{3.66}$$

For the mode function u_s, we find the solution

$$u_s(\tau) = \sqrt{f(\tau)}\left[c_1(k)\int_{-1/k}^{\tau}\frac{d\bar{\tau}}{f(\bar{\tau})} + c_2(k)\right], \tag{3.67}$$

where $c_1(k)$ and $c_2(k)$ are constants of integration. Choosing $c_1(k)$ and $c_2(k)$ so that u_s and u'_s match the Bunch-Davies solution, $(1/\sqrt{2k})e^{-ik\tau}$, at horizon crossing

$(-\tau = 1/k)$, yields

$$c_1(k) = \frac{e^i \left(f'\left(-1/k\right) + 2ikf\left(-1/k\right)\right)}{2\sqrt{2kf\left(-1/k\right)}}, \tag{3.68}$$

$$c_2(k) = \frac{e^i}{\sqrt{2kf\left(-1/k\right)}}. \tag{3.69}$$

For fast-growing f, the integral in Eq. (3.67) is very closely approximated by $(1/k)(1/f(-1/k))$ at late times. With Eqs. (3.68) and (3.69), the entropic mode function is given by

$$u_s = \Sigma(k)\sqrt{f(\tau)} \tag{3.70}$$

where

$$\Sigma(k) \equiv \frac{e^i \left(-f'\left(-1/k\right) + (2-2i)kf\left(-1/k\right)\right)}{2\sqrt{2}k^{3/2} f\left(-1/k\right)^{3/2}}. \tag{3.71}$$

Substituting this result into the right side of the adiabatic equation, Eq. (3.52), we find that u_σ satisfies

$$u_\sigma'' + 2\frac{\mu^2-4}{(\mu^2-2)^2}\frac{1}{(-\tau)^2}u_\sigma = 4\frac{\mu^2-6}{\mu(\mu^2-2)^2}\frac{c\Sigma(k)}{(-\tau)^2} \tag{3.72}$$

with solution

$$u_\sigma = c_3(k)(-\tau)^{\frac{\mu^2-4}{\mu^2-2}} + c_4(k)(\tau)^{\frac{2}{\mu^2-2}} + 2\frac{\mu^2-6}{\mu(\mu^2-4)}c\Sigma(k) \tag{3.73}$$

where $c_3(k)$ and $c_4(k)$ are constants. The first two terms vanish as $\tau \to 0$ by property P4. This shows that our assumption in Eq. (3.65) is justified.

From the solutions for the mode functions in Eqs. (3.67) and (3.73), it is clear that both the adiabatic and the entropic spectra are proportional to $k^3|\Sigma(k)|^2$. Scale invariance is obtained if and only if

$$|\Sigma(k)|^2 = \xi k^{-3}, \tag{3.74}$$

for some constant ξ that is independent of k. Eq. (3.74) is a first order differential equation for the coupling function f, namely

$$\left(\frac{f'}{f}\right)^2 - \frac{4}{(-\tau)}\frac{f'}{f} = 8\xi f - \frac{8}{(-\tau)^2}; \tag{3.75}$$

its solution is given by

$$f(\tau) = \frac{\sec^2\left(\ln|\tau/\tau_0|\right)}{2\xi(-\tau)^2}, \tag{3.76}$$

where τ_0 is an integration constant. This is clearly not monotonic as $\tau \to 0^-$, and therefore, it violates property P1. Hence, we conclude scale-invariance is impossible for fast-growing f.

3.4.2 Slow growth: $|f_{,\sigma}/f| \lesssim 1$

If $|f_{,\sigma}/f| \lesssim 1$, then $|f'/f| \lesssim 1/(-\tau)$. To leading order, both mode functions satisfy

$$u'' + 2\frac{(\mu^2-4)}{(\mu^2-2)^2}\frac{1}{(-\tau)^2}u = 0, \tag{3.77}$$

as is clear from Eqs. (3.52), (3.53) and (3.54)-(3.62). In this case, both the adiabatic and the entropic spectra are given by

$$n_s = 4 - \left|\frac{\mu^2-6}{\mu^2-2}\right|, \tag{3.78}$$

which is blue by property P4. Hence, we conclude scale invariance is impossible for slow-growing f.

3.4.3 "Just-so" growth: $|f_{,\sigma}/f| \sim 1$

If $|f_{,\sigma}/f| \sim 1$, $f(\sigma) = e^{-\lambda\sigma}$ for some $\lambda \in \mathbb{R}$ such that $\mathrm{sgn}(\lambda) = \mathrm{sgn}(\mu)$. The coupling functions $\alpha, \beta, \gamma, \delta$ are all proportional to $1/\sqrt{f}$ so the right sides of Eqs. (3.52) and

(3.53) can be neglected. The mode functions effectively decouple and the adiabatic spectral index is again given by Eq. (3.78); the entropic spectral index is

$$n_s = 4 - \left| 2\frac{\lambda\mu - 2}{\mu^2 - 2} + 1 \right|, \tag{3.79}$$

which is scale invariant when $\lambda = \mu$. For a given $\mu > \sqrt{6}$, any $n_s < (3\mu^2 - 2)/(\mu^2 - 2)$ can be achieved by choosing $\lambda = (n_s - 1)/\mu - \mu(n_s - 3)/2$.

Note that since "just-so" growth implies $f(\sigma) = e^{-\lambda\sigma}$ (and property P2 requires $h(\sigma) = e^{-\mu\sigma}$), the Lagrangian density is given by

$$\mathcal{L} = \frac{1}{2}R - \frac{1}{2}(\partial\sigma)^2 - \frac{1}{2}e^{-\lambda\sigma}(\partial\phi)^2 - V_0 e^{-c\phi}e^{-\mu\sigma}, \tag{3.80}$$

which is equivalent to the Lagrangian density in Eq. (3.48) with the identifications

$$\begin{aligned} \sigma &\longleftrightarrow \psi, \\ \phi &\longleftrightarrow \chi. \end{aligned} \tag{3.81}$$

3.5 Discussion

Recall that in chapter 2, we studied matter-like contracting universes. We showed that such universes have no hope of explaining the fine-tuning problems of standard big bang cosmology without introducing the worse fine-tuning problem associated with the unstable growth anisotropy. We argued above that these same conclusions extend to any contracting universe whose dominant energy density blueshifts slower than anisotropy. This led us to consider ekpyrotic universes because these have the attractive feature that they obviate this anisotropy problem. Notwithstanding, Tolley and Wesley pointed out that many ekpyrotic models of observational interest– *i.e.*,

those that generate the observed fluctuation spectrum– suffer from a different kind of fine-tuning problem that manifests as a sensitivity to initial conditions.

In this chapter, we presented explicit ekpyrotic models, with and without shift symmetry, that generate a scale-invariant spectrum of entropic fluctuations and *do not* require finely tuned initial conditions. Rather, we showed that although the negative eigenvalue identified by Tolley and Wesley can indicate a true instability in some models, in others it simply implies the existence of a fixed-curve solution rather than a fixed point. For the actions discussed here, the fixed curve is a stable attractor; fine-tuning of initial conditions is thereby avoided.

It is worthwhile to pause to examine these beneficial features in a broader context. First, as with all ekpyrotic models, those discussed here avoid the mutiverse problem of inflation and therefore make falsifiable predictions that are the same in all parts of the universe without resorting to additional inputs like anthropic arguments or probability measures. From an aesthetic perspective, it is remarkable that the avoidance of finely tuned initial conditions alleviates, rather than exacerbates, concomitant requirements on the equation of state, ϵ, during the ekpyrotic phase. These models no longer require ultra-stiff pressures (*i.e.*, $\epsilon \gg 3$) to obtain a scale-invariant spectrum of density perturbations; the observed spectral index can be achieved– and fine-tuning problems averted– if ϵ is only marginally greater than 3. Moreover, as in all ekpyrotic models, these naturally generate an undetectable spectrum of primordial gravitational waves (the ratio of the tensor-perturbation amplitude to the scalar-perturbation amplitude, $r \approx 0$), consistent with current bounds [47, 112]. They also generate zero non-Gaussianity during the ekpyrotic contraction phase. A small amount of local non-Gaussianity may be generated during the bounce, but at a level well within current observational bounds on $f_{\rm NL}$ [113, 114].

Interestingly, as observational constraints impose tighter bounds on r, inflation and ekpyrosis are moving in diametrically opposed directions in terms of parameters,

degrees of freedom, and initial conditions. That is, inflationary models are becoming more complicated [28] while ekpyrotic models are becoming simpler.

3.6 Appendix A: Deriving the coordinate transformation

In this appendix, we will derive the coordinate transformation in Eqs. (3.23) and (3.24). We will work in three steps. First, we will show quite generally that the symmetry transformation in Eq. (3.2) guarantees that the existence of a Killing field, namely ξ^a, on field space. Next, we will specialize to the model in Eq. (3.21), showing that it possesses the symmetry and then constructing the corresponding Killing field. Finally, we will choose coordinates (ϕ, σ) on field space such that the Killing direction is ϕ and the orthogonal direction is σ, thereby producing Eqs. (3.23) and (3.24).

Showing existence of the Killing field from symmetry

In order to conform to the (standard) notation that contravariant vector indices appear as superscripts and that covariant covector indices appear as subscripts, we will depart from the (nonstandard) convention taken in Eq. (3.1), in which Φ_a with lower index denotes field-space coordinates and in which G^{ab} with upper indices denotes field-space metric components. Rather, henceforth, Φ^a with upper indices will denote field-space coordinates, and G_{ab} with lower indices will denote field-space metric components. This should present no ambiguity.

The instability argument in Ref. [106] applies to actions of the form in Eq. (3.1), which in this new notation reads

$$S = \int d^4x\sqrt{-g}\left(\frac{1}{2}R - \frac{1}{2}G_{ab}g^{\mu\nu}\partial_\mu\Phi^a\partial_\nu\Phi^b - V(\Phi)\right) \equiv S_R + S_K + S_V. \tag{3.82}$$

Perturbing Eq. (3.2) about an arbitrary point $\kappa = \kappa_0$, we find that under

$$\Phi^a(x;\kappa_0) \to \Phi^a(x;\kappa_0+\epsilon) = \Phi^a(x;\kappa_0) + \xi^a(\Phi(x;\kappa_0))\epsilon + O(\epsilon^2) \tag{3.83}$$

$$g_{\mu\nu}(x;\kappa_0) \to g_{\mu\nu}(x;\kappa_0+\epsilon) = e^{\epsilon} g_{\mu\nu}(x;\kappa_0) \tag{3.84}$$

the action transforms as

$$S(\kappa_0) \to S(\kappa_0+\epsilon) = e^{\epsilon} S(\kappa_0). \tag{3.85}$$

To first order in ϵ, we have from Eqs. (3.83) and (3.84) that

$$\delta_\epsilon \Phi^a \equiv \frac{\partial \Phi^a(x;\kappa_0+\epsilon)}{\partial \epsilon}\Big|_{\epsilon=0} = \xi^a \tag{3.86}$$

$$\delta_\epsilon g_{\mu\nu} \equiv \frac{\partial g_{\mu\nu}(x;\kappa_0+\epsilon)}{\partial \epsilon}\Big|_{\epsilon=0} = g_{\mu\nu}. \tag{3.87}$$

Then the demand that the action transforms as in Eq. (3.85) implies

$$\delta_\epsilon S \equiv \frac{dS(\kappa_0+\epsilon)}{d\epsilon}\Big|_{\epsilon=0} = S(\kappa_0). \tag{3.88}$$

or equivalently that

$$0 = \delta_\epsilon S - S \tag{3.89}$$

$$= (\delta_\epsilon S_R - S_R) + (\delta_\epsilon S_K - S_K) + (\delta_\epsilon S_V - S_V). \tag{3.90}$$

The first term in parentheses vanishes trivially since in 3+1 dimensions, $\delta_\epsilon(\sqrt{-g}g^{\mu\nu}) = \sqrt{-g}g^{\mu\nu}$. Expanding the other two terms gives

$$
\begin{aligned}
0 &= \delta_\epsilon\left(\int d^4x\sqrt{-g}\left(g^{\mu\nu}G_{ab}\partial_\mu\Phi^a\partial_\nu\Phi^b + V(\Phi)\right)\right) - S_K - S_V && (3.91)\\
&= \int d^4x\Big(\delta_\epsilon(\sqrt{-g}g^{\mu\nu})G_{ab}\partial_\mu\Phi^a\partial_\nu\Phi^b + \sqrt{-g}g^{\mu\nu}\delta_\epsilon G_{ab}\partial_\mu\Phi^a\partial_\nu\Phi^b \\
&\quad + \sqrt{-g}g^{\mu\nu}G_{ab}\partial_\mu\delta_\epsilon\Phi^a\partial_\nu\Phi^b + \sqrt{-g}g^{\mu\nu}G_{ab}\partial_\mu\Phi^a\partial_\nu\delta_\epsilon\Phi^b + \delta_\epsilon(\sqrt{-g}V)\Big) \\
&\quad - S_K - S_V && (3.92)\\
&= \int d^4x\sqrt{-g}\Big[g^{\mu\nu}\left(\delta_\epsilon G_{ab}\partial_\mu\Phi^a\partial_\nu\Phi^b + 2G_{ab}\partial_\mu\delta_\epsilon\Phi^a\partial_\nu\Phi^b\right) + \delta_\epsilon V + V\Big] && (3.93)
\end{aligned}
$$

Since G_{ab} and ξ^a depend only on Φ^a, we can use the chain rule to write

$$\delta_\epsilon G_{ab} = \frac{\partial G_{ab}}{\partial\Phi^c}\delta_\epsilon\Phi^c \tag{3.94}$$

and

$$\partial_\mu\delta_\epsilon\Phi^a = \partial_\mu(\Phi^c)\frac{\partial\delta_\epsilon\Phi^a}{\partial\Phi^c}. \tag{3.95}$$

Using these and relabeling indices, we can rewrite the term in the square brackets in Eq. (3.93) as

$$\left(\frac{\partial G_{ab}}{\partial\Phi^c}\delta_\epsilon\Phi^c + G_{ac}\frac{\partial\delta_\epsilon\Phi^c}{\partial\Phi^b} + G_{cb}\frac{\partial\delta_\epsilon\Phi^c}{\partial\Phi^a}\right)g^{\mu\nu}\partial_\mu\Phi^a\partial_\nu\Phi^b + \left(\frac{dV}{d\Phi^a}\delta_\epsilon\phi^a + V\right). \tag{3.96}$$

Recalling Eq. (3.86), this expression is

$$(\mathcal{L}_\xi G_{ab})g^{\mu\nu}\partial_\mu\Phi^a\partial_\nu\Phi^b + \left(\frac{dV}{d\Phi^a}\xi^a + V\right). \tag{3.97}$$

Since this transformation is to hold for all fields and all metrics, both terms in parentheses must vanish separately, *i.e.*, $(\mathcal{L}_\xi G)_{ab} = 0$ and $\delta_\epsilon V = -V$. Thus, we have shown

that if the symmetry transformation in Eq. (3.2) holds, then ξ^a is a Killing field on field space (and moreover that $V \to e^{-\kappa} V$).

Constructing the Killing field

The model in Eq. (3.21) possesses the symmetry in Eq. (3.2). Note that under

$$\psi \to \psi + \frac{\kappa}{\lambda}, \tag{3.98}$$

$$\chi \to \chi_0 + e^{\kappa/2}(\chi - \chi_0), \tag{3.99}$$

$$g_{\mu\nu} \to e^{\kappa} g_{\mu\nu}, \tag{3.100}$$

the action indeed changes as $S \to e^{\kappa} S$. Therefore, by the argument of the previous section, the field-space metric possesses a Killing field. In the rest of this section, we will derive a formula for the general Killing field. Then, by choosing the appropriate Killing direction to be ϕ and the orthogonal direction to be σ, we will reproduce the variable transformation in Eqs. (3.23) and (3.24).

For the purposes of solving Killing's equation, it is useful to change field-space variables $(\psi, \chi) \mapsto (X, Y)$ where

$$X = \chi - \chi_0 \tag{3.101}$$

$$Y = \frac{2}{\lambda} e^{\frac{\lambda}{2}\psi}. \tag{3.102}$$

In these variables, it is clear that field-space is the well-known Poincaré half-plane [115]

$$d\psi^2 + e^{-\lambda\psi} d\chi^2 = \left(\frac{2}{\lambda}\right)^2 \left(\frac{dX^2 + dY^2}{Y^2}\right). \tag{3.103}$$

It is also useful to rewrite Killing's equation for a vector field K^a in terms of its covariant components by substituting the identity

$$\Gamma_{\nu\rho\mu} + \Gamma_{\mu\rho\nu} = G_{\mu\nu,\rho} \tag{3.104}$$

into the first term on the right side of

$$(\mathcal{L}_K G)_{\mu\nu} = G_{\mu\nu,\rho} K^\rho + G_{\mu\sigma} X^\sigma{}_{,\nu} + G_{\sigma\nu} K^\sigma{}_{,\mu}, \tag{3.105}$$

where $\Gamma_{\nu\rho\mu} \equiv G_{\nu\sigma}\Gamma^\sigma_{\rho\mu}$ and $\Gamma^\sigma_{\rho\mu}$ are the components of the Levi-Civita connection for the field-space metric. This yields

$$\begin{aligned}
(\mathcal{L}_K G)_{\mu\nu} &= \left(G_{\nu\sigma}\Gamma^\sigma_{\rho\mu} + G_{\mu\sigma}\Gamma^\sigma_{\rho\nu}\right) K^\rho + G_{\mu\sigma} K^\sigma{}_{,\nu} + G_{\nu\sigma} K^\sigma{}_{,\mu} && (3.106)\\
&= G_{\nu\sigma} K^\sigma{}_{;\mu} + G_{\mu\sigma} K^\sigma{}_{;\nu} && (3.107)\\
&= K_{\nu;\mu} + K_{\mu;\nu} && (3.108)\\
&= K_{\nu,\mu} + K_{\mu,\nu} - 2\Gamma^\rho_{\nu\mu} K_\rho = 0 && (3.109)
\end{aligned}$$

For the field-space metric in Eq. (3.103), the only nontrivial connection components are $\Gamma^Y_{XX} = -\Gamma^X_{XY} = -\Gamma^Y_{YY} = Y^{-1}$. Thus, Eq. (3.109) yields from the $(\mu,\nu) = (X,X),(X,Y),(Y,Y)$ components, respectively, the following differential equations, for K_X and K_Y

$$\begin{aligned}
K_{X,X} &= Y^{-1} K_Y, && (3.110)\\
K_{X,Y} + 2Y^{-1} K_X &= -K_{Y,X}, && (3.111)\\
K_{Y,Y} &= -Y^{-1} K_Y. && (3.112)
\end{aligned}$$

Equation (3.112) integrates immediately to

$$K_Y = \mathcal{X}_{,X}(X)/Y, \tag{3.113}$$

where $\mathcal{X}(X)$ is an arbitrary function of X. Putting this into Eq. (3.110) yields

$$K_{X,X} = \frac{\mathcal{X}_{,X}(X)}{Y^2} \implies K_X = \frac{\mathcal{X}(X)}{Y^2} + \mathcal{Y}(Y) \tag{3.114}$$

where $\mathcal{Y}(Y)$ is an arbitrary function of Y. Substituting Eqs. (3.113) and (3.114) into Eq. (3.111) and rearranging yields the separable equation

$$\mathcal{X}_{,XX} = -Y\mathcal{Y}_{,Y} - 2\mathcal{Y}, \tag{3.115}$$

from which it follows that both sides are equal to the same constant, which we set to A. The remaining integrals are trivial and give

$$\mathcal{X}(X) = \frac{A}{2}X^2 + BX + C, \tag{3.116}$$

$$\mathcal{Y}(Y) = -\frac{A}{2} + \frac{D}{Y^2}, \tag{3.117}$$

where B, C, and D are integration constants. Putting these into Eqs. (3.113) and (3.114) and raising the indices yields

$$K^X = \left(\frac{\lambda}{2}\right)^2 \left(\frac{A}{2}(X^2 - Y^2) + BX + (C + D)\right), \tag{3.118}$$

$$K^Y = \left(\frac{\lambda}{2}\right)^2 (AXY + BY). \tag{3.119}$$

Thus, we have derived the most general Killing field of the field-space metric. It is a linear combination of the independent Killing fields, $K_1 \equiv (X^2 - Y^2)\partial_X + 2XY\partial_Y$, $K_2 \equiv X\partial_X + Y\partial_Y$, and $K_3 \equiv \partial_X$.

Selecting the coordinates

We will now choose coordinates (ϕ, σ) such that ϕ increases along K_2^a, namely $\partial_\phi^a = \omega K_2^a$, where ω is a constant. This implies

$$\frac{\partial X}{\partial \phi} = \omega X \implies X = \alpha(\sigma) e^{\omega\phi}, \tag{3.120}$$

$$\frac{\partial Y}{\partial \phi} = \omega Y \implies Y = \beta(\sigma) e^{\omega\phi}, \tag{3.121}$$

where α and β are functions of σ that will be chosen such that the Lagrangian density takes the form in Eq. (3.3). Comparing to the field-space metric,

$$\left(\frac{2}{\lambda}\right)^2 \left(\frac{dX^2 + dY^2}{Y^2}\right) = \frac{1}{(\omega\beta)^2}\Big((\alpha_{,\sigma}^2 + \beta_{,\sigma}^2) d\sigma^2 + \omega^2(\alpha^2 + \beta^2) d\phi^2 - \omega(\alpha\alpha_{,\sigma} + \beta\beta_{,\sigma})(d\phi d\sigma + d\sigma d\phi)\Big), \tag{3.122}$$

this requires

$$\alpha_{,\sigma}^2 + \beta_{,\sigma}^2 = \omega\beta^2 \tag{3.123}$$

$$\alpha\alpha_{,\sigma} + \beta\beta_{,\sigma} = \frac{1}{2}\frac{d}{d\sigma}\left(\alpha^2 + \beta^2\right) = 0 \tag{3.124}$$

Equation (3.124) integrates to $\alpha^2 + \beta^2 = c_1^2$ for some constant c_1. Parameterizing the solution as

$$\alpha(\sigma) = c_1 \tanh\left(F(\sigma)\right), \tag{3.125}$$

$$\beta(\sigma) = c_1 \operatorname{sech}\left(F(\sigma)\right), \tag{3.126}$$

for some function $F(\sigma)$, we can substitute into Eq. (3.123). This yields $F_{,\sigma}^2 = \omega^2$, which has a solution

$$F(\sigma) = \omega\sigma + c_2. \tag{3.127}$$

Substituting into Eqs. (3.120) and (3.121) gives

$$X = c_1 \tanh(\omega\sigma + c_2) e^{\omega\phi} \tag{3.128}$$

$$Y = c_1 \mathrm{sech}(\omega\sigma + c_2) e^{\omega\phi}. \tag{3.129}$$

Using Eqs. (3.101) and (3.102), we find (setting $c_2 = 0, c_1 = \frac{2}{\lambda} e^{\frac{\lambda}{2}\psi_0}, \omega = \lambda/2$),

$$\psi = \phi + \frac{2}{\lambda} \ln\left[\mathrm{sech}\left(\frac{\lambda\sigma}{2}\right)\right] + \psi_0, \tag{3.130}$$

$$\chi = \frac{2}{\lambda} e^{\frac{\lambda}{2}(\phi+\psi_0)} \tanh\left(\frac{\lambda\sigma}{2}\right) + \chi_0, \tag{3.131}$$

in agreement with Eqs. (3.23) and (3.24).

3.7 Appendix B: Deriving the properties

In this appendix, we derive the four properties listed at the beginning of Sec. 3.4 using a series of lemmas:

Lemma 1 *$x = 0$ cannot generate a scale-invariant adiabatic spectrum without fine-tuning.*

If $x = 0$, $z = z_0 = const.$ Since $z \equiv \sigma$, this means that $\sigma \equiv z_0$ along the solution. Defining

$$\bar{\sigma} \equiv \sigma - z_0, \tag{3.132}$$

$$\bar{\phi} \equiv \sqrt{f(z_0)}\left(\phi - \frac{1}{c}\ln h(z_0)\right), \tag{3.133}$$

$$\bar{c} \equiv \frac{c}{\sqrt{f(z_0)}}, \tag{3.134}$$

$$F(\bar{\sigma}) \equiv \frac{f(\bar{\sigma} + z_0)}{f(z_0)}, \tag{3.135}$$

$$H(\bar{\sigma}) \equiv \frac{h(\bar{\sigma} + z_0)}{h(z_0)}, \tag{3.136}$$

the Lagrangian density can be recast as

$$\mathcal{L} = \frac{1}{2}R - \frac{1}{2}(\partial\bar{\sigma})^2 - \frac{1}{2}F(\bar{\sigma})(\partial\bar{\phi})^2 - V_0 H(\bar{\sigma})e^{-\bar{c}\bar{\phi}}. \tag{3.137}$$

Eq. (3.137) has the shift-symmetric form of Eq. (3.3) with the solution $(x, z) = (0, z_0)$ at $(x, \bar{z}) = (0, 0)$ (with $\bar{z} \equiv \bar{\sigma}$) for which Tolley and Wesley proved that any solutions of interest are unstable. For fixed-point solutions like this (as opposed to fixed-curve solutions) instability implies the need for finely tuned initial conditions. Thus, we conclude $|\sigma| \to \infty$; we are forced to fixed-curve solutions.

Lemma 2 *$f \to const$ cannot generate a scale-invariant adiabatic or entropic spectrum without fine tuning.*

When $f = f_0 = const$, the non-canonical coupling becomes canonical. Then, the background Eqs. (3.5) and (3.6) give $(w, x) = (w_0, x_0)$ with $x_0 \neq 0$ (cf. lemma 1). Then $h = e^{-\sqrt{6}x_0\sigma}$. In such canonically coupled theories, the adiabatic perturbation decouples from the entropic perturbation and has a blue tilt. More precisely, the equations of motion corresponding to the Lagrangian density

$$\mathcal{L} = \frac{1}{2}R - \frac{1}{2}(\partial\sigma)^2 - \frac{1}{2}f_0(\partial\phi)^2 - V_0 e^{-c\phi}e^{-d\sigma} \tag{3.138}$$

linearized around $(w_0, x_0) = (d/\sqrt{6}, c/\sqrt{6f_0})$ yield the same equation for both the adiabatic and the entropic mode functions

$$u'' + \left(k^2 + \frac{2f_0\left(c^2 + (d^2-4)\,f_0\right)}{\left(c^2 + (d^2-2)\,f_0\right)^2}\frac{1}{(-\tau)^2}\right)u = 0 \tag{3.139}$$

so that the spectral index is given by

$$n_s = 4 - \left|\frac{c^2 + (d^2-6)\,f_0}{c^2 + (d^2-2)\,f_0}\right|. \tag{3.140}$$

Avoiding fine tuning, (*i.e.,* negative eigenvalues in the linearized equations of motion) requires $c^2/f_0 + d^2 > 6$. In this regime, the spectral indices are blue for both the adiabatic and entropic spectra.

Lemma 3 *If $w \neq 0$ then $f \to const$ at late times.*

For scaling solutions, the background equation for w, Eq. (3.5), can be recast as

$$\frac{df}{dz} = A\sqrt{f}\left(\sqrt{f} - B\right), \tag{3.141}$$

with $A \equiv \sqrt{6}\left(w^2 + x^2 - 1\right)/x$ and $B \equiv c/(\sqrt{6}w)$. There are various cases to consider, depending on the sign of A and B. For example, if $A > 0$ and $B > 0$, then $x > 0$ so that $z' < 0$. Then $\mathrm{sgn}(f') = -\mathrm{sgn}(df/dz)$, so that f decreases whenever the right side of Eq. (3.141) is positive ($\sqrt{f} > B$) and increases whenever it is negative ($\sqrt{f} < B$). It follows that at late times $f \to B^2 = const$. The other cases can be analyzed similarly, with the result that $f \to (B^2 \text{ or } 0)$. With lemma 2, we only have to consider the case $w = 0$.

Lemma 4 *If $w = 0$, then $f \to \infty$ at late times.*

If $w = 0$, then Eq. (3.5) becomes $w_{,N} = 3(x^2 - 1) \times (-c/(\sqrt{6}f))$. The condition $w = 0$ is maintained only if $f \to \infty$.

To this point, we have shown that any ekpyrotic, scaling attractor that generates a scale-invariant spectrum of either adiabatic or entropic perturbations lies at $w = 0$ with $f \to \infty$ and $x \neq 0$. Defining $\mu \equiv \sqrt{6}x$, Eq. (3.6) implies $h_{,z}/h = -\mu$, from which we conclude, given that $z \equiv \sigma$, $h(\sigma) \propto e^{-\mu\sigma}$ (property P2).

Lemma 5 *The scaling solution must correspond to the limit given in property P3.*

With $h(\sigma) = e^{-\mu\sigma}$, the only scaling solutions of Eqs. (3.5) and (3.6) are $(w, x) = \left\{(0, \pm 1), (0, \mu/\sqrt{6})\right\}$ if $f_{,\sigma}/f \neq const$. For the first two solutions, $\epsilon = 3$. Since ekpyrosis corresponds to $\epsilon > 3$, we only consider the third solution (property P3).

Note, if $f_{,\sigma}/f = const \equiv -\lambda$, there is another scaling solution at

$$(w, x) = \left(\pm \frac{\sqrt{\mu(\lambda+\mu) - 6}}{|\lambda+\mu|}, \frac{\sqrt{6}}{\lambda+\mu} \right). \tag{3.142}$$

At late times, this solution is equivalent to one in Ref. [100] that was shown never to be an attractor.

Lemma 6 *The coupling $f(\sigma)$ must grow monotonically.*

Since the solution in property P3 is a fixed curve, it can be parameterized by one variable, z. For any finite $|z|$, f will be finite so that even if the system lies at $(w, x) = (0, \mu/\sqrt{6})$, the kinetic energy of the ekpyrotic field evolves as $w_{,N} = -3c(\mu^2/6-1)/\sqrt{f}$ (cf. Eq. (3.5)). Thus, in any interval over which f shrinks, $|w_{,N}|$ grows. For this reason, we only consider solutions for which f grows monotonically (property P2). Linearizing Eqs. (3.5) and (3.6) about the background in property P3 yields

$$(\delta w)_{,N} = \left(3\left(\frac{\mu^2}{6} - 1 \right) - \frac{\mu f_{,z}}{2f} \right) \delta x, \tag{3.143}$$

$$(\delta x)_{,N} = 3\left(\frac{\mu^2}{6} - 1 \right) \delta x, \tag{3.144}$$

where $\delta w \equiv w$ and $\delta x \equiv x - \mu/\sqrt{6}$. The eigenvalues of this system are $\{(\mu^2-6)/2, (\mu^2 - 6 - \mu f_{,z}/f)/2\}$. Since $\mu f_{,z}/f < 0$, this reduced 2×2 system is stable *i.e.*, has positive eigenvalues, if $|\mu| > \sqrt{6}$ (property P4).

Chapter 4

Warm ekpyrosis

Most of this chapter was published in Ref. [67] in collaboration with a fellow graduate student Gustavo Turiaci, who has granted permission for its reproduction here.

4.1 Introduction

In chapter 3, we demonstrated that the best understood two-field models of ekpyrosis can simultaneously resolve the standard puzzles of big bang cosmology and generate the observed primordial spectrum of fluctuations, without introducing additional fine-tuning problems. This chapter explores whether these same successes can be achieved utilizing a single ekpyrotic scalar field. As we show below, this is indeed possible, but at the cost of imposing greater fine-tuning constraints to be discussed. The key ingredient is a coupling between the single field and a perfect fluid of ultra-relativistic matter. This coupling introduces a friction term into the equation of motion for the field, opposing the Hubble anti-friction, which can be chosen such that an exactly scale-invariant (or nearly scale-invariant) spectrum of adiabatic density perturbations is continuously produced throughout the ekpyrotic phase. An obvious advantage compared with the two-field models is that the spectrum is immediately adiabatic, and hence no conversion is necessary.

To provide some context, it is useful to reexamine the history of ekpyrotic cosmologies, and in particular their efficacy at both explaining the fluctuations and resolving the standard puzzles. As mentioned in chapter 3, the earliest models of ekpyrosis involved a single, minimally coupled scalar field with a steep, negative exponential potential. After some debate, it was shown that these models cannot produce the observed scale-invariant, adiabatic spectrum because the comoving curvature perturbation acquires a strong blue tilt [93, 94, 95, 96, 97]. However, it was noticed in Ref. [116] that when a second scalar field is added– also with a steep, negative potential– there exists a background solution along the potential energy surface whose entropic perturbations acquire a scale-invariant spectrum. After the ekpyrotic smoothing phase, it was argued in Ref. [99], the entropic perturbations will convert into a scale-invariant spectrum of adiabatic perturbations if the background solution undergoes a bend in field-space. This two-step process, first of generating scale-invariant entropic perturbations and then of converting them to adiabatic perturbations, has been dubbed the "entropic mechanism" [58, 100]. As remarked in chapter 3, this is similar to the "curvaton mechanism" described in Refs. [117, 118, 119]. The first models making use of the entropic mechanism require finely tuned initial conditions because the background solution is unstable to small perturbations [106, 102, 103, 104, 105].

The more recent two-field models discussed in chapter 3 have cured this instability by introducing non-canonical kinetic terms [107, 120, 114, 66]. Such terms provide friction in the equation of motion for the non-canonically coupled field [121]. This friction has two effects: 1) it damps the background evolution for the non-canonically coupled field, thereby making it the entropy direction in field-space and 2) it alters the spectrum of perturbations in this direction: scale-invariant entropic spectra are produced even though the entropy field has no potential. These newer models have the attractive features that they generate no detectable spectrum of primordial gravitational waves (the ratio of the tensor-perturbation amplitude to the scale-perturbation

amplitude, $r \approx 0$) and zero non-Gaussianity during the ekpyrotic contraction phase; only a small amount of local non-Gaussianity ($f_{\rm NL} = \mathcal{O}(1)$) is generated by the conversion process [112, 113, 114]. These models also impose less stringent constraints on the equation of state parameter of the universe and hence require less fine-tuning of parameters than actions with canonical kinetic terms.

In all of these models, during the slow contracting phase, the ekpyrotic fields are assumed to have no direct interaction with any other fields. They simply traverse their potential energy surface in a supercooled universe, and only after the ekpyrotic phase is the universe assumed to reheat, either through some coupling to Standard Model particles or through stringy, higher dimensional effects [58]. In this chapter, we consider a single, ekpyrotic field coupled to a perfect fluid of ultra-relativistic matter (*e.g.,* radiation) in thermal equilibrium. As the field falls down its steep, negative potential, it decays continuously into lighter fields which are thermally excited, thus generating a dissipative friction term in its equation of motion. We assume that the dissipation occurs under adiabatic conditions in which the microscopic dynamical processes operate much faster than the macroscopic evolution of the field and of the universe [122]. In this way, we approximate the dissipation to be local in time, a condition which may be difficult to achieve in a microphysical model. We return to this point in Sec. 4.4. As in the non-canonical, two-field models discussed above, this friction term allows a scale-invariant spectrum to be produced. In contrast to the non-canonical models, the scale-invariant spectrum is immediately adiabatic; no conversion is necessary.

To describe the interaction between the fluid and scalar field, we strive for generality, leaving the details of specific microphysical model-building for future work. Therefore, we work at the level of the equations of motion, adding generic dissipative and noise terms. As we will show, if the dissipation is too strong, the radiation fluid dominates the energy density of the universe; if it is too weak, the scalar field

dominates. Hence, our results require that the dissipation coefficient evolve in fixed proportion to the Hubble parameter. This is the main source of fine-tuning (although this tuning can be relaxed somewhat by changing the details of the interaction).

The idea of particle production during a cosmological smoothing and flattening phase has been investigated previously in models referred to as warm inflation, where thermal fluctuations sourced by radiation-induced noise were shown to dominate over vacuum fluctuations [123, 124, 125, 126, 122, 127]. Similar effects appear in models such as trapped inflation [128]. In contracting universes, however, the thermal fluctuations are suppressed on the largest scales, and the density perturbations are dominated by vacuum fluctuations. The reason is that contracting universes grow hotter with time, so that longer modes cross the horizon at lower temperature with correspondingly smaller thermal fluctuations.

This chapter is organized as follows. In Sec. 4.2, we solve and analyze the background evolution, showing the appearance of a new family of attractors introduced by the interaction between the ekpyrotic field and the radiation fluid. In Sec. 4.3, we compute the power spectrum for the comoving curvature perturbation by studying scalar perturbations to linear order. This results in a Langevin-like equation that we solve using Green's function techniques. We find that the thermal contribution to the power spectrum is subleading to the vacuum contribution over the observable modes, and we show how to fix the parameters of the model to obtain scale invariance. In Sec. 4.4, we discuss implications of our results and directions for future work.

4.2 Background

In this section, we derive an explicit solution for the background cosmology. The main results of this section are Eqs. (4.17) and Fig. 4.1.

We employ reduced Planck units in which $8\pi G_N = k_B = \hbar = c_L = 1$ where G_N is Newton's gravitational constant, k_B is Boltzmann's constant, $\hbar$ is the reduced Planck's constant, and c_L is the speed of light. We use the metric signature $(-,+,+,+)$. Commas denote ordinary derivatives, and semicolons denote covariant derivatives.

We consider a contracting universe populated with a radiation fluid and a minimally coupled scalar field obeying Einstein's equations,

$$G_{ab} = T_{ab}. \tag{4.1}$$

Here, G_{ab} is the Einstein tensor, and $T_{ab} = T^{(r)}_{ab} + T^{(\phi)}_{ab}$ is the total energy-momentum tensor which has been decomposed into a term describing the radiation fluid, denoted by the superscript (r), and a term describing the scalar field, denoted by the superscript (ϕ). The radiation fluid is characterized by a four-velocity, u^a, an energy density, ρ_r, and a pressure, p_r, so that its energy-momentum tensor is given by

$$T^{(r)}_{ab} = (\rho_r + p_r)u_a u_b + p_r g_{ab}. \tag{4.2}$$

For simplicity, we take $p_r = \rho_r/3$, although this is not central to our results. The scalar field is characterized by a potential energy density, $V(\phi)$, so that its energy-momentum tensor is given by

$$T^{(\phi)}_{ab} = \phi_{,a}\phi_{,b} - \left(\frac{1}{2}\phi^{;c}\phi_{;c} + V(\phi)\right) g_{ab}. \tag{4.3}$$

For convenience, we take the negative, exponential form, $V(\phi) = V_0 e^{-c\phi}$, where $V_0 < 0$ and $c > 0$. The interaction between the radiation fluid and the scalar field is described

by a flux term, $Q_a \equiv -\Gamma u^b \phi_{,b} \phi_{,a}$, satisfying

$$T^{(r)b}{}_{a;b} = -T^{(\phi)b}{}_{a;b} = Q_a. \tag{4.4}$$

In a spatially flat, Friedmann-Robertson-Walker spacetime, the background metric takes the form

$$ds^2 = a^2(\tau)\left(-d\tau^2 + \delta_{ij}dx^i dx^j\right) = -dt^2 + a^2(t)\delta_{ij}dx^i dx^j, \tag{4.5}$$

where a is the scale factor, $t < 0$ is cosmic time, and $\tau < 0$ is conformal time defined by $d\tau \equiv dt/a$. At background, Eqs. (4.4) gives two equations (from the t-component)

$$\ddot{\phi} + 3H\dot{\phi} + V_{,\phi} = -\Gamma\dot{\phi}, \tag{4.6}$$

$$\dot{\rho}_r + 4H\rho_r = \Gamma\dot{\phi}^2, \tag{4.7}$$

where overdots represent derivatives with respect to cosmic time and $H \equiv \dot{a}/a < 0$ is the Hubble parameter. The flux term, proportional to Γ, describes the decay of the ϕ-field into the particles comprising the radiation fluid. It appears in two places: on the right side of Eq. (4.7), it sources the energy density of the radiation, ensuring that ρ_r is not rapidly outstripped by the energy density in the ekpyrotic field, ϕ; but most important, in Eq. (4.6) it manifests as a dissipative friction term for ϕ. As we will see, this friction term is critical for the production of a scale-invariant spectrum.

As it stands, Eq. (4.6) for the scalar field is incomplete. It is well understood in the context of classical and quantum theory that whenever a process generates an effective dissipative interaction, it also generates fluctuations that can be described by a stochastic noise source, Ξ, with zero mean [129]. Thus, Eq. (4.6) should read

$$\ddot{\phi} + 3H\dot{\phi} + V_{,\phi} = -\Gamma\dot{\phi} + \Xi. \tag{4.8}$$

If the microphysical process responsible for this noise, Ξ, is in thermal equilibrium at some temperature, T, then the Fluctuation-Dissipation Theorem relates the dissipation it induces, Γ, to its correlation function via

$$\langle \Xi(x,\tau)\Xi(x',\tau')\rangle = 2\Gamma T\delta^{(3)}(x-x')\delta(\tau'-\tau), \tag{4.9}$$

where angular brackets denote ensemble averaging. If this process is not in thermal equilibrium, then its correlation, $\langle \Xi\Xi\rangle$, can depend more generally on (x,τ) and (x',τ'). As discussed in Sec. 4.1, this noise term is critical in warm inflation because it significantly enhances the power spectrum of scalar perturbations relative to the vacuum result. In the contracting models considered here, the opposite is true: as we will show, the noise, Ξ, is completely irrelevant to the power spectrum of the comoving curvature perturbation. Moreover, since it has zero mean, $\langle \Xi\rangle$, it is irrelevant to the background dynamics as well and will be omitted in the reminder of this section.

To find the background dynamics, Eqs. (4.6) and (4.7) must be solved subject to the Friedmann constraint (from the t-t component of Eq. (4.1)),

$$H^2 = \frac{1}{3}\left(\frac{1}{2}\dot{\phi}^2 + V + \rho_r\right). \tag{4.10}$$

To this end, it proves useful to introduce the dimensionless "Ω-variables," (or more properly their square roots)

$$(x,y,z) \equiv \left(\frac{\dot{\phi}}{\sqrt{6}H}, -\frac{\sqrt{|V|}}{\sqrt{3}H}, -\frac{\sqrt{\rho_r}}{\sqrt{3}H}\right), \tag{4.11}$$

characterizing respectively the fractional kinetic energy density in the scalar field, the fractional potential energy density in the scalar field, and the fractional energy density in the radiation fluid. In terms of these variables, Eq. (4.10) can be rewritten as $y = \sqrt{x^2+z^2-1}$, where we have taken the positive root since $H<0$ in a contracting

universe. The equation of state of the universe takes the simple form

$$\epsilon \equiv -\dot{H}/H^2 = 3x^2 + 2z^2, \tag{4.12}$$

as can be obtained by differentiating Eq. (4.10) and substituting Eqs. (4.6) and (4.7). Therefore, ekpyrosis occurs whenever $3x^2 + 2z^2 > 3$. Meanwhile, Eqs. (4.6) and (4.7) can be rewritten as

$$\frac{dx}{d\ln a} = 3(x^2 + z^2 - 1)\left(x - \frac{c}{\sqrt{6}}\right) - x\left(z^2 + \frac{\Gamma}{H}\right), \tag{4.13}$$

$$\frac{dz}{d\ln a} = (3x^2 + 2z^2 - 2)z + \frac{\Gamma}{H}\frac{x^2}{z}. \tag{4.14}$$

Note that Γ appears only in the ratio $\gamma \equiv \Gamma/H < 0$. It is at this point that the fine-tuning enters: we assume in this chapter that γ is a constant, independent of time. To motivate this assumption, note that if $|\gamma|$ grows rapidly, the universe becomes dominated by radiation only, and if it shrinks rapidly, the universe becomes dominated by the ekpyrotic field only. It is only when γ is roughly constant that these two components coexist. Therefore, we assume it in what follows, and merely observe in passing that if, *e.g.,* $\Gamma \propto T^2$ or $\sqrt{\rho_\phi}$, where $\rho_\phi \equiv \frac{1}{2}\dot{\phi}^2 + V$, then γ is constant along the solution of interest, and our assumption is justified. With this assumption, Eqs. (4.13) and (4.14) admit a fixed-point, scaling solution at (x_0, z_0) with

$$x_0 \equiv \left[\left(24\left(c^2+4\right)\gamma + 9\left(c^2-4\right)^2 + 16\gamma^2\right)^{1/2} + 3c^2 + 4\gamma + 12\right](6\sqrt{6}c)^{-1}, \tag{4.15}$$

$$z_0 \equiv [(\gamma+3)(\sqrt{9c^4 + 24(\gamma-3)c^2 + 16(\gamma+3)^2} + 4\gamma + 12) - 3c^2(\gamma-3)]^{1/2}(3\sqrt{2}c)^{-1}. \tag{4.16}$$

As a consistency check, note that in the absence of radiation, *i.e.,* when $\gamma = 0$, this solution reduces to $(x, z) = (c/\sqrt{6}, 0)$, which reproduces ordinary, single-field ekpyrosis (when $c > \sqrt{6}$).

To summarize, Eqs. (4.15) and (4.16) describe a cosmological background whose evolution is given by

$$\begin{aligned} a &= (t/t_{\rm e})^{\frac{1}{\epsilon}} & a &= (\tau/\tau_{\rm e})^{\frac{1}{\epsilon-1}} \\ H \equiv \dot{a}/a &= \frac{1}{\epsilon t} & \mathcal{H} \equiv a'/a &= \frac{1}{(\epsilon-1)\tau} \\ \phi &= \phi_{\rm e} + \frac{\sqrt{6}x_0}{\epsilon}\ln\left(t/t_{\rm e}\right) & \phi &= \phi_{\rm e} + \frac{\sqrt{6}x_0}{\epsilon-1}\ln\left(\tau/\tau_{\rm e}\right) \\ \rho_r &= \frac{3z_0^2}{\epsilon^2 t^2} & \rho_r &= \frac{3z_0^2\left(\tau/\tau_{\rm e}\right)^{-2\epsilon/(\epsilon-1)}}{\tau_{\rm e}^2(\epsilon-1)^2}, \end{aligned} \tag{4.17}$$

where $' \equiv d/d\tau$ and we have normalized the scale factor to unity when ekpyrosis ends at some time $t_{\rm e} < 0$. For convenience, we have included the results in conformal time and defined $\tau_{\rm e} \equiv \epsilon(\epsilon-1)^{-1}t_{\rm e}$ and

$$\phi_{\rm e} \equiv \frac{1}{c}\ln\left(-\frac{V_0\tau_{\rm e}^2(\epsilon-1)^2}{3\left(x_0^2+z_0^2-1\right)}\right). \tag{4.18}$$

These dynamics are pictured in Fig. 4.1, which shows that this solution is an attractor for a wide range of initial conditions.

We close this section by noting that if the flux term is changed to $Q_a = \Gamma(u^b\phi_{,b})^n\phi_{,a}$, for $n > 1$, it can be shown that the updated equations of motion admit a similar attractor so long as $\Gamma \propto H^{2-n}$. This alleviates the finely-tuned time dependence of Γ required for the stability of the background solution.

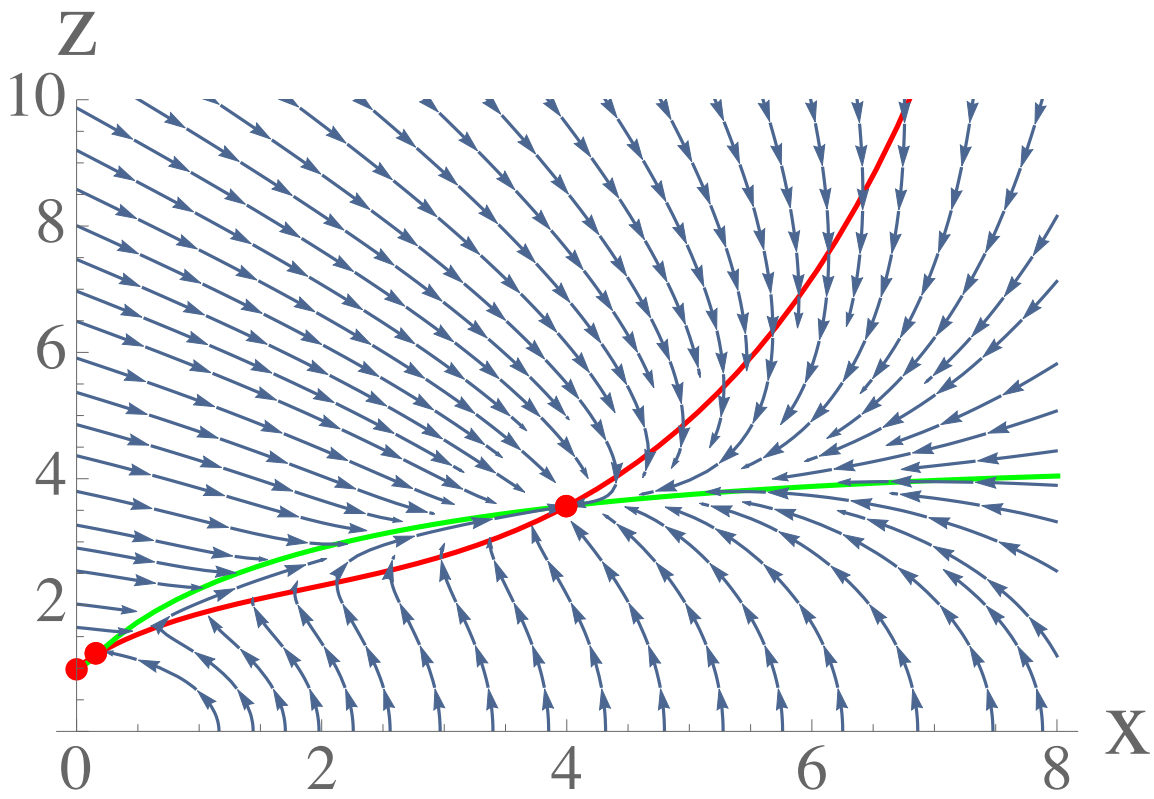

Figure 4.1: This streamplot shows that the warm ekpyrotic background solution is an attractor for a wide range of initial conditions. For illustration, we have chosen parameter values $(c, \gamma) = (15, -56.8)$. Any set of initial conditions for ϕ, $\dot{\phi}$, $\dot{\rho}$, and a corresponds to a particular point in this plane $(x, z) \equiv \left(\dot{\phi}/(\sqrt{6}H), -\sqrt{\rho_r}/(\sqrt{3}H)\right)$. The background solution follows the blue arrows originating at this point. The red and green curves are included simply to guide the eye: they are nullclines, where $dx/d\ln a = 0$ (red) and $dz/d\ln a = 0$ (green). The intersections of the nullclines are shown as red dots. These so called "fixed-point, scaling solutions" are special because the blue streamlines vanish here. If the background solution starts at one of these points, it stays there. The rightmost such point corresponds to (x_0, z_0) defined in Eqs. (4.15) and (4.16). Clearly, it is an attractor for a wide range of initial conditions. The analysis below shows that the comoving curvature perturbation generated by this solution acquires a scale-invariant spectrum on large scales.

4.3 Perturbations

In this section, we study scalar perturbations to linear order about the background solution described in Eqs. (4.17). We show that there exists a wide range in parameter space (*i.e.,* choices of c and γ) for which the comoving curvature perturbation acquires a scale-invariant power spectrum. This result is displayed in Fig. 4.2; it is the main result of this chapter.

A full derivation of the scalar perturbation equations in spatially-flat gauge is presented in Appendix 4.5. In this gauge, all perturbed quantities can be expressed in terms of the scalar potentials of the four-velocities of the radiation fluid, δu_r, and of the scalar field, δu_ϕ. In particular, the comoving curvature perturbation is

$$\mathcal{R} \equiv -\frac{H}{2\epsilon}(6x_0^2\delta u_\phi + 4z_0^2\delta u_r). \tag{4.19}$$

These potentials satisfy the coupled system

$$\delta u_\phi'' + \frac{C_1}{\tau}\delta u_\phi' + \left(k^2 + \frac{C_2}{\tau^2}\right)\delta u_\phi = \mathcal{J}_r(\delta u_r, k, \tau) + \xi(k,\tau), \tag{4.20}$$

$$\delta u_r'' + \frac{C_5}{\tau}\delta u_r' + \left(\frac{k^2}{3} + \frac{C_6}{\tau^2}\right)\delta u_r = \mathcal{J}_\phi(\delta u_\phi, k, \tau), \tag{4.21}$$

where

$$\mathcal{J}_r(\delta u_r, k, \tau) \equiv \frac{C_3}{\tau^2}\delta u_r + \frac{C_4}{\tau}\delta u_r', \tag{4.22}$$

$$\mathcal{J}_\phi(\delta u_\phi, k, \tau) \equiv \frac{C_7}{\tau^2}\delta u_\phi + \frac{C_8}{\tau}\delta u_\phi', \tag{4.23}$$

$\xi \equiv \Xi/\dot{\phi}^2$, and the C_i are constants that depend on c and γ, whose explicit definitions are given in Eqs. (4.71) and (4.62)-(4.69).

The purpose of the rest of this section is to solve Eqs. (4.20) and (4.21) for general c and γ so that we can find $\mathcal{R}$ via Eq. (4.19). Before solving this system in general (Sec. 4.3.2), we first review the solution in the cold case when $\gamma = 0$ (Sec. 4.3.1).

4.3.1 Cold ekpyrosis

In this subsection, we reproduce the result of standard, single-field ekpyrosis, *i.e.*, without radiation, for which a scale-invariant spectrum for $\mathcal{R}$ is impossible [97].

Recall that with no radiation ($\gamma = 0$) and a sufficiently steep potential ($c > \sqrt{6}$), the background solution in Eqs. (4.15) and (4.16) reduces to $(x_0, z_0) = (c/\sqrt{6}, 0)$. As for the perturbations, δu_r vanishes identically, and Eq. (4.20) becomes

$$\delta u_\phi'' + \frac{C_1}{\tau}\delta u_\phi' + \left(k^2 + \frac{C_2}{\tau^2}\right)\delta u_\phi = 0, \tag{4.24}$$

with $C_1 = -2$ and $C_2 = 2c^2\left(c^2-3\right)\left(c^2-2\right)^{-2}$. The selection of Bunch-Davies vacuum fixes

$$\delta u_\phi(k,\tau) = \frac{\epsilon - 1}{\sqrt{2\epsilon}}\sqrt{\frac{\pi}{4}}(-\tau)^{\frac{1-C_1}{2}} H^{(1)}_{\nu_\phi}(-k\tau), \tag{4.25}$$

where, in terms of the function

$$\nu(X,Y) \equiv \frac{1}{2}\sqrt{(X-1)^2 - 4Y}, \tag{4.26}$$

we have defined $\nu_\phi \equiv \nu(C_1, C_2)$. In the next subsection, we will use this same normalization for the perturbation, δu_ϕ, since at early times, the temperature, T, and dissipation, Γ, are small. In the super-horizon limit, $-k\tau \to 0$, Eq. (4.25) approaches $\delta u_\phi \propto k^{-\nu_\phi}$, so the spectral index is given by

$$n_s \;=\; 4 - 2\nu_\phi = 3 + \frac{4}{c^2-2}, \tag{4.27}$$

which is clearly blue (in particular > 3) for ekpyrosis (which requires $c > \sqrt{6}$). Thus, scale-invariance is impossible in the single-field model.

4.3.2 Warm ekpyrosis

In this subsection, we consider the "warm" case when $\gamma \neq 0$. The presence of the radiation fluid introduces into Eqs. (4.20) and (4.21) two crucial differences: the first is that C_1 and C_2 depend not only on the steepness, c, of the potential, but also on the dissipation rate, γ; the second is that δu_r is no longer negligible.

To solve the system, we decompose the scalar potential for the four-velocity of the radiation fluid as $\delta u_r = \delta u_r^{\rm h} + \delta u_r^{\rm p}$, where the first term is a homogeneous solution to Eq. (4.21) with $\mathcal{J}_\phi$ set to 0, *i.e.*,

$$\delta u_r^{\rm h}(k,\tau) = (-k\tau)^{\frac{1-C_5}{2}}[a_1(k)J_{\nu_r}(-k\tau) + a_2(k)Y_{\nu_r}(-k\tau)], \tag{4.28}$$

and the second term is the particular solution given by integrating over the retarded Green's function, *i.e.*,

$$\delta u_r^{\rm p}(k,\tau) = k^{-1}\int_{-\infty}^{\tau} G_r(-k\tau,-k\bar{\tau})\mathcal{J}_\phi(\delta u_\phi,k,\bar{\tau})d\bar{\tau}. \tag{4.29}$$

In the above, $a_1(k)$ and $a_2(k)$ are integration constants and

$$G_r(z,y) \equiv \frac{\pi}{2} y\,(z/y)^{\frac{1-C_5}{2}}\left[J_{\nu_r}\left(z/\sqrt{3}\right)Y_{\nu_r}\left(y/\sqrt{3}\right) - Y_{\nu_r}\left(z/\sqrt{3}\right)J_{\nu_r}\left(y/\sqrt{3}\right)\right] \tag{4.30}$$

with $\nu_r \equiv \nu(C_5, C_6)$. In Appendix 4.6, we show that the integral in Eq. (4.29) can be approximated by

$$\delta u_r^{\rm p} \approx (C_7/C_6)\theta(1-k|\tau|)\delta u_\phi, \tag{4.31}$$

where $\theta(x)$ is the Heaviside step function. That is, $\delta u_r^{\rm p}$ is negligible before horizon crossing and is a constant multiple of δu_ϕ after horizon crossing (see Fig. 4.4).

Armed with these solutions, we now turn to Eq. (4.20). The right side is a sum of three terms, $\mathcal{J}_r(\delta u_r^{\rm p}, k, \tau) + \mathcal{J}_r(\delta u_r^{\rm h}, k, \tau) + \xi$. The last term is negligible as discussed in detail in Appendix 4.7. The second term is a rapidly decreasing function that depends on the initial state of $\delta u_r^{\rm h}$. We restrict attention to models where this term begins sufficiently small that it can be neglected. Therefore, we need only consider $\mathcal{J}_r(\delta u_r^{\rm p})$. Inside the horizon, it has no effect, but outside the horizon, it renormalizes the "dissipation" and "frequency" terms on the left side of Eq. (4.20)

$$C_1 \to \tilde{C}_1 \equiv C_1 - C_4 C_7 C_6^{-1}, \tag{4.32}$$

$$C_2 \to \tilde{C}_2 \equiv C_2 - C_3 C_7 C_6^{-1}, \tag{4.33}$$

as is clear from substituting Eq. (4.31) into Eq. (4.22) and putting the result into Eq. (4.20).

Therefore, the subhorizon solution is given by

$$\delta u_\phi^{\rm sub} = \frac{\epsilon - 1}{\sqrt{2\epsilon}} \sqrt{\frac{\pi}{4}} (-\tau)^{\frac{1-C_1}{2}} H^{(1)}_{\nu_\phi}(-k\tau), \tag{4.34}$$

and the superhorizon solution is given by

$$\delta u_\phi^{\rm sup} = (-\tau)^{\frac{1-\tilde{C}_1}{2}} \left(\kappa_1 J_{\tilde{\nu}_\phi}(-k\tau) + \kappa_2 Y_{\tilde{\nu}_\phi}(-k\tau) \right), \tag{4.35}$$

where $\tilde{\nu}_\phi \equiv \nu(\tilde{C}_1, \tilde{C}_2)$, and κ_1 and κ_2 are approximated by the following matching conditions at horizon crossing ($-k\tau = 1$)

$$\delta u_\phi^{\rm sub} = \delta u_\phi^{\rm sup}, \tag{4.36}$$

$$(\delta u_\phi^{\rm sup})' - (\delta u_\phi^{\rm sub})' = -C_4 C_7 C_6^{-1} k \, \delta u_\phi^{\rm sub}, \tag{4.37}$$

i.e.,

$$\begin{aligned}\kappa_1 &= -\frac{\pi^{3/2}(\epsilon-1)}{8\sqrt{2}C_6\sqrt{\epsilon}}\Bigg(H^{(1)}_{\nu_\phi}(1)(Y_{\tilde{\nu}_\phi}(1)(\tilde{C}_1 - C_1 \\ &\quad +2(C_4C_7C_6^{-1}+\tilde{\nu}_\phi-\nu_\phi)) - 2Y_{\tilde{\nu}_\phi-1}(1)) \\ &\quad +2H^{(1)}_{\nu_\phi-1}(1)Y_{\tilde{\nu}_\phi}(1)\Bigg)\times k^{\frac{C_1-\tilde{C}_1}{2}}, \qquad (4.38)\\ \kappa_2 &= \frac{\pi^{3/2}(\epsilon-1)}{8\sqrt{2}C_6\sqrt{\epsilon}}\Bigg(H^{(1)}_{\nu_\phi}(1)(J_{\tilde{\nu}_\phi}(1)(\tilde{C}_1 - C_1 \\ &\quad +2(C_4C_7C_6^{-1}+\tilde{\nu}_\phi-\nu_\phi)) - 2J_{\tilde{\nu}_\phi-1}(1)) \\ &\quad +2H^{(1)}_{\nu_\phi-1}(1)J_{\tilde{\nu}_\phi}(1)\Bigg)\times k^{\frac{C_1-\tilde{C}_1}{2}}, \qquad (4.39)\end{aligned}$$

Substituting the solution in Eq. (4.35), together with Eqs. (4.38) and (4.39), into Eq. (4.19), we find that the primordial power spectrum of the comoving curvature perturbation on superhorizon scales is given by

$$\Delta^2_{\mathcal{R}}(k,\tau) \equiv \frac{k^3}{2\pi^2}|\mathcal{R}|^2 \approx \mathcal{O}(10^{-4})V_{\rm end}^{\frac{1+\tilde{C}_1+2\tilde{\nu}_\phi}{2}}k^{n_s-1}, \qquad (4.40)$$

where $V_{\rm end} \equiv |V_0|e^{-c\phi_{\rm e}}$ is the magnitude of the potential energy density when ekpyrosis ends, and the spectral index is given by

$$n_s = 4 - 2\tilde{\nu}_\phi + (C_1 - \tilde{C}_1), \qquad (4.41)$$

which is plotted in Fig. 4.2.

Given any point in the c-γ plane, the height of the surface above that point shows the spectral index, n_s. The color scheme reflects that for $n_s > 1$, the spectrum is blue and for $n_s < 1$, the spectrum is red. The thick, blue curve at $\gamma = 0$ reproduces the results of ordinary, single-field ekpyrosis from Eq. (4.27). As discussed in Sec. 4.3.1, this curve describes a blue-tilted spectrum that is inconsistent with observation. However, note the effect of particle production on the spectral index: at any value of c, increas-

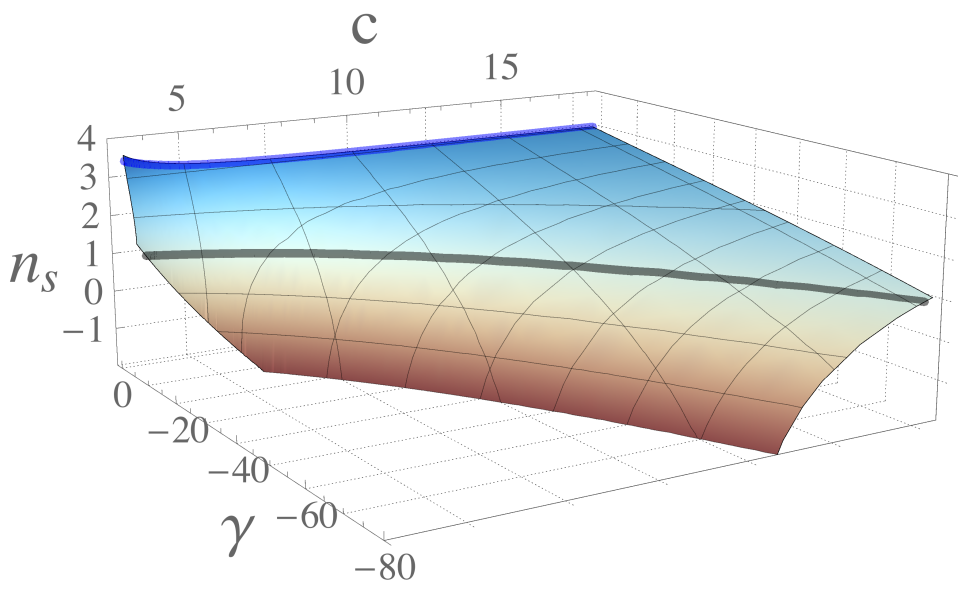

Figure 4.2: This shows n_s as a function of c and γ for the background solution in Eqs. (4.17).

ing the dissipation rate, $|\gamma|$, reddens the spectrum. In particular, the thick, black curve has $n_s = 1$. Any choice of c and γ along this curve corresponds to an exactly scale-invariant spectrum. For such a choice, the exponent of $V_{\rm end}$ in Eq. (4.40) can be computed and is roughly .61, so that to match the observed amplitude, $V_{\rm end}$ must be made of order $V_{\rm end}^{1/4} \sim 10^{16}$ GeV, which is high enough to recover the successful predictions of hot big bang nucleosynthesis.

In this section, we have ignored isocurvature perturbations. The reason is that even though they are not negligible at the end of ekpyrosis, reheating will render them thus, provided the universe reheats in local thermal and chemical equilibrium with no nonzero conserved quantities (see Ref. [130]). Therefore, our assumption that isocurvature perturbations can be ignored amounts to this rather mild constraint on reheating. This can be achieved, *e.g.,* if the ϕ-field completely decays into thermalized radiation at sufficiently early time.

4.4 Discussion

In this chapter, we have presented a scenario for ekpyrosis that continuously generates a scale-invariant spectrum of adiabatic perturbations. The key is the continuous decay of the ekpyrotic field; this decay introduces a friction term that allows a scale-invariant spectrum to be achieved. More generally, as can be seen by following a curve of constant c along the surface in Fig. 4.2, we showed that the effect of particle production is to redden the power spectrum of the supercooled theory.

We view the elimination of the second scalar field and hence any subsequent conversion mechanism as a major simplification, and a return to the spirit of the original formulation of ekpyrosis, since the hydrodynamical behavior at finite temperature is universal regardless of the details of its microscopic origin. While we have not attempted to embed this phase into a complete cosmological history, the decay into radiation presents the tantalizing possibility of evading the need for additional reheating (provided the radiation so generated does not present complications for realizing a bounce).

There are two key assumptions that merit attention. The first is that the dissipation rate must scale with the Hubble parameter. This scaling represents the greatest source of fine-tuning (although see the last paragraph of Sec. 4.2 for a possible alternative). The second is that the initial fluctuations of the fluid, δu_r^{h}, are small enough to be neglected. If these conditions are met, it is always possible to choose the parameters c and γ such that a scale-invariant spectrum is achieved.

There are many directions for future work. One possibility is to consider generalizations of the radiation fluid within the framework presented here, as was done in warm inflation [131]. For example, one could analyze a fluid with a non-relativistic equation of state or that is out of thermal equilibrium. One could also include viscosity by adding corrections to its energy-momentum tensor, $T_{ab}^{(r)}$.

Another possibility is to devise a microphysical theory– to identify the microscopic degrees of freedom comprising the fluid that realizes the effective dynamics described here. For example, one could try to reproduce the trapped inflation scenario in a contracting universe [128]. In warm inflation, this is difficult, though not impossible [132, 133, 134], to achieve because, as argued in Ref. [135], the dissipation coefficient, Γ, appears as the result of a small correction to a sub-leading thermal correction to the potential energy density of the inflaton, which must be extremely flat to support inflation. Thus, non-negligible Γ requires large thermal corrections, which spoil the extreme flatness of the potential. In ekpyrosis, such extreme flatness is neither required nor permitted. Nevertheless, constructing a microphysical model may also prove difficult for warm ekpyrosis. We assumed in this chapter that the degrees of freedom in the thermal bath induce a dissipation coefficient that is local in time. However, as indicated above, interactions between a scalar field and the degrees of freedom in an ambient thermal bath generically lead to non-local terms in the equation of motion for the scalar field. These terms can be approximated with a local friction term only when the microphysical dynamics of these degrees of freedom operate much faster than the evolution of the ekpyrotic field and the contraction of the universe. Since the background solution in Eq. (4.17) involves only a logarithmic dependence of the ekpyrotic field on time, it may be possible to find a model where these non-local interactions are well approximated by a local term, but we leave this for future work. In addition, the scaling $\Gamma \propto H$ may require nontrivial microphysics. For example, if the dissipation coefficient depends only on temperature, this scaling requires $\Gamma \propto T^2$, which may be difficult to achieve [136, 137, 138, 135, 139, 140].

It is important to understand to what extent dissipation affects the tensor-to-scalar ratio. One does not expect dissipation to alter the tensor spectrum from the predictions of ordinary, single-field ekpyrosis, in which it is strongly blue-tilted and exponentially suppressed on large scales [112]. Since we have shown that dissipation

flattens the scalar spectrum, we expect the tensor-to-scalar ratio to be exponentially suppressed on observable scales.

It is also important to understand the effects of dissipation on the non-Gaussian signatures. A reason to be optimistic is that, as we have shown, neither the steepness, c, of the potential nor the equation of state parameter of the universe, ϵ, needs to be tuned particularly large. As discussed above, one microphysical realization for which the machinery already exists to compute non-Gaussianities would be an ekpyrotic analog of the trapped inflation scenario [128]. In such a realization, the ekpyrotic field falls down its potential, transferring its kinetic energy into the production of other particles via couplings of the form

$$\frac{1}{2}\sum g_i^2(\phi-\phi_i)\chi_i^2. \tag{4.42}$$

As ϕ passes each ϕ_i, the particles corresponding to the field χ_i become light and are copiously produced with an energy density controlled by g_i. As a consequence, the ekpyrotic field receives an effective friction term in its equation of motion– also controlled by the $\{g_i\}$– which can be chosen to approximate the dissipative dynamics studied here. In trapped inflation, these effects were used to support slow roll on potentials that were otherwise too steep. The techniques developed in Ref. [128] for the computation of non-Gaussianities would apply as well to ekpyrotic potentials. For comparison, the models discussed in Refs. [107, 120, 114, 66] generate no non-Gaussianity during the ekpyrotic phase.

4.5 Appendix A: Perturbation equations

In this appendix, we will derive the linearized perturbation equations. We will follow the notation of Ref. [141] (see also Ref. [142]). To simplify the derivation, we will

find the linearized equations for the ensemble expectation values of the fields. This implies that any stochastic contribution to these equations will vanish.

A metric with the most general scalar-type perturbation in a flat Friedman-Robertson-Walker background is

$$ds^2 = -a^2(1+2\alpha)d\tau^2 - 2a^2\beta_{,i}d\tau dx^i + a^2\left[\delta_{ij}(1+\varphi) + 2\psi_{,ij}\right]dx^i dx^j \tag{4.43}$$

Ignoring anisotropic stress, the energy-momentum tensor for the fluid can be decomposed as

$$\begin{aligned} T^{(r)\tau}{}_{\tau} &= -(\rho_r + \delta\rho_r) && (4.44)\\ T^{(r)\tau}{}_{i} &= a(\rho_r + p_r)\delta u_{r,i} && (4.45)\\ T^{(r)i}{}_{j} &= (p_r + \delta p_r)\delta_{ij}, && (4.46) \end{aligned}$$

Thus, perturbations in the fluid are parameterized by $\delta\rho_r, \delta p_r$ and δu_r. For simplicity, we will assume $\delta p_r = \delta\rho_r/3$, though this is not central to our results. In writing the perturbation equations, it is useful to define the shear, $\chi \equiv a(\beta + a\dot{\psi})$, and the perturbed expansion of the normal-frame vector field $\kappa \equiv 3(-\dot{\varphi} + H\alpha) + \frac{k^2}{a^2}\chi$. In Fourier space, the perturbation equations are

$$\begin{aligned} -\frac{k^2}{a^2}\varphi + H\kappa &= -\frac{1}{2}\delta\rho, && (4.47)\\ \kappa - \frac{k^2}{a^2}\chi + \frac{3}{2}\sum_{i=r,\phi}(\rho_i + p_i)\delta u_i &= 0, && (4.48)\\ \dot{\chi} + H\chi - \alpha - \varphi &= 0, && (4.49)\\ \dot{\kappa} + 2H\kappa + \left(3\dot{H} - \frac{k^2}{a^2}\right)\alpha &= \frac{1}{2}(\delta\rho + 3\delta p), && (4.50)\\ \delta\dot{\rho}_r + 3H(\delta\rho_r + \delta p_r) + \frac{k^2}{a^2}(\rho_r + p_r)\delta u_r &= +\delta q_r + \dot{\rho}_r\alpha + (\rho_r + p_r)\kappa, && (4.51)\\ \frac{-1}{a^3(\rho_r + p_r)}\frac{d}{dt}\left[a^3(\rho_r + p_r)\delta u_r\right] &= \frac{\delta p_r}{\rho_r + p_r} + \alpha - \frac{j_r}{\rho_r + p_r}, && (4.52)\\ \delta\ddot{\phi} + 3H\delta\dot{\phi} + \left(\frac{k^2}{a^2} + V_{,\phi\phi}\right)\delta\phi &= \dot{\phi}(\kappa + \dot{\alpha}) - \delta q_\phi + (2\ddot{\phi} + 3H\dot{\phi})\alpha, && (4.53) \end{aligned}$$

where

$$\delta\rho \equiv \delta\rho_r + \dot{\phi}\delta\dot{\phi} - \dot{\phi}^2\alpha + V_{,\phi}\delta\phi, \tag{4.54}$$

$$\delta p \equiv \delta p_r + \dot{\phi}\delta\dot{\phi} - \dot{\phi}^2\alpha - V_{,\phi}\delta\phi, \tag{4.55}$$

$$\delta u_\phi \equiv -\delta\phi/\dot{\phi}, \tag{4.56}$$

$$\delta q_r \equiv \delta\Gamma\dot{\phi}^2 + 2\Gamma\dot{\phi}\delta\dot{\phi} - 2\alpha\Gamma\dot{\phi}^2, \tag{4.57}$$

$$\delta q_\phi \equiv \delta\Gamma\dot{\phi} - \Gamma\alpha\dot{\phi} + \Gamma\delta\dot{\phi}, \tag{4.58}$$

$$j_r \equiv -\Gamma\dot{\phi}\delta\phi. \tag{4.59}$$

Eqs. (4.47)-(4.52) are, respectively, the G^t_t component of the field equations, the G^t_i component, the $G^i_j - \frac{1}{3}\delta^i_j G^k_k$ component, the $G^i_i - G^t_t$ component, the $T^{(r)b}{}_{i;b} = Q_i$ component, the $T^{(r)b}{}_{t;b} = Q_t$ component, and the $T^{(\phi)b}{}_{t;b} = -Q_t$ component.

Henceforth, we work in spatially flat gauge ($G = \varphi = 0$). Then Eqs. (4.47) and (4.48) can be solved algebraically for the metric variables α and β in terms of the matter variables $\delta\phi, \delta u_r$, and $\delta\rho_r$. Eq. (4.52) can then be solved algebraically for $\delta\rho_r$ in terms of δu_r and $\delta\phi$. Substituting these results into Eqs. (4.51) and (4.53) leaves two closed equations for the variables δu_r and δu_ϕ. Specializing to the background solution in Eqs. (4.17), these are

$$\delta\ddot{u}_\phi + c_1 H\delta\dot{u}_\phi + \left(\frac{k^2}{a^2} + c_2 H^2\right)\delta u_\phi = c_3 H^2\delta u_r + c_4 H\delta\dot{u}_r \tag{4.60}$$

$$\delta\ddot{u}_r + c_5 H\delta\dot{u}_r + \left(\frac{k^2}{3a^2} + c_6 H^2\right)\delta u_r = c_7 H^2\delta u_\phi + c_8 H\delta\dot{u}_\phi, \tag{4.61}$$

with the constants c_i defined by

$$
\begin{aligned}
c_1 &\equiv -\frac{\sqrt{6}cz_0^2}{x_0} - \sqrt{6}cx_0 + \frac{\sqrt{6}c}{x_0} - \gamma - 3, && (4.62)\\
c_2 &\equiv 6\sqrt{6}cx_0^3 + 6\sqrt{6}cx_0z_0^2 - 6\sqrt{6}cx_0 - 18x_0^4 \\
&\quad -24x_0^2z_0^2 + 27x_0^2 + 2\gamma z_0^2 + 6z_0^2 + \frac{\sqrt{6}}{2}c\gamma x_0, && (4.63)\\
c_3 &\equiv -\frac{2\sqrt{6}cz_0^4}{x_0} - 2\sqrt{6}cx_0z_0^2 + \frac{2\sqrt{6}cz_0^2}{x_0} \\
&\quad -8\gamma x_0^2 + 12x_0^2z_0^2 + 16z_0^4 - 2\gamma z_0^2 - 8z_0^2, && (4.64)\\
c_4 &\equiv -4z_0^2, && (4.65)\\
c_5 &\equiv \frac{4\gamma x_0^2}{z_0^2} - 1, && (4.66)\\
c_6 &\equiv -\frac{2\sqrt{6}c\gamma x_0^3}{z_0^2} - 2\sqrt{6}c\gamma x_0 + \frac{2\sqrt{6}c\gamma x_0}{z_0^2} \\
&\quad -\frac{6\gamma x_0^4}{z_0^2} - 7\gamma x_0^2 - \frac{4\gamma^2 x_0^2}{z_0^2} - \frac{6\gamma x_0^2}{z_0^2} \\
&\quad -8x_0^2z_0^2 + 3x_0^2 - 8z_0^4 + 10z_0^2, && (4.67)\\
c_7 &\equiv -\frac{2\sqrt{6}c\gamma x_0^3}{z_0^2} - 3\sqrt{6}cx_0^3 - 2\sqrt{6}c\gamma x_0 + \frac{2\sqrt{6}c\gamma x_0}{z_0^2} \\
&\quad -3\sqrt{6}cx_0z_0^2 + 3\sqrt{6}cx_0 + 12x_0^4 - 5\gamma x_0^2 - \frac{4\gamma^2 x_0^2}{z_0^2} \\
&\quad -\frac{6\gamma x_0^2}{z_0^2} + 12x_0^2z_0^2 - 18x_0^2, && (4.68)\\
c_8 &\equiv \frac{5\gamma x_0^2}{2z_0^2} + 2x_0^2, . && (4.69)
\end{aligned}
$$

For concreteness, we have assumed $\Gamma \propto \sqrt{V(\phi)}$, independent of ρ_r and $\dot{\phi}$, *i.e.,* $\Gamma = -\gamma\sqrt{-V(\phi)/(3(x_0^2+z_0^2-1))}$. For this choice, $\delta\Gamma = \gamma cH\delta\phi/2$. Of course, for a realistic model, Γ should depend on the temperature of the radiation fluid [136]; the field dependence is not required [137, 138, 135]. One possibility, which preserves the $\Gamma \propto H$ scaling necessary for the warm ekpyrotic background solution, is $\Gamma \propto T^2/M$, where M is some mass scale fixed by the background solution. More generally, Γ can be any function of T and ϕ, provided the scaling $\Gamma \propto H$ is preserved.

We have performed the analysis for the two extreme cases, where $\Gamma \propto \sqrt{V(\phi)}$ and where $\Gamma \propto T^2$ and found that both cases give qualitatively similar results, namely, a scale-invariant scalar spectrum is possible. There are only minor differences, *e.g.,* in the c_i in Eqs. (4.62)-(4.69). This is important because in warm inflation, a temperature dependence in the dissipation coefficient can have large effects on the primordial scalar spectrum as shown in Refs. [136, 139, 140].

As we explained above, in deriving these equations, we have averaged out the stochastic fluctuations. However, at background level, we know that whatever microphysical process generates the dissipation, Γ, in the equation of motion for the scalar field, must also be accompanied by a stochastic source, Ξ, whose correlation satisfies the Fluctuation-Dissipation Theorem (see Appendix 4.7 for details). That is, Eq. (4.60) must be replaced with

$$\delta\ddot{u}_\phi + c_1 H \delta\dot{u}_\phi + \left(\frac{k^2}{a^2} + c_2 H^2\right)\delta u_\phi = c_3 H^2 \delta u_r + c_4 H \delta\dot{u}_r + \xi(k,t), \tag{4.70}$$

where $\xi \equiv \Xi/\dot{\phi}^2$ with the extra factors of $\dot{\phi}$ in the denominator coming from the change of variables from $\delta\phi$ to δu_ϕ. In conformal time, Eqs. (4.70) and (4.61) become Eqs. (4.20) and (4.21) , with

$$C_i = \begin{cases} \frac{c_i - 1}{\epsilon - 1} & \text{if } i = 1, 5 \\ \frac{c_i}{(\epsilon-1)^2} & \text{if } i = 2, 3, 6, 7 \\ \frac{c_i}{\epsilon - 1} & \text{if } i = 4, 8 \end{cases} \tag{4.71}$$

where again $\epsilon \equiv 3x_0^2 + 2z_0^2$.

4.6 Appendix B: Locality of fluid response

Since, in general, fluids behave non-locally we will show in this appendix how locality can be recovered in the late time limit. This is because the sources for the fluid are $\tau^{-2}\delta u_\phi(k,\tau), \tau^{-1}\delta u'_\phi(k,\tau)$ and not δu_ϕ itself. Using the expression for the source, $\mathcal{J}_\phi$, in Eq. (4.23) and integrating the derivative term by parts, the particular solution for the radiation fluid in Eq. (4.29) can be rewritten as

$$\delta u_r^{\rm p}(z) = \int_z^\infty dy K_r(z,y)\delta u_\phi(y), \tag{4.72}$$

where $z \equiv -k\tau$ and we defined the kernel

$$K_r(z,y) \equiv \frac{C_7+C_8}{y^2}G_r(z,y) - \frac{C_8}{y}G_{r,y}(z,y). \tag{4.73}$$

Now, we will show that this kernel behaves locally in the small z (superhorizon) approximation. It follows from the explicit expression of the Green's functions that $K_r(z,z) \to \infty$ and $K_r(z,y) \to 0$ for $z \neq y$ as $z \to 0$. These properties are illustrated in Fig. 4.3. To compute the particular solution for the radiation fluid, we can therefore make the local approximation

$$\delta u_r^{\rm p}(z) = \int_z^\infty dy K_r(z,y)\delta u_\phi(y) \approx \delta u_\phi(z)\int_z^\infty dy K_r(z,y). \tag{4.74}$$

In the small z limit, this integral can be done exactly and gives

$$\int_z^\infty dy K_r(z,y) = \frac{C_7}{C_6} + \mathcal{O}(z^{\frac{1-C_5+2\nu_r}{2}}). \tag{4.75}$$

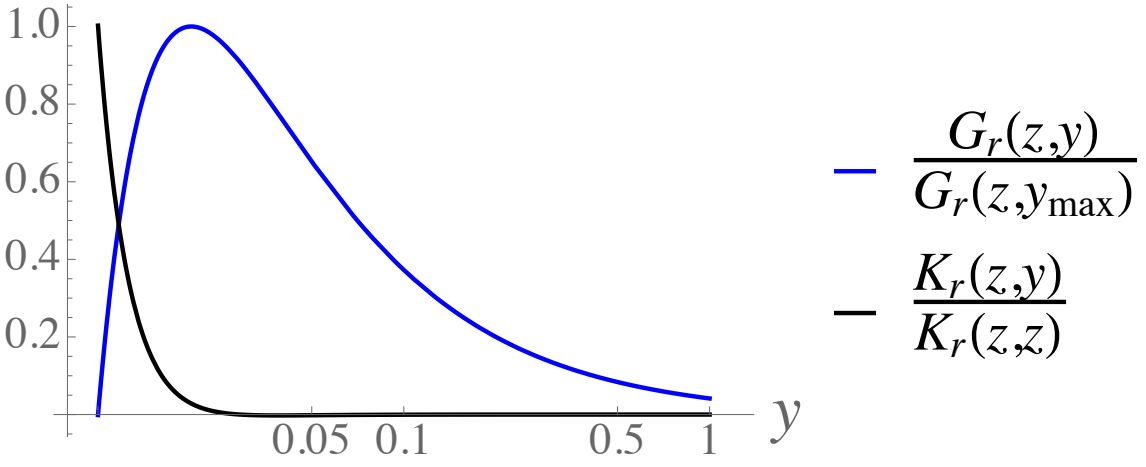

(a)

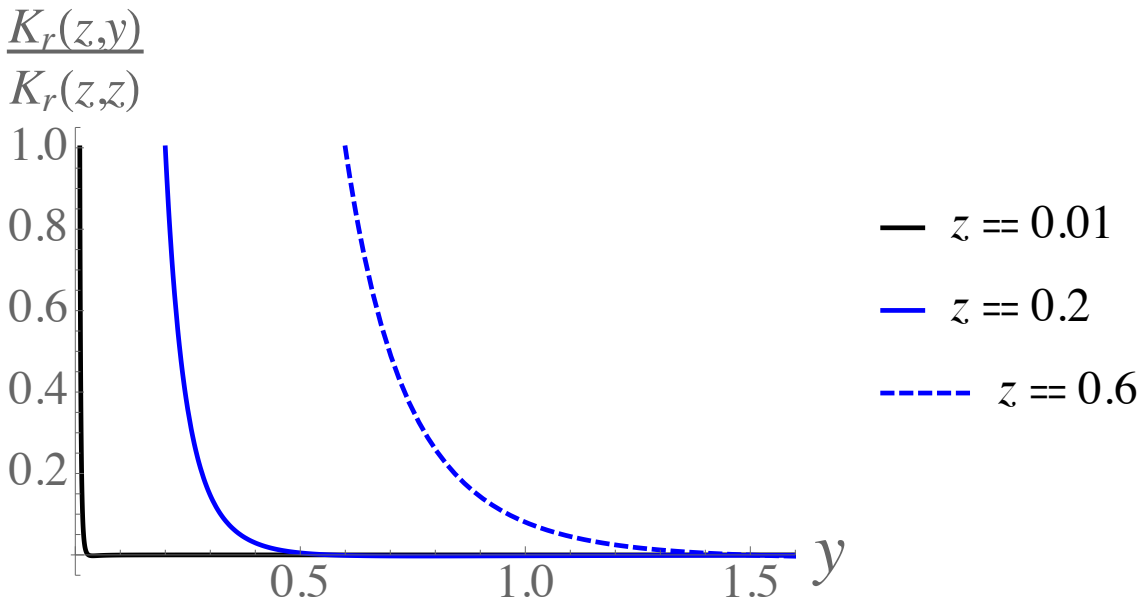

(b)

Figure 4.3: (a) Comparison of the locality of the Green's function, G_r, (blue) and the kernel, K_r, (black) for $z = 10^{-2}$. Both are normalized such that their maximum value is 1: as should be clear, $y_{\max}$ is the argument for which $G_r(z, y)$ is maximized. Note the logarithmic scale on the horizontal axis. (b) Comparison of the fluid kernel, K_r at different final times, z. As modes are stretched beyond the horizon $z \ll 1$, this kernel becomes increasingly local. For both plots, we used $(c, \gamma) = (15, -56.8)$.

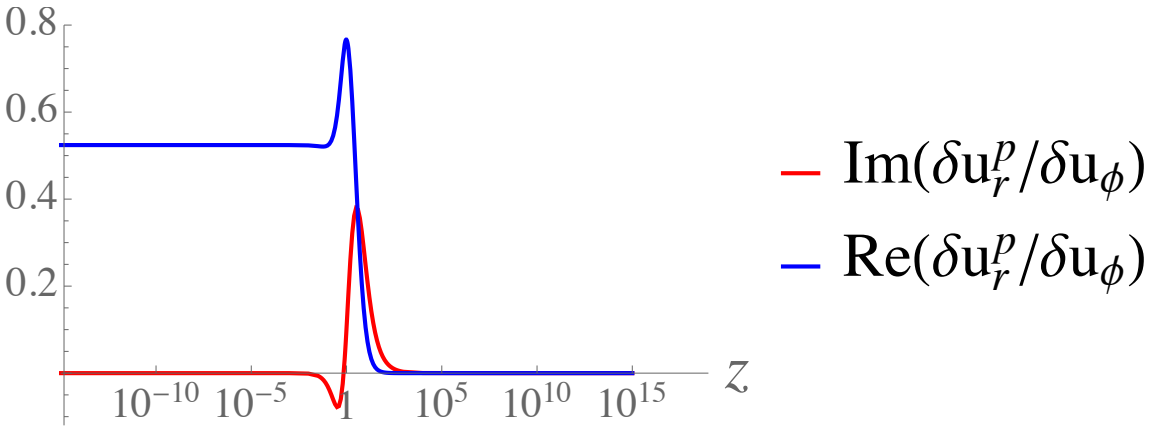

Figure 4.4: This plot shows the time dependence of the real (blue) and imaginary (red) parts of the ratio $\delta u_r^{\rm p}/\delta u_\phi$ when $(c,\gamma) = (15,-56.8)$. Recall δu_ϕ is given by Eqs. (4.34) and (4.35) and $\delta u_r^{\rm p}$ is given by Eq. (4.29), or, equivalently, by Eq. (4.72). There is a sharp transition once a mode exits the horizon. Inside the horizon ($z > 1$), the particular solution for the fluid $\delta u_r^{\rm p}$ is negligible. Outside ($z < 1$) it rapidly approaches a constant factor, roughly C_7/C_6, times δu_ϕ. This justifies the mode matching procedure in the text.

Therefore, in this limit, we make the approximation (see Fig. 4.4)

$$\delta u_r^{\rm p}(z) \approx (C_7/C_6)\delta u_\phi(z) + \mathcal{O}(z^{\frac{1-C_5+2\nu_r}{2}}). \tag{4.76}$$

4.7 Appendix C: Thermal contribution to the scalar spectrum

In this appendix, we will show that the thermal contribution to the power spectrum of the comoving curvature perturbation, $\Delta^2_{\mathcal{R}}$, is negligible for the observable modes in comparison to the vacuum, scale-invariant contribution.

To prove this, we write the particular solution for the scalar field perturbation in terms of the stochastic noise

$$\delta u_\phi(\mathbf{k},\tau_{\rm e}) = k^{-1}\int_{-\infty}^{\tau_{\rm e}} d\tau G_\phi(-k\tau_{\rm e},-k\tau)\xi(\mathbf{k},\tau), \tag{4.77}$$

where G_ϕ is the retarded Green's function for Eq. (4.20), and again, $\tau_{\rm e}$ is the time at which ekpyrosis ends. The two-point function of the noise follows from the Fluctuation-Dissipation Theorem in Eq. (4.9)

$$\langle \xi(\mathbf{k},\tau)\xi(\mathbf{k}',\tau')\rangle = \mathcal{N}_{\rm FD}(2\pi)^3\delta(\mathbf{k}+\mathbf{k}')\delta(\tau-\tau'), \tag{4.78}$$

where the noise kernel is given by

$$\mathcal{N}_{\rm FD} \equiv 2\Gamma T/\dot\phi^2, \tag{4.79}$$

with the extra factors of $\dot\phi$ in the denominator coming from the change of variables from $\delta\phi$ to δu_ϕ. Substituting Eq. (4.78) into Eq. (4.77) and changing the integration variable to $y=-k\tau$, the thermal power spectrum for δu_ϕ is given by

$$\begin{aligned}&\langle \delta u_\phi(\mathbf{k},\tau_{\rm e})\delta u_\phi(\mathbf{k}',\tau_{\rm e})\rangle \\ &= \frac{1}{k^3}\left\{\int_{-k\tau_{\rm e}}^{\infty}[G_\phi(-k\tau_{\rm e},y)]^2\mathcal{N}_{\rm FD}dy\right\}\times \\ &(2\pi)^3\delta^{(3)}(\mathbf{k}+\mathbf{k}').\end{aligned} \tag{4.80}$$

To compute this integral, we separate out the time dependence of the noise kernel, *i.e.*, $\mathcal{N}_{\rm FD} = \mathcal{N}_0(-\tau)^{\frac{1}{2}+\frac{1}{2(\epsilon-1)}}$ with

$$\mathcal{N}_0 \equiv \frac{-\gamma(\epsilon-1)^{1/2}}{3x_0^2}\left(\frac{45}{\pi^2}z_0^2\right)^{1/4}(-\tau_{\rm e})^{-\frac{1}{2(\epsilon-1)}}. \tag{4.81}$$

For the Green's function, G_ϕ, we use the same approximation we used to compute δu_ϕ in Eqs. (4.34) and (4.35), namely finding the solutions for $y > 1$ and $y < 1$ and matching at horizon crossing, taking account of the effect of $\mathcal{J}_r$ according to the change in dissipation and frequency in Eqs. (4.32) and (4.33).

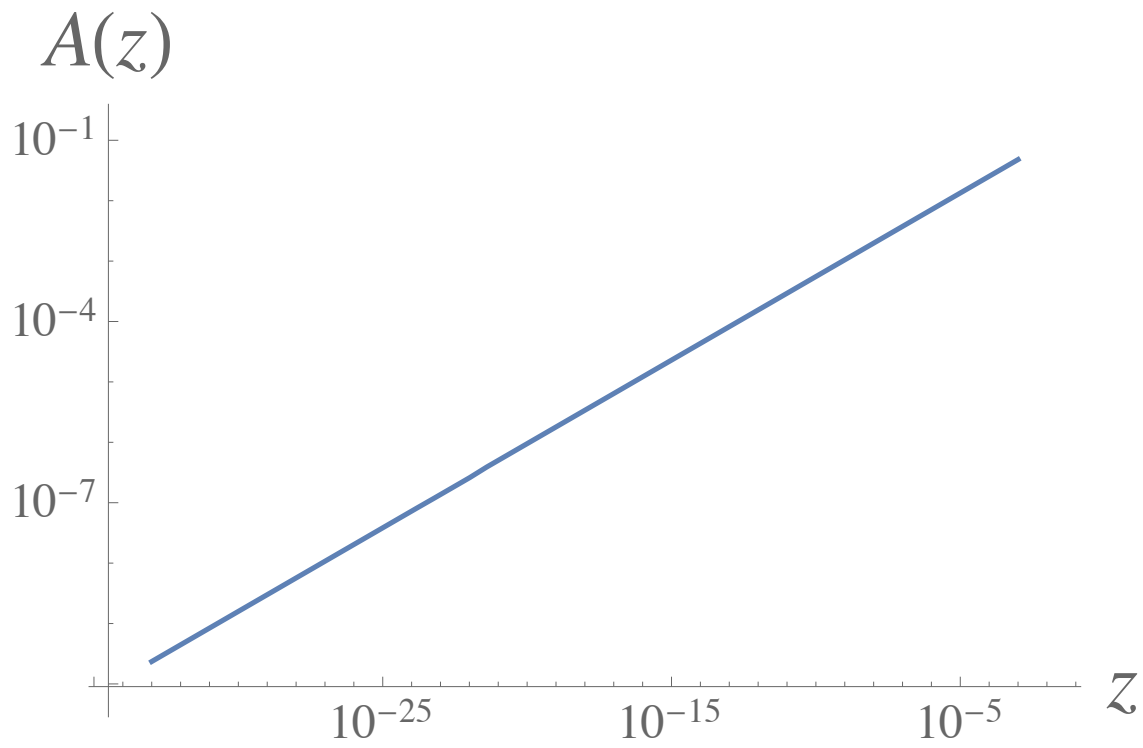

Figure 4.5: This plot shows the result for $\mathcal{A}(z)$ obtained by matching the different solutions at horizon crossing. The largest scales correspond to the smallest values of z. Thus, there is a strong suppression of the thermal contribution to $\Delta^2_{\mathcal{R}}$ on the largest scales. Again, we have used the parameter choice $(c, \gamma) = (15, -56.8)$.

Then, dropping the arguments on the left side of Eq. (4.80), the power spectrum is

$$\begin{aligned} k^3\langle \delta u_\phi^2 \rangle &= \mathcal{N}_0(-\tau_{\rm e})^{\frac{1}{2}+\frac{1}{2(\epsilon-1)}}\mathcal{A}(-k\tau_{\rm e}) \times \\ &\quad (2\pi)^3\delta^{(3)}(\mathbf{k}+\mathbf{k}') \end{aligned} \tag{4.82}$$

where the function

$$\mathcal{A}(z) \equiv z^{-\frac{1}{2}-\frac{1}{2(\epsilon-1)}} \int_z^\infty dy [G_\phi(z,y)]^2 y^{\frac{1}{2}+\frac{1}{2(\epsilon-1)}} \tag{4.83}$$

is plotted in Fig. 4.5. Using Eqs. (4.81), (4.82), and (4.19) in Eq. (4.40), we find that this contribution to $\Delta^2_{\mathcal{R}}$ is suppressed relative to the vacuum result by a factor that is weakly dependent on c and γ and is of order $\mathcal{A}(-k\tau_{\rm e})V_{\rm end}^{.14}$, *e.g.*, for the choice $(c,\gamma) = (15,-56.8)$. Thus, the ratio of this thermal contribution to the vacuum contribution is of order $\mathcal{O}(10^{-9})$ for the largest observable modes.

Chapter 5

Conclusion and outlook

Early Universe theories were introduced to address fine-tuning problems with standard big bang cosmology. To date, inflation remains the most popular proposal, but open questions remain– both phenomenological and conceptual. In this thesis, we studied bouncing alternatives in which the large-scale structure of the present-day Universe originates from the contracting phase before the bounce. These scenarios have the attractive features that they avoid a multiverse and make falsifiable predictions for cosmological observables.

Throughout the duration of my PhD (2012-2017), early Universe cosmology has undergone a paradigm shift. In 2013, the BICEP2 collaboration reported a detection of B-modes in the polarization of the CMB at large angular scales (around $\ell \approx 80$)– a detection they concluded was "well-fit by a lensed-ΛCDM + tensor theoretical model with tensor-to-scalar ratio $r = 0.20^{+0.07}_{-0.05}$" [6]. At the time, this detection was hailed as "smoking gun" evidence for cosmic inflation. After all, when combined with previous bounds from, *e.g.,* PLANCK2013 on the spectral index of the scalar perturbation spectrum, $n_s = 0.9603 \pm 0.0073$ [143], the simplest, single-field inflationary models predict a primordial gravitational wave spectrum with a tensor-to-scalar ratio con-

sistent with the claimed detection. Bets were settled and champagne was poured in celebration of this putative verification of inflation.

As time passed, more detailed studies revealed that the B-mode polarization detected by BICEP2 was caused not by primordial gravitational waves but by a local contaminant that obscures our view of the CMB– the polarized emission of dust within our galaxy. Taking proper account of the contribution of dust, a joint analysis of data from the BICEP2/Keck Array and the Planck collaboration revised the bounds on the tensor-to-scalar ratio, $r_{0.05} < 0.12$ at 95% confidence [144]. With that, the simple models of inflation– those that precipitated the uncorking of champagne bottles– were suddenly disfavored by the data. One would think that if a detection of primordial gravitational waves proves inflation, then a non-detection should disprove it. But this is not so for a theory as versatile as inflation because it can accommodate nearly any cosmological observables (see Ref. [145] for a recent inflationary model consistent with the revised bounds). Some view unfalsifiability as a feature. It certainly affords theorists a justification for permanent employment. But it also means that no observation can rule it out, a big problem for any scientific theory.

Along with these recent phenomenological obstacles, inflation comes with the more serious philosophical hurdle of the multiverse– a nearly unavoidable consequence of quantum fluctuations coupled with accelerated, exponential expansion. With the multiverse, any and every cosmological outcome is produced an infinite number of times. The multiverse predicts everything, and so it predicts nothing. In light of these shortcomings, early Universe cosmologists have two options: we can either seek to redress these shortcomings within the inflationary framework, or we can search for alternative mechanisms for resolving the standard problems. In this thesis, we have taken the second approach, choosing to focus our efforts on two popular bouncing paradigms.

Chapter 2 was based on work published in Ref. [65]. In it, we assessed the matter bounce scenario. We showed that its instability to anisotropic stresses renders it fundamentally unable to address the standard fine-tuning problems without introducing a more extreme fine-tuning requirement of its own. In particular, since the growth of anisotropies is exponentially sensitive to the number of scale-invariant modes that leave the Hubble horizon during the matter-like phase, any implementation must involve a powerful mechanism for suppressing anisotropy beforehand. We argued that orchestrating such a suppression requires that the degrees of freedom responsible for the matter-like phase be coupled to those driving the isotropizing phase. As we pointed out, there are two possibilities: either the isotropizing degrees of freedom must decay directly into matter or they must drive the matter-like contraction themselves. We showed that both possibilities impose extraordinary, exponential fine-tuning requirements on any realization. As a result of these considerations, we arrived at two robust conclusions: 1) new insights are required for the viability of the matter bounce scenario and 2) ekpyrosis is a seemingly indispensable ingredient in any bouncing cosmology that hopes to explain the standard puzzles within the framework of Einstein gravity.

Chapter 3 was based on work published in Ref. [66] in collaboration with Dr. Anna Ijjas and Professor Paul Steinhardt. In it, we examined recent models of two-field ekpyrosis. For these models, we found no such fine-tuning challenges. On the contrary, we illustrated that the simplest realizations are strong attractors for a wide range of initial conditions. The attractor behavior is produced by a non-canonical kinetic coupling between the adiabatic and entropic fields. The coupling introduces friction into the equation of motion for the entropic field, stabilizing it against perturbations, thereby avoiding the need for finely tuned initial conditions. The entropic field acquires (nearly) scale-invariant perturbations, which convert into curvature perturbations via the entropic mechanism. These models generate zero non-Gaussianity

during the ekpyrotic phase and an undetectable spectrum of primordial gravitational waves, consistent with current bounds. Therefore, detecting large-amplitude primordial gravitational waves would represent an unequivocal falsification of this scenario.

Finally, chapter 4 was based on work published in Ref. [67] in collaboration with my fellow graduate student, Gustavo Turiaci. In it, we introduced a new model called "warm ekpyrosis," which is also an attractor and has the aesthetic advantage of requiring only a single scalar field. We showed that an ekpyrotic field decaying into hot radiation receives dissipative corrections to its equation of motion, which can be chosen such that its fluctuations acquire a (nearly) scale-invariant spectrum. The spectrum is immediately adiabatic, and thus no conversion is necessary– another significant advantage. It is notable that the same ingredient responsible for the scale-invariant spectrum– the dissipation induced by the decay– also provides a framework for explaining reheating, a largely unexplored topic in the context of ekpyrotic cosmologies and one that merits further study. The general hydrodynamical analysis we applied provides many directions for future work, chief among them to devise a microphysical realization that reproduces the effective dynamics described here. As with all ekpyrotic scenarios, this too would be falsified by a detection of large-amplitude primordial gravitational waves.

These results suggest that ekpyrotic bouncing cosmologies hold promise for describing the early Universe. In the near future, high-sensitivity measurements of B-mode polarization in the CMB will yield tighter constraints on the tensor-to-scalar ratio, providing a crucial discriminant between these different early Universe scenarios. Within the framework of Einstein gravity, it is difficult to imagine an ekpyrotic universe that can generate large-scale primordial gravitational waves. Both mechanisms studied in this thesis for producing scale-invariant curvature perturbations (noncanonical kinetic couplings in chapter 3 and direct decay in chapter 4) altered only the scalar (compressional) modes; they left the tensor (radiative) perturbations intact

with respect to single-field ekpyrosis [112]. All models to date generate no detectable spectrum of primordial gravitational waves. To alter this spectrum, one might imagine tensorial corrections to the anisotropic inertia (see *e.g.*, π_{ij}^{T} in Eq. (5.1.43) of Ref. [146]). Such terms vanish for perfect fluid matter or for matter in local thermal equilibrium, but in general they can act as sources for the production of primordial gravitational waves. We leave the investigation of such effects for future work.

Bibliography

[1] E. Harrison, *Darkness at night: A riddle of the universe*. Harvard University Press, 1987.

[2] A. Einstein, "Die Grundlage der allgemeinen Relativitätstheorie," *Annalen der Physik*, vol. 354, pp. 769–822, 1916.

[3] P. S. Wesson, "Olbers's paradox and the spectral intensity of the extragalactic background light," *The Astrophysical Journal*, vol. 367, pp. 399–406, 1991.

[4] A. A. Penzias and R. W. Wilson, "A measurement of excess antenna temperature at 4080 mc/s.," *The Astrophysical Journal*, vol. 142, pp. 419–421, 1965.

[5] J. Kovac, E. M. Leitch, C. Pryke, J. E. Carlstrom, N. W. Halverson, and W. L. Holzapfel, "Detection of polarization in the cosmic microwave background using DASI," *Nature*, vol. 420, pp. 772–787, 2002.

[6] P. A. R. Ade *et al.*, "Detection of B-Mode Polarization at Degree Angular Scales by BICEP2," *Phys. Rev. Lett.*, vol. 112, no. 24, p. 241101, 2014.

[7] D. Hanson *et al.*, "Detection of B-mode Polarization in the Cosmic Microwave Background with Data from the South Pole Telescope," *Phys. Rev. Lett.*, vol. 111, no. 14, p. 141301, 2013.

[8] J. Dunkley, R. Hlozek, J. Sievers, V. Acquaviva, P. A. Ade, P. Aguirre, M. Amiri, J. Appel, L. Barrientos, E. S. Battistelli, *et al.*, "The atacama cosmol-

ogy telescope: cosmological parameters from the 2008 power spectrum," *The Astrophysical Journal*, vol. 739, no. 1, p. 52, 2011.

[9] S. Masi *et al.*, "The BOOMERanG experiment and the curvature of the universe," *Prog. Part. Nucl. Phys.*, vol. 48, pp. 243–261, 2002. [,243(2002)].

[10] B. P. Crill *et al.*, "SPIDER: A Balloon-borne Large-scale CMB Polarimeter," *Proc. SPIE Int. Soc. Opt. Eng.*, vol. 7010, p. 2P, 2008.

[11] G. F. Smoot, C. L. Bennett, A. Kogut, E. Wright, J. Aymon, N. Boggess, E. Cheng, G. De Amici, S. Gulkis, M. Hauser, *et al.*, "Structure in the cobe differential microwave radiometer first-year maps," *The Astrophysical Journal*, vol. 396, pp. L1–L5, 1992.

[12] D. N. Spergel, L. Verde, H. V. Peiris, E. Komatsu, M. Nolta, C. Bennett, M. Halpern, G. Hinshaw, N. Jarosik, A. Kogut, *et al.*, "First-year wilkinson microwave anisotropy probe (wmap)* observations: determination of cosmological parameters," *The Astrophysical Journal Supplement Series*, vol. 148, no. 1, p. 175, 2003.

[13] P. A. R. Ade *et al.*, "Planck 2013 results. XVI. Cosmological parameters," *Astron. Astrophys.*, vol. 571, p. A16, 2014.

[14] C. W. Misner, "Mixmaster universe," *Phys. Rev. Lett.*, vol. 22, pp. 1071–1074, May 1969.

[15] R. Dicke, "Gravitation and the universe, volume 78 of memoirs of the american philosophical society, jayne lecture for 1969," *American Philosophical Society, Philadelphia, USA*, vol. 82, 1970.

[16] A. H. Guth, "The Inflationary Universe: A Possible Solution to the Horizon and Flatness Problems," *Phys.Rev.*, vol. D23, pp. 347–356, 1981.

[17] A. Albrecht and P. J. Steinhardt, "Cosmology for grand unified theories with radiatively induced symmetry breaking," *Phys.Rev.Lett.*, vol. 48, pp. 1220–1223, 1982.

[18] A. D. Linde, "A New Inflationary Universe Scenario: A Possible Solution of the Horizon, Flatness, Homogeneity, Isotropy and Primordial Monopole Problems," *Phys.Lett.*, vol. B108, pp. 389–393, 1982.

[19] S. W. Hawking, "The development of irregularities in a single bubble inflationary universe," *Physics Letters B*, vol. 115, no. 4, pp. 295–297, 1982.

[20] A. A. Starobinsky, "Dynamics of phase transition in the new inflationary universe scenario and generation of perturbations," *Physics Letters B*, vol. 117, no. 3-4, pp. 175–178, 1982.

[21] A. H. Guth and S.-Y. Pi, "Fluctuations in the new inflationary universe," *Physical Review Letters*, vol. 49, no. 15, p. 1110, 1982.

[22] A. Vilenkin, "Quantum Fluctuations in the New Inflationary Universe," *Nucl. Phys.*, vol. B226, pp. 527–546, 1983.

[23] J. M. Bardeen, P. J. Steinhardt, and M. S. Turner, "Spontaneous creation of almost scale-free density perturbations in an inflationary universe," *Phys. Rev. D*, vol. 28, pp. 679–693, Aug 1983.

[24] R. Penrose, "Difficulties with inflationary cosmology," *Annals N.Y.Acad.Sci.*, vol. 571, pp. 249–264, 1989.

[25] G. Gibbons and N. Turok, "The Measure Problem in Cosmology," *Phys.Rev.*, vol. D77, p. 063516, 2008.

[26] L. Berezhiani and M. Trodden, "How Likely are Constituent Quanta to Initiate Inflation?," *Phys. Lett.*, vol. B749, pp. 425–430, 2015.

[27] S. Ferrara, R. Kallosh, A. Linde, and M. Porrati, "Minimal Supergravity Models of Inflation," *Phys. Rev.*, vol. D88, no. 8, p. 085038, 2013.

[28] A. Ijjas, P. J. Steinhardt, and A. Loeb, "Inflationary paradigm in trouble after Planck2013," *Phys.Lett.*, vol. B723, pp. 261–266, 2013.

[29] A. Ijjas and P. J. Steinhardt, "Inflationary cheat sheet," *unpublished*, 2016.

[30] P. J. Steinhardt, "Natural inflation," in *Very Early Universe* (G. W. Gibbons, S. W. Hawking, and S. T. C. Siklos, eds.), pp. 251–266, 1983.

[31] A. Vilenkin, "The Birth of Inflationary Universes," *Phys.Rev.*, vol. D27, p. 2848, 1983.

[32] A. H. Guth, "Inflation and eternal inflation," *Phys.Rept.*, vol. 333, pp. 555–574, 2000.

[33] A. H. Guth, "Quantum Fluctuations in Cosmology and How They Lead to a Multiverse," 2013.

[34] A. H. Guth, D. I. Kaiser, and Y. Nomura, "Inflationary paradigm after Planck 2013," *Phys.Lett.*, vol. B733, pp. 112–119, 2014.

[35] A. Linde, "Inflationary Cosmology after Planck 2013," in *Proceedings, 100th Les Houches Summer School: Post-Planck Cosmology: Les Houches, France, July 8 - August 2, 2013*, pp. 231–316, 2015.

[36] A. H. Guth, "Eternal inflation and its implications," *J. Phys.*, vol. A40, pp. 6811–6826, 2007.

[37] A. Borde, A. H. Guth, and A. Vilenkin, "Inflationary space-times are incompletein past directions," *Phys. Rev. Lett.*, vol. 90, p. 151301, 2003.

[38] I. Bars, P. J. Steinhardt, and N. Turok, "Cyclic Cosmology, Conformal Symmetry and the Metastability of the Higgs," *Phys. Lett.*, vol. B726, pp. 50–55, 2013.

[39] A. Friedmann, "Über die krümmung des raumes," *Zeitschrift für Physik*, vol. 10, no. 1, pp. 377–386, 1922.

[40] A. Einstein and W. De Sitter, "On the relation between the expansion and the mean density of the universe," *Proceedings of the National Academy of Sciences*, vol. 18, no. 3, pp. 213–214, 1932.

[41] A. Einstein, "Cosmological considerations on the general theory of relativity," *The Principle of Relativity. Dover Books on Physics. June 1, 1952. 240 pages. 0486600815, p. 175-188*, pp. 175–188, 1952.

[42] A. G. Lemaitre, "A homogeneous universe of constant mass and increasing radius accounting for the radial velocity of extra-galactic nebulae," *Monthly Notices of the Royal Astronomical Society*, vol. 91, no. 5, pp. 483–490, 1931.

[43] R. C. Tolman, "On the theoretical requirements for a periodic behaviour of the universe," *Physical Review*, vol. 38, no. 9, p. 1758, 1931.

[44] R. C. Tolman, *Relativity, thermodynamics, and cosmology*. Courier Corporation, 1987.

[45] V. A. Belinskii, I. M. Khalatnikov, and E. M. Lifshitz, "Oscillatory approach to a singular point in the relativistic cosmology," *Advances in Physics*, vol. 19, no. 80, pp. 525–573, 1970.

[46] P. J. Steinhardt and N. Turok, "The cyclic model simplified," *New Astronomy Reviews*, vol. 49, no. 2âĂŽÄì6, pp. 43 – 57, 2005. Sources and Detection of Dark

Matter and Dark Energy in the Universe 6th {UCLA} Symposium on Sources and Detection of Dark Matter and Dark Energy in the Universe.

[47] J. Khoury, B. A. Ovrut, P. J. Steinhardt, and N. Turok, "The Ekpyrotic universe: Colliding branes and the origin of the hot big bang," *Phys.Rev.*, vol. D64, p. 123522, 2001.

[48] J. K. Erickson, D. H. Wesley, P. J. Steinhardt, and N. Turok, "Kasner and mixmaster behavior in universes with equation of state w >= 1," *Phys. Rev.*, vol. D69, p. 063514, 2004.

[49] J. Acacio de Barros, M. A. Sagioro Leal, and M. Pinto-Neto, "The Causal Interpretation of Dust and Radiation Fluids Non-Singular Quantum Cosmologies," in *Recent Developments in Theoretical and Experimental General Relativity, Gravitation, and Relativistic Field Theories* (T. Piran and R. Ruffini, eds.), p. 1403, 1999.

[50] M. Bojowald, "Absence of singularity in loop quantum cosmology," *Phys. Rev. Lett.*, vol. 86, pp. 5227–5230, 2001.

[51] P. J. Steinhardt and N. Turok, "A cyclic model of the universe," *Science*, vol. 296, no. 5572, pp. 1436–1439, 2002.

[52] L. Smolin, "An Invitation to loop quantum gravity," in *Proceedings, 3rd International Symposium on Quantum theory and symmetries (QTS3): Cincinnati, USA, September 10-14, 2003*, pp. 655–682, 2004. [Submitted to: Rev. Mod. Phys.(2004)].

[53] N. Turok, B. Craps, and T. Hertog, "From big crunch to big bang with ads/cft," *arXiv preprint arXiv:0711.1824*, 2007.

[54] S. Gielen and N. Turok, "Perfect Quantum Cosmological Bounce," *Phys. Rev. Lett.*, vol. 117, no. 2, p. 021301, 2016.

[55] P. Peter and N. Pinto-Neto, "Primordial perturbations in a nonsingular bouncing universe model," *Physical Review D*, vol. 66, no. 6, p. 063509, 2002.

[56] L. E. Allen and D. Wands, "Cosmological perturbations through a simple bounce," *Physical Review D*, vol. 70, no. 6, p. 063515, 2004.

[57] Y.-F. Cai, T. Qiu, X. Zhang, Y.-S. Piao, and M. Li, "Bouncing universe with quintom matter," *Journal of High Energy Physics*, vol. 2007, no. 10, p. 071, 2007.

[58] E. I. Buchbinder, J. Khoury, and B. A. Ovrut, "New Ekpyrotic cosmology," *Phys.Rev.*, vol. D76, p. 123503, 2007.

[59] P. Creminelli and L. Senatore, "A smooth bouncing cosmology with scale invariant spectrum," *Journal of Cosmology and Astroparticle Physics*, vol. 2007, no. 11, p. 010, 2007.

[60] T. Qiu, J. Evslin, Y.-F. Cai, M. Li, and X. Zhang, "Bouncing galileon cosmologies," *Journal of Cosmology and Astroparticle Physics*, vol. 2011, no. 10, p. 036, 2011.

[61] D. A. Easson, I. Sawicki, and A. Vikman, "G-bounce," *Journal of Cosmology and Astroparticle Physics*, vol. 2011, no. 11, p. 021, 2011.

[62] Y.-F. Cai, D. A. Easson, and R. Brandenberger, "Towards a Nonsingular Bouncing Cosmology," *JCAP*, vol. 1208, p. 020, 2012.

[63] A. Ijjas and P. J. Steinhardt, "Classically stable nonsingular cosmological bounces," *Physical Review Letters*, vol. 117, no. 12, p. 121304, 2016.

[64] A. Ijjas and P. J. Steinhardt, "Fully stable cosmological solutions with a non-singular classical bounce," *Phys. Lett.*, vol. B764, pp. 289–294, 2017.

[65] A. M. Levy, "Fine-tuning challenges for the matter bounce scenario," *Phys. Rev. D*, vol. 95, p. 023522, Jan 2017.

[66] A. M. Levy, A. Ijjas, and P. J. Steinhardt, "Scale-invariant perturbations in ekpyrotic cosmologies without fine-tuning of initial conditions," *Phys. Rev.*, vol. D92, no. 6, p. 063524, 2015.

[67] A. M. Levy and G. J. Turiaci, "Warm Ekpyrosis," *Phys. Rev.*, vol. D94, no. 8, p. 083514, 2016.

[68] E. Komatsu *et al.*, "Five-Year Wilkinson Microwave Anisotropy Probe (WMAP) Observations: Cosmological Interpretation," *Astrophys. J. Suppl.*, vol. 180, pp. 330–376, 2009.

[69] P. Ade *et al.*, "Planck 2015. XX. Constraints on inflation," 2015.

[70] P. A. R. Ade *et al.*, "Planck 2015 results. XVII. Constraints on primordial non-Gaussianity," 2015.

[71] J. L. Sievers *et al.*, "The Atacama Cosmology Telescope: Cosmological parameters from three seasons of data," *JCAP*, vol. 1310, p. 060, 2013.

[72] D. Wands, "Duality invariance of cosmological perturbation spectra," *Phys. Rev.*, vol. D60, p. 023507, 1999.

[73] F. Finelli and R. Brandenberger, "On the generation of a scale invariant spectrum of adiabatic fluctuations in cosmological models with a contracting phase," *Phys. Rev.*, vol. D65, p. 103522, 2002.

[74] L. E. Allen and D. Wands, "Cosmological perturbations through a simple bounce," *Phys. Rev.*, vol. D70, p. 063515, 2004.

[75] R. H. Brandenberger, "The Matter Bounce Alternative to Inflationary Cosmology," 2012.

[76] R. Brandenberger and P. Peter, "Bouncing Cosmologies: Progress and Problems," 2016.

[77] G. W. Gibbons, S. W. Hawking, and S. Siklos, *The Very Early Universe: Proceedings of the Nuffield Workshop, Cambridge 21 June to 9 July, 1982.* CUP Archive, 1985.

[78] A. H. Guth, "Inflationary universe: A possible solution to the horizon and flatness problems," *Phys. Rev. D*, vol. 23, pp. 347–356, Jan 1981.

[79] J. Quintin, Z. Sherkatghanad, Y.-F. Cai, and R. H. Brandenberger, "Evolution of cosmological perturbations and the production of non-Gaussianities through a nonsingular bounce: Indications for a no-go theorem in single field matter bounce cosmologies," *Phys. Rev.*, vol. D92, no. 6, p. 063532, 2015.

[80] Y.-B. Li, J. Quintin, D.-G. Wang, and Y.-F. Cai, "Matter bounce cosmology with a generalized single field: non-Gaussianity and an extended no-go theorem," 2016.

[81] Y.-F. Cai, R. Brandenberger, and X. Zhang, "The Matter Bounce Curvaton Scenario," *JCAP*, vol. 1103, p. 003, 2011.

[82] E. Wilson-Ewing, "The Matter Bounce Scenario in Loop Quantum Cosmology," *JCAP*, vol. 1303, p. 026, 2013.

[83] Y.-F. Cai and E. Wilson-Ewing, "A ΛCDM bounce scenario," *JCAP*, vol. 1503, no. 03, p. 006, 2015.

[84] A. Fertig, J.-L. Lehners, E. Mallwitz, and E. Wilson-Ewing, "Converting entropy to curvature perturbations after a cosmic bounce," *JCAP*, vol. 1610, no. 10, p. 005, 2016.

[85] Y.-F. Cai, A. Marciano, D.-G. Wang, and E. Wilson-Ewing, "Bouncing cosmologies with dark matter and dark energy," *Universe*, vol. 3, p. 1, 2017.

[86] Y.-F. Cai, R. Brandenberger, and P. Peter, "Anisotropy in a Nonsingular Bounce," *Class. Quant. Grav.*, vol. 30, p. 075019, 2013.

[87] V. Bozza and M. Bruni, "A Solution to the anisotropy problem in bouncing cosmologies," *JCAP*, vol. 0910, p. 014, 2009.

[88] K. Story, C. Reichardt, Z. Hou, R. Keisler, K. Aird, B. Benson, L. Bleem, J. Carlstrom, C. Chang, H.-M. Cho, *et al.*, "A measurement of the cosmic microwave background damping tail from the 2500-square-degree spt-sz survey," *The Astrophysical Journal*, vol. 779, no. 1, p. 86, 2013.

[89] J. Middleton and J. D. Barrow, "The Stability of an Isotropic Cosmological Singularity in Higher-Order Gravity," *Phys. Rev.*, vol. D77, p. 103523, 2008.

[90] R. Brandenberger, "Matter Bounce in Horava-Lifshitz Cosmology," *Phys. Rev.*, vol. D80, p. 043516, 2009.

[91] Y.-F. Cai, S.-H. Chen, J. B. Dent, S. Dutta, and E. N. Saridakis, "Matter Bounce Cosmology with the f(T) Gravity," *Class. Quant. Grav.*, vol. 28, p. 215011, 2011.

[92] Y.-F. Cai and E. Wilson-Ewing, "Non-singular bounce scenarios in loop quantum cosmology and the effective field description," *JCAP*, vol. 1403, p. 026, 2014.

[93] R. Brandenberger and F. Finelli, "On the spectrum of fluctuations in an effective field theory of the Ekpyrotic universe," *JHEP*, vol. 11, p. 056, 2001.

[94] D. H. Lyth, "The Primordial curvature perturbation in the ekpyrotic universe," *Phys. Lett.*, vol. B524, pp. 1–4, 2002.

[95] J.-c. Hwang, "Cosmological structure problem in the ekpyrotic scenario," *Phys. Rev.*, vol. D65, p. 063514, 2002.

[96] J. Hwang and H. Noh, "Identification of perturbation modes and controversies in ekpyrotic perturbations," *Phys. Lett.*, vol. B545, pp. 207–213, 2002.

[97] P. Creminelli, A. Nicolis, and M. Zaldarriaga, "Perturbations in bouncing cosmologies: Dynamical attractor versus scale invariance," *Phys. Rev.*, vol. D71, p. 063505, 2005.

[98] J.-L. Lehners, "Ekpyrotic and Cyclic Cosmology," *Phys.Rept.*, vol. 465, pp. 223–263, 2008.

[99] J.-L. Lehners, P. McFadden, N. Turok, and P. J. Steinhardt, "Generating ekpyrotic curvature perturbations before the big bang," *Phys.Rev.*, vol. D76, p. 103501, 2007.

[100] F. Di Marco, F. Finelli, and R. Brandenberger, "Adiabatic and isocurvature perturbations for multifield generalized Einstein models," *Phys.Rev.*, vol. D67, p. 063512, 2003.

[101] F. Finelli, "A contracting universe driven by two scalar fields," *Physics Letters B*, vol. 545, no. 1–2, pp. 1 – 7, 2002.

[102] K. Koyama, S. Mizuno, and D. Wands, "Curvature perturbations from ekpyrotic collapse with multiple fields," *Class.Quant.Grav.*, vol. 24, pp. 3919–3932, 2007.

[103] K. Koyama and D. Wands, "Ekpyrotic collapse with multiple fields," *JCAP*, vol. 0704, p. 008, 2007.

[104] E. I. Buchbinder, J. Khoury, and B. A. Ovrut, "On the initial conditions in new ekpyrotic cosmology," *JHEP*, vol. 0711, p. 076, 2007.

[105] K. Hinterbichler and J. Khoury, "The Pseudo-Conformal Universe: Scale Invariance from Spontaneous Breaking of Conformal Symmetry," *JCAP*, vol. 1204, p. 023, 2012.

[106] A. J. Tolley and D. H. Wesley, "Scale-invariance in expanding and contracting universes from two-field models," *JCAP*, vol. 0705, p. 006, 2007.

[107] M. Li, "Note on the production of scale-invariant entropy perturbation in the Ekpyrotic universe," *Physics Letters B*, vol. 724, pp. 192–197, July 2013.

[108] J. M. Bardeen, "Gauge-invariant cosmological perturbations," *Phys. Rev. D*, vol. 22, pp. 1882–1905, Oct 1980.

[109] M. Sasaki, "Large Scale Quantum Fluctuations in the Inflationary Universe," *Prog.Theor.Phys.*, vol. 76, p. 1036, 1986.

[110] V. Mukhanov, "Quantum theory of gauge-invariant cosmological perturbations," *Zh. Eksp. Teor. Fiz*, vol. 94, p. 1, 1988.

[111] Z. Lalak, D. Langlois, S. Pokorski, and K. Turzynski, "Curvature and isocurvature perturbations in two-field inflation," *JCAP*, vol. 0707, p. 014, 2007.

[112] L. A. Boyle, P. J. Steinhardt, and N. Turok, "The Cosmic gravitational wave background in a cyclic universe," *Phys. Rev.*, vol. D69, p. 127302, 2004.

[113] A. Fertig, J.-L. Lehners, and E. Mallwitz, "Ekpyrotic Perturbations With Small Non-Gaussian Corrections," 2013.

[114] A. Ijjas, J.-L. Lehners, and P. J. Steinhardt, "General mechanism for producing scale-invariant perturbations and small non-Gaussianity in ekpyrotic models," *Phys.Rev.*, vol. D89, no. 12, p. 123520, 2014.

[115] M. Deserno, "Notes on differential geometry," 2004.

[116] F. Finelli, "Assisted contraction," *Phys. Lett.*, vol. B545, pp. 1–7, 2002.

[117] D. H. Lyth and D. Wands, "Generating the curvature perturbation without an inflaton," *Phys. Lett.*, vol. B524, pp. 5–14, 2002.

[118] D. H. Lyth, C. Ungarelli, and D. Wands, "Primordial density perturbation in the curvaton scenario," *Phys. Rev. D*, vol. 67, p. 023503, Jan 2003.

[119] D. H. Lyth and D. Wands, "Cold dark matter isocurvature perturbation in the curvaton scenario," *Phys. Rev. D*, vol. 68, p. 103516, Nov 2003.

[120] M. Li, "Entropic mechanisms with generalized scalar fields in the Ekpyrotic universe," *Phys.Lett.*, vol. B741, pp. 320–326, 2015.

[121] A. Notari and A. Riotto, "Isocurvature perturbations in the ekpyrotic universe," *Nucl. Phys.*, vol. B644, pp. 371–382, 2002.

[122] A. Berera, I. G. Moss, and R. O. Ramos, "Warm Inflation and its Microphysical Basis," *Rept. Prog. Phys.*, vol. 72, p. 026901, 2009.

[123] A. Berera and L.-Z. Fang, "Thermally induced density perturbations in the inflation era," *Phys. Rev. Lett.*, vol. 74, pp. 1912–1915, 1995.

[124] A. Berera, "Warm inflation," *Phys. Rev. Lett.*, vol. 75, pp. 3218–3221, 1995.

[125] A. Berera, "Thermal properties of an inflationary universe," *Phys. Rev.*, vol. D54, pp. 2519–2534, 1996.

[126] A. Berera, "The warm inflationary universe," *Contemp. Phys.*, vol. 47, pp. 33–49, 2006.

[127] M. Bastero-Gil and A. Berera, "Warm inflation model building," *Int. J. Mod. Phys.*, vol. A24, pp. 2207–2240, 2009.

[128] D. Green, B. Horn, L. Senatore, and E. Silverstein, "Trapped Inflation," *Phys. Rev.*, vol. D80, p. 063533, 2009.

[129] E. Calzetta and B. Hu, *Nonequilibrium Quantum Field Theory.* Cambridge Monographs on Mathematical Physics, Cambridge University Press, 2008.

[130] S. Weinberg, "Must cosmological perturbations remain non-adiabatic after multi-field inflation?," *Phys. Rev.*, vol. D70, p. 083522, 2004.

[131] M. Bastero-Gil, A. Berera, I. G. Moss, and R. O. Ramos, "Cosmological fluctuations of a random field and radiation fluid," *JCAP*, vol. 1405, p. 004, 2014.

[132] A. Berera, M. Gleiser, and R. O. Ramos, "A First principles warm inflation model that solves the cosmological horizon / flatness problems," *Phys. Rev. Lett.*, vol. 83, pp. 264–267, 1999.

[133] A. Berera, M. Gleiser, and R. O. Ramos, "Strong dissipative behavior in quantum field theory," *Phys. Rev.*, vol. D58, p. 123508, 1998.

[134] S. Bartrum, M. Bastero-Gil, A. Berera, R. Cerezo, R. O. Ramos, and J. G. Rosa, "The importance of being warm (during inflation)," *Phys. Lett.*, vol. B732, pp. 116–121, 2014.

[135] J. Yokoyama and A. D. Linde, "Is warm inflation possible?," *Phys. Rev.*, vol. D60, p. 083509, 1999.

[136] I. G. Moss and C. Xiong, "Dissipation coefficients for supersymmetric inflatonary models," 2006.

[137] M. Bastero-Gil, A. Berera, and R. O. Ramos, "Dissipation coefficients from scalar and fermion quantum field interactions," *JCAP*, vol. 1109, p. 033, 2011.

[138] M. Bastero-Gil, A. Berera, R. O. Ramos, and J. G. Rosa, "General dissipation coefficient in low-temperature warm inflation," *JCAP*, vol. 1301, p. 016, 2013.

[139] M. Bastero-Gil, A. Berera, and R. O. Ramos, "Shear viscous effects on the primordial power spectrum from warm inflation," *JCAP*, vol. 1107, p. 030, 2011.

[140] M. Bastero-Gil, A. Berera, R. O. Ramos, and J. G. Rosa, "Warm Little Inflaton," 2016.

[141] J.-c. Hwang and H. Noh, "Cosmological perturbations with multiple fluids and fields," *Class. Quant. Grav.*, vol. 19, pp. 527–550, 2002.

[142] K. A. Malik and D. Wands, "Adiabatic and entropy perturbations with interacting fluids and fields," *JCAP*, vol. 0502, p. 007, 2005.

[143] P. Ade *et al.*, "Planck 2013 results. XXII. Constraints on inflation," *Astron.Astrophys.*, vol. 571, p. A22, 2014.

[144] P. A. R. Ade *et al.*, "Joint Analysis of BICEP2/$KeckArray$ and *Planck* Data," *Phys. Rev. Lett.*, vol. 114, p. 101301, 2015.

[145] A. Linde, "Does the first chaotic inflation model in supergravity provide the best fit to the planck data?," *Journal of Cosmology and Astroparticle Physics*, vol. 2015, no. 02, p. 030, 2015.

[146] S. Weinberg, *Cosmology*. Oxford University Press, 2008.